UNIVERSITEIT VAN PRETORIA
UNIVERSITY OF PRETORIA
YUNIBESITHI YA PRETORIA

DYNAMIC ANALYSIS OF STEEL RAILWAY BRIDGE SUBJECTED TO TRAIN LOADS

RAHEL DELELEGNE SHIBESHI

2015

UNIVERSITEIT VAN PRETORIA
UNIVERSITY OF PRETORIA
YUNIBESITHI YA PRETORIA

DYNAMIC ANALYSIS OF STEEL RAILWAY BRIDGE SUBJECTED TO TRAIN LOADS

RAHEL DELELEGNE SHIBESHI

A preliminary copy of dissertation submitted in partial fulfilment of the requirements for the degree of

MASTER OF ENGINEERING (STRUCTURAL ENGINEERING)

In the

FACULTY OF CIVIL ENGINEERING

UNIVERSITY OF PRETORIA

APRIL 2015

DISSERTATION SUMMARY

DYNAMIC ANALYSIS OF STEEL RAILWAY BRIDGE SUBJECTED TO TRAIN LOADS

RAHEL DELELEGNE SHIBESHI

Supervisor: Professor CP Roth

Department: Civil Engineering

University: University of Pretoria

Degree: Master of Engineering (Structural engineering)

The continuous need of rail infrastructure development worldwide indicates the necessity of thoroughly understanding the various types of responses of railway bridges and how the responses of these bridges are affected by various factors. One of the motivations for conducting this research is to understand the different possible approaches that exist for the dynamic analysis of simply supported single span railway bridges, and to understand the effect of the different parameters on each response. The different parameters considered in the scope of this research include: the speed and the axle load of a train, the span length, the moment of inertia and the mass of the bridge. These parameters can affect the magnitude and pattern of the bridge's response. In the following research the dynamic analysis of a single span simply supported steel truss railway bridge when subjected to train loads is analysed. The study is approached using three different methodologies: modal analysis using three dimensional FEM of a bridge; a time history analysis formulated from mathematically derived equations of motion; and supporting data obtained by conducting field measurement on an existing bridge. The author believes there is insufficient research work done on existing railway bridges in South Africa.

The purpose of the study is to contribute additional value to the clarity of the specified subject matter. The methodology used in this research can be taken as a reference during the construction of new railway bridges or when upgrading existing bridges, for instance when the speed limit needs to be increased. The author also believes that bridges' structural integrity may be compromised or that failure may occur as a result of fatigue in the structure due to insufficient consideration being given to the dynamic response of the bridge. This suggests that there is a definite need for further research to be conducted on this subject matter. Therefore, the information obtained from conducting this study is believed to

contribute to further research on the subject matter, and to influence the course of action followed during fatigue analysis.

The results of this research indicate that the responses of a bridge are sensitive to change in any of the identified bridge parameters, as well as the train speed. Generally it can be concluded that the mathematical approach provided good estimation to the actual displacement value. The FEM also gave good estimation to the frequency as compared to the frequency extracted from acceleration data using FFT. However the magnitude of measured acceleration is not reliable that may have resulted from the difference in the laboratory and actual condition set up in addition to the other factors. It is also observed that the maximum acceleration due to certain speeds has passed the limit set by Safety and Serviceability Standards of Bridges.

ABSTRACT

Title: Dynamic Analysis of Steel Railway Bridge Subjected to Train Loads

Author: Rahel Delelegne Shibeshi

Supervisor: Professor CP Roth

Department: Civil Engineering

University: University of Pretoria

Degree: Master of Engineering (Structural engineering)

ARTICLE INFO

Article history

ABSTRACT

In this research a single span simply supported steel truss railway bridge is analyzed when subjected to train loads. The study was conducted by using three different methodologies namely modal analysis using three dimensional finite element models of a bridge based on As-built drawn from scratch; a time history analysis and field measurement on an existing bridge. The finite element models of the bridge were modeled using two methodologies; using beam and shell elements. A time history analysis involves developing an equation of motion for the forced and free vibration of the bridge when subjected to both a single- and successive train loads. The dynamic responses studied include the displacement, acceleration and natural frequency of the bridge which were compared for different train speeds, span length, and the mass of the bridge. Field measurement was conducted using accelerometers and displacement transducers which were mounted on a self-designed mounting section.

Keywords: Finite element modeling, Time history analysis, field measurement, steel truss railway bridge, accelerometer, displacement transducer, train, dynamic analysis

DECLARATION (VERKLARING)

I, the undersigned hereby declare that:

I understand what plagiarism is and I am aware of the University's policy in this regard;

The work contained in this thesis is my own original work;

I did not refer to work of current or previous students, lecture notes, handbooks or any other study material without proper referencing;

Where other people's work has been used this has been properly acknowledged and referenced;

I have not allowed anyone to copy any part of my thesis;

I have not previously in its entirety or in part submitted this thesis at any university for a degree.

Signature of student

Rahel D.Shibeshi

11307952

ACKNOWLEDGEMENT (ERKENNING)

I wish to express my appreciation to the following organisations and persons who made this project dissertation possible:

a) PRASA for providing me access and permission to perform field measurement on the steel truss bridge at Irene, Centurion. I appreciate their coordination before and during the measurement.

b) University of Pretoria for financial support and the use of laboratory facilities during the course of the study.

c) Oasys for providing me access to use the finite element software package, OaSYS GSA.

d) Professor CP Roth, my supervisor, for his guidance and support.

e) The following persons are gratefully acknowledged for their assistance during the course of the study:

   i) Prof EP Kearsley for creating the opportunity for me to study with the University of Pretoria. I appreciate her willingness to help.

   ii) Prof Wynand Steyn for providing me permission to use the accelerometers. I appreciate his willingness to help.

   iii) Prof PJ(Hannes) Grabe for introducing me to PRASA. I appreciate his willingness to help.

   iv) Berhanu B.Bogale, Pr.Eng, PMP, for his suggestions.

f) Miss Talita Van Graan for grammar proofing

g) My husband, Berhanu B.Bogale, my two daughters, Naomi and Soliana B.Bogale, my father, Delelegne S.Mengesha, and my whole family for their patience, encouragement and continuous support during the study.

TABLE OF CONTENTS

LIST OF TABLES

LIST OF FIGURES

LIST OF ACRONYMS

AASHTO	American Association of State Highway and Transportation Officials
AREMA	American Railway Engineering and Maintenance-of-Way Association
DRC	Democratic Republic of Congo
E	Modulus of Elasticity
EI	Flexural rigidity
FEM	Finite element modelling
FFT	Fast Fourier transform
RFDM	Regional Freight Demand Model
GSA	Finite element modelling package used whose full name is OaSYS GSA
GCDC	Gulf Coast Data Concepts
HBM	Hottinger Baldwin Messtechnik
HSR	High speed train
I	Moment of Inertia
ICP	Integrated Circuit Piezoelectric
LTPF	Long Term Planning Framework.
MDOF	Multiple degree of freedom
MEMS	Micro Electromechanical Systems
OHBD	Ontario Highway Bridge Design
PRASA	Passenger Rail Agency of South Africa
SAIIA	South African Institute of International Affairs
SDOF	Single degree of freedom
SNCF	Société Nationale des Chemins de fer Français (French National Railways)
TC	Trailer Coach
USB	Universal Serial Bus

LIST OF SYMBOLS

SYMBOL	DESCRIPTION	UNIT
D	Critical length of the train	m or any unit of length
D_{dyn}	Dynamic deflection	mm or any unit of length
D_{st}	Static deflection	mm or any unit of length
e	Axle spacing	m or any unit of length
$EI(x)$	Flexural rigidity of bridge per unit length	kNm^2
$f_I(x,t)$	Fictitious force	N
$H(\bullet)$	Unit step function	Unit less
$\tilde{k}$	Generalised stiffness of bridge	N/m
L	Span length of the bridge	m or any unit of length
L_c	Distance between the two wheel assemblies of a coach, and	m or any unit of length
L_d	Distance between the rear wheel assembly of a coach and the front wheel assembly of the following coach.	m or any unit of length
$\tilde{m}$	Generalised mass of bridge	kg
$m(x)$	Mass of the bridge per unit length	kg/m
$M(x,t)$	Internal bending moment	Nm or any unit of moment
N	Total number of moving loads considered.	Unit less
P	Series of lumped loads from two axle loads of a bogie, P_0	N or any unit of force
P_0	Axle load moving	N or any unit of force
$P(x,t)$	Expression of single load	N
$\tilde{P}(V,t)$	Expression of the train front wheel loads	Unit less
$\tilde{P}(V,t-t_c)$	Expression of the train rear wheel loads	Unit less
$\tilde{P}(t)$	Generlaized force	N or any unit of force
s	Speed parameter	Unit less
T_n	Natural period calculated from the natural frequency	s
t_c	Time lag between the front and rear wheel two sets of moving loads	s
t_d	Time to cross the bridge	s

t_j	Arriving time of the j^{th} load at the beam or bridge	s
$u\,(x,t)$	Displacement at distance *'x'* and time *'t'*	m or any unit of length
$\ddot{u}(x,t)$	Acceleration expressed as second derivative of displacement with respect to time	m/s^2
$u''(x,t)$	Curvature expressed as second derivative of displacement with respect to distance	m^{-1}
V	Speed of the train	m/s or any unit of speed
V_{cr}	Critical speed	m/s or any unit of speed
x	Distance from one edge of bridge where the response is required	m or any unit of length
$\ddot{z}(t)$	Acceleration coordinate	m/s^2
$(Z_{st})_0$	Static deflection from generlaized model	m or any unit of length
$\delta\,\kappa(x)$	Virtual curvature	Unit less
$\delta\,u\,(x)$	Virtual displacement or fictitious displacement	m or any unit of length
$\delta(x-Vt)$	Dirac delta function centred at x= vt	Unit less
$\delta\,W_E$	Virtual external work	Nm or any unit of work
$\delta\,W_I$	Virtual internal work	Nm or any unit of work
(λ)	Wavelength of irregularity	m or any unit of length
$\psi(x)$	Shape function of the bridge	unit less
ω_1	Frequency of the first vertical mode of vibration of the bridge	rad/s
ω	Fundamental frequency of the bridge in rad/s	rad/s
Ω	Track irregularity	rad/m

1 INTRODUCTION

1.1 GENERAL BACKGROUND

Worldwide, the current generation is expressing a keen interest in the expansion of an integrated, rapid and classier passengers train, and far from being localised to any one country; this may increase the need of rail network infrastructure development. In developing countries such as South Africa, this is a matter that requires more attention and further research. The author believes that a properly integrated, high speed transport system will reduce the travelling time from their home to their work place, which indirectly has a significant impact on the economy and social well-being of the country.

The Maputo corridor initiative is an example of the need of railway infrastructure development and expansion. According to the Maputo corridor logistics initiative, the Maputo corridor is planned to connect the South African areas of Gauteng, Limpopo and Mpumalanga with the Mozambican capital, Maputo (Policy Briefing 54, August 2012). Another useful example is the Regional Freight Demand Model (RFDM) which investigates the transport infrastructure projects development plan in 17 countries in sub-Saharn Africa. The countries listed are: Angola, Botswana, Burundi, Congo, Democratic Republic of Congo(DRC), Kenya, Lesotho, Malawi, Mozamique, Namibia, Rwanda, South Africa, Swaziland, Tanzania, Uganda, Zambia and Zimbabwe (Transnet, 2014). East-African countries such as Ethiopia need to expand their rail infrastructures connecting different parts of the country's main cities. Generally, a closer look at the rail infrastructure network in Africa shows the importance of rail infrastructure development and expansion on the functioning of numerous sectors of the country.

Most expansion of railway infrastructure may involve construction of new railway bridges or upgrading of existing railway bridges, the construction of ducts, embankments and other related features that form part of a rail system. In some cases where the construction of a new bridge is not viable, the upgrading of existing bridges is the only alternative. In these instances, a detailed analysis of the existing bridge is mandatory.

One of the key factors that may affect bridges' static and dynamic response is the type of construction materials used. Concrete is commonly used as a construction material for shorter span bridges as it is cheaper to construct and easier to maintain. However, steel is also a viable alternative material for steel railway bridge construction, especially in areas

where longer span bridges need to be constructed. Steel is believed to be advantageous over concrete by saving on construction time and weighing less, which results in cheaper foundation costs. It also creates less disruption and pollution during the process of construction. Therefore understanding the behaviour of steel bridges is important for future flexibility in selecting construction material.

1.2 PROBLEM STATEMENT

The continuous need of rail infrastructure development increases the necessity of thoroughly understanding the various types of responses of a bridge subjected to train loads. Some of the motivations for conducting this research include:

a) To add more clarity to the subject matter of the dynamic response of a single span simply supported steel railway bridge when subjected to train loads.

b) To understand the different approaches for dynamic analysis: Finite Element Modelling (FEM), Mathematical Approach and Field Measurement.

c) To understand the effect of parameters on dynamic response of new or existing railway bridges. Some of the parameters of concern to this study were: train speed, axle load of the train, span length and the mass of the bridge.

d) To enrich South Africa's research works in the subject area. To the author's knowledge, there are no research works related to dynamic analysis of railway bridges in South Africa.

1.3 OBJECTIVE OF THE STUDY

The main objectives of this research include:

a) To analyse the dynamic response of a single span simply supported steel bridge when subjected to train loads, using three methodologies: FEM, Mathematical Approach and Field Measurement. These mentioned methodologies were analysed in this study as discussed in Chapters 3 to 8 of this dissertation.

b) To compare the extent of responses within the values existing in references and from empirical formulas as obtained from previous research works. These findings are summarized in Chapter 6.

c) To observe the effect of different parameters more specifically train speed on the dynamic behaviour of a steel truss railway.

1.4 SCOPE OF THE STUDY

The dynamic responses of a single span simply supported steel truss railway bridge when subjected to train loads will be discussed in this research. The scope of the work includes an analytical representation of the situation using FEM and mathematical approaches, as well as performing field measurement as discussed in Section 1.5. This involves:

a) Selecting a representative steel railway bridge that is mainly based on its availability, ease of access, visibility of the strucutal frame work and from which the form and size of structural elements can be measured.
b) Developing an As-built drawing from scratch, based on visual inspection and measurement of the bridge,
c) Selecting a FEM package based on the accuracy of the results obtained, the availability of the software licence and the ease, analysis speed and versatility of the modelling used.
d) FEM using shell and beam elements and comparing their modal analysis results. The results of this analysis will be discussed in detail in Chapter 4.
e) Time history analysis based on the equation of motion developed will be presented in Chapter 5 of this research project.
f) Conducting field measurement on the actual bridge located at Irene, Centurion as described in Chapter 3.
g) Comparison and discussion of the results obtained in the analysis set out above, and in concurrence with existing available references and literature on the subject.

The assumptions that were made during the course of the study were:

a) The entire steel truss bridge was assumed to behave as a generalized beam.
b) A perfectly straight rail with no discontinuity or roughness, no damping on the structure, no shear deformation, and no eccentricity of the position of axle load therefore imply that a torsion effect was not considered.
c) The axle load of the train can be represented as a force crossing the bridge at a constant speed.
d) The initial conditions were assumed at rest when developing the equation of motion.

The study entailed some limitations which may have significantly altered the results obtained. These limitations include:

a) Non-linear analysis was not included in the scope of this research.
b) Three-dimensional mathematical approach was not covered; therefore the response at any local point on the structure cannot be extracted from the mathematical approaches.

c) The mathematical approach is only applicable to single span simply supported bridges. The equation of motion must be changed to match the boundary condition of bridges exceeding one span or different boundary conditions.

d) Only vertical response for the first mode of vibration was observed.

e) The mathematical approach could be taken as a generalized solution whereby approximate responses were extracted. A more detailed analysis may be required if one is studying the subject in order to observe the specific nature of different types of bridges such as truss or plate girder railway bridge.

f) Factors such as rail roughness and irregularity, the wind effect, fatigue and vehicle bridge interaction was not included as it exceeds the scope possible within this research.

g) The effect of damping was not considered.

h) The effect of speeds above 90km/h on dynamic response was not measured, but was only analysed mathematically and compared with existing literature and references. The reason for this is that the maximum speed limit on actual bridge under consideration was 90km/h.

1.5 METHODOLOGY

The methodologies applied in this research include: FEM, Mathematical Approach and Field Measurement on a specifically selected bridge.

1) A mathematical representation of a single and simply supported span bridge was formulated from existing theory. The equations developed were manipulatable which makes observing the differences in response when the span length, train speed or bridge mass varies easier. This is discussed in more detail in Chapter 5 and 6.
2) The second step is the FEM. This includes;
    - A single span steel railway bridge is selected which could be used as a case study. Critical data on the bridge was not readily available, therefore an initial field investigation was mandatory. Dimensional drawings were developed from scratch by taking actual field measurement on the field. Some of the parameters such as boundary conditions; the connection details between elements and the property of materials corresponding to the real condition were assumed as based on visual inspection. These assumptions were then applied in the FEM presented in Chapter 4.
    - Modal analysis is then performed on the FEM.

- Different types of models were used for the FEM of the selected bridge, including modelling using shell and beam elements. This exercise involved the inclusion and exclusion of secondary elements such as bottom and side bracings, rail and sleepers. It was believed this will save time when conducting future analysis of such cases as the difference obtained from these models and previous research works were analysed and compared in this research.

3) Field measurement was undertaken using Universal Serial Bus (USB) accelerometer obtained from Gulf Coast Data Concepts (GCDC) and Hottinger Baldwin Messtechnik (HBM)'s WA50 type displacement transducer. Prior to the actual field measurement, verification of each pre-calibrated instrument was performed as discussed in Chapter 3. The accuracy and ease of fixing of the instrument was one of the issues discussed in this aforementioned chapter. Selecting an appropriate instrument of measurement was mandatory as the bridge is built approximately 8m high above a river with no deck or ballast which made the fixing of instrument of measurement a challenging task. Generally the research strategy followed can be represented with chart shown in Figure 1.1.
4) All results obtained from the three methodology discussed is compared and discussed in Chapter 7.

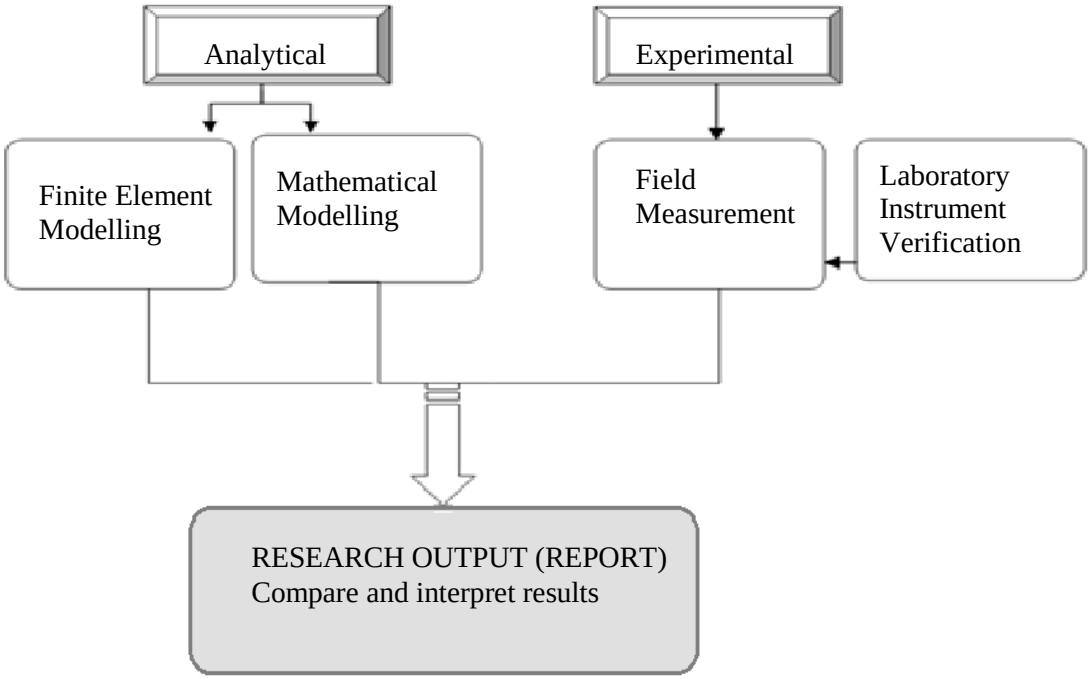

Figure 1.1: Schematic presentation of the research strategy

1.6 ORGANIZATION OF THE REPORT

This dissertation is structured as follows:

Chapter 1:

This chapter consists of the general introduction and background related to the study followed by research problem statement. The scope of the study including limitation of the research and assumptions taken during the research is also briefly described. A short description of the research methodology is also included.

Chapter 2:

In this chapter a literature review is presented from which the research methodology explained in chapter 1 is selected. Existing knowledge on different methodologies for dynamic analysis and determining dynamic responses are introduced based on different research works. The methodologies introduced are mathematical approach for time history analysis, using FEM to extract modal frequencies and field measurement for comparison of the real life conditions and theoretical approach. Different factors that may alter the dynamic response significantly are discussed. The mathematical approaches incudes the theoretical background and principles used to derive equation of motion of the system subjected to single and successive moving loads of train. Some of the excluded item which is beyond the scope of this research is introduced in short. Discussion on FEM consists of different kinds of modelling methodologies and their effect on the results. The field measurement part discusses how measuring instrument is calibrated, how to locate sensor on site, type of sensor that can be used, how to section measuring field in phase or how to measure step by step, duration of measurement, possible data acquisition systems, method of extracting result from field measurement, different limiting values presented by different references are also included. Other important parameters which is not the main part of the research such as effect of damping, track irregularity and roughness, rail discontinuity, resonance, importance and application of dynamic factors and effect of skewness of the bridge are introduced. This chapter is therefore the basis for the following chapters.

Chapter 3:

It describes the field observation undertaken on the actual steel truss railway bridge during the study. Brief description on the type of instrument utilized, where and how it is set on the field, the parameters measured, method of gathering and analysis of the data. Finally results are plotted and discussed.

Chapter 4:

This contains a description different FEM models that are assumed to represent the real life condition of the bridge described in chapter 3. The FEM package is also briefly described. Different methods of modelling techniques are also shown in different model presented that included FEM using beam and shell elements. The effect of modelling the bridge at different depth of detailing on modal analysis result is discussed.

Chapter 5:

Here all the theoretical background used for mathematical approach is included. An approximate method of finding the dynamic responses of structure is presented. Equations of motion for the bridge subjected to single load and train loads is developed and discussed.

Chapter 6:

A brief explanation on how equations developed in chapter 5 is utilized is included here.The result is plotted and discussed here.

Chapter 7:

This chapter includes discussion and comparison of result obtained using the three methodologies applied which are discussed from Chapters 3 to 6. Some additional calculations such as calculation of impact factor and natural frequencies using empirical formula are included based on formula obtained from literature review. Finally a conclusion is made based on the comparison.

Chapter 8:

This is the last chapter of dissertation which includes the general conclusion of the research. Here the summary of methodologies, different bridge responses obtained, comparision of results with limits set by existing references and effect of train speed on the bridge responses are discussed. Finally a recommendation and possible future advancement on the area of research is also suggested at the end of the chapter.

Appendix:

The appendix includes the list of calculation and derivations (by author), demonstration of application of equations, typical field measurement data, supporting documents, snap shots and finite element modeling outputs.

2 LITERATURE REVIEW

2.1 INTRODUCTION

Structures such as buildings, roads, bridges or dams respond when subjected to dynamic loads. In this research, a systematic approach was implemented to study the response of a simply supported single span railway bridge in the vertical direction. The method that was suggested and applied for the dynamic analysis of such a bridge when subjected to a train loads is to first analyse the situation mathematically or numerically using time history analysis; to perform the modal analysis using FEM software package and finally to conduct field measurement under controlled traffic and normal traffic conditions on a steel truss railway bridge located at Irene, Centurion. Detailed discussions of these methodologies are included in Chapters 3 to 7 of this dissertation.

The mathematical approach followed for dynamic analysis includes developing the right equation of motion. This can be referred to in Chapter 5. The equations that were used for this study purpose were specifically chosen for the type of bridge examined in the study, while an advanced methodology can be applied, depending on the extent of response required. One method of approaching the scenario involved simplifying the simply supported single span system having Multiple Degrees of Freedom (MDOF) to a generalized Single Degree of Freedom (SDOF) of the whole system as discussed in Chopra (2007) and Yang *et al* (2004) in order to obtain an approximate closed form solution. In this instance, the train loads was assumed to be represented as moving loads. A second, more detailed approach which can render a relatively more accurate response involves obtaining the response by considering vehicle-bridge interaction independently.

To consider the interaction between two components, a separate equation for the vehicle and components of bridges must be written. This is done by initially dividing the bridge in the few numbers of units having finite Degree of Freedom (DOF) and by representing the system as layers of springs as shown in Section 2.3.1 in a similar way as presented by Kargarnovin *et al* (2005). This helps to formulate a closed form of solution in a matrix form. The latter approach is used mainly when sensitive case analysis is a key concern of the study. Some of the sensitive analyses includes determining the riding comfort, rail irregularity, vehicle response or similar natures of work which exceed the scope of this research report and as such has been omitted. One may refer the work of Yang *et al* (2004) for more detailed information on this approach for a two- and three dimensional systems.

Modal analysis using FEM software packages is utilised to extract the natural frequency and mode shape of the structure. Modal analysis can be performed using various FEM packages such as ABAQUS (Kaliyaperumal *et al*, 2008; Madshus and Kaynia, 2000) and OaSYS GSA (to the best of the author's knowledge, this package was used for the first time in this specific kind of research). The results from various research works are presented in this chapter for the purpose of comparison. Possible methodologies and the instrumentation for conducting field measurement are compared with the methodology applied in this research work as described in Chapter 3.

Different limiting values set by different references for different dynamic responses such as vertical and lateral acceleration and frequency as reported by Kargarnovin *et al* (2005), Goicolea and Gabaldon (2008) and Xia *et al (*2005) are presented here for the purpose of comparison. Michaltsos *et al* (2010) introduced various research works that have been published since 1905, including where the works vary from simple beam to bridge dynamic response. Information on their respective complete solution shows the extent of study that has previously been undertaken.

A few important related concepts are also included in this paragraph and also summarized in Chapter 7 which however are only briefly reviewed in this research. These include the effect of the skewness of the bridge (Ashebo *et al*, 2007); the riding comfort of high-speed trains travelling over railway bridges (Kargarnovin *et al*, 2005); the track irregularity and roughness; rail discontinuity; the influence of train critical speed (Michaltsos *et al*, 2010); the ballast stiffness and damping from the structure or from the train suspension system. Dynamic factors such as derail factors; offload factors; wheel/rail forces and coach-body acceleration which are considered as running safety and stability parameters – may be referred from work of Xia *et al* (2005).

2.2 MATHEMATICAL APPROACH

The Mathematical approach for the dynamic analysis of structures subjected to any external forces such as vehicles, trains, wind or earthquakes usually involves developing an equation of motion that expresses the entire force-structure system. The depth of the approach used differs, depending on the extent of the accuracy and detailed nature of the results required.

There are a few mathematical approaches that can be applied for studying dynamic responses. The first approach is studying the dynamic response of the structure directly from a simple generalized equation of motion developed where the axle load of the train is treated as an external force. This approach is used in the time history analysis discussed further in Chapter 5. The second approach is studying the interaction between the vehicle (train) and the bridge which includes modelling them separately, followed by finding a relationship between them. This may involve noting all the determining parameters such as mass, stiffness and damping constant of the system in a matrix form to find a closed form of solution.

Unlike the first approach, the later approach requires a computer analysis depending on the size of the matrices which is formulated to account for each unit the structure is divided into for the purpose of analysis. Both methods may share few common functions to express force function such as the external applied force or the force in between the bodies. The common expression or function that is applied by both approaches is the Dirac delta function, which is briefly defined in Chapter 5.

Kargarnovin *et al* (2005) utilized this function to define the forces between bogies and wheel sets and wheel-rail contact forces from all wheel sets. Chopra (2007) and Yang *et al* (2004) used it to define a single moving load passing across a bridge. The latter one has been further advanced and is used to define successive wheel loads on two and three dimensional mathematical approach of the vehicle and bridge interaction system. Michaltsos *et al* (2010) also used the Dirac delta function with a Heaviside's unit-step one to develop equation of motion of a train moving at a constant velocity on a single span bridge. For the purpose of this research, two methods were used to account for successive moving loads from the train. The first method uses Heaviside's unit-step as described by Yang *et al* (2004) and the second method sums up the effect of each single axle load entering the bridge at different time as further described in Chapter 5. As Michaltsos *et al* (2010) explains, it may not be possible to find accurate closed-form solution from equation developed for a bridge subjected to successive loads, therefore one should expect an approximate solution based on previous research works.

Some of the responses such as frequency may also be obtained from empirical expression developed through statistical evaluation and regression analysis of large number of field measurements (Kaliyaperumal *et al*, 2008) as presented in Section 2.3. The magnitude of the frequency is extracted from field measured data by changing the time-domain data to

frequency domain data by using Fourier transform, commonly used by previous research works such as proposed by Kargarnovin *et al* (2005).

2.2.1 Dynamic response from generalized equation of motion

The simplified equation of a system subjected to moving loads is derived based on the assumption that the system is generalized and simplified. As a result, the interaction between the bridge and vehicle will be ignored. As mentioned by Yang *et al* (2004), generalizing a system is only sufficient to determine the response of the bridge. Generally when the mass ratio of the vehicle to bridge is large, the bridge sub-system or vehicle's response is influenced easily by the vehicle-bridge interaction. However this research is limited to simulation of the movement of the bridge from a generalized system of bridge as referred to in Chapter 5.

2.2.2 Dynamic response from equation of motion of finite bridge units and vehicle

One of the typical assumptions made while studying the interaction between rail and bridge is assuming the rail and bridge components as layers of parallel springs. A typical presentation of a spring model where the rail and bridge components are assumed as layers of parallel springs is presented in Figure 2.1. Kargarnovin *et al* (2005) provides a complete detailed discussion of the concept or refer to the equations developed. Below only the introduction is presented.

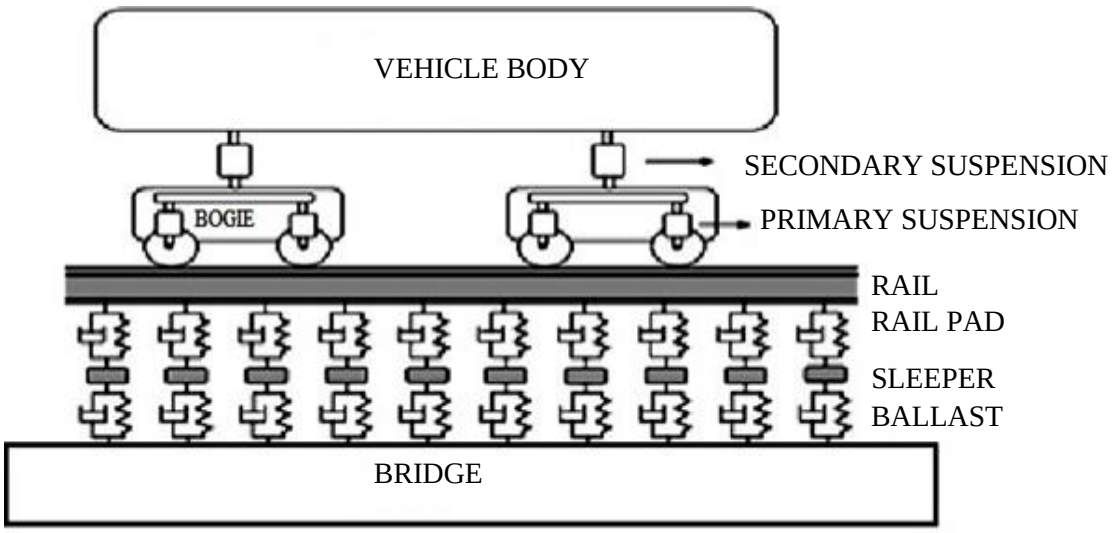

Figure 2.1: Vehicle, track and bridge model (taken from Kargarnovin *et al*, 2005)

A similar model is presented by Liu *et al* (2009). The track of a railway bridge is a part of a structure consisting of the rails, pads, sleepers, ballast and the underlying sub grade for a railroad. However, for the purpose of this research the whole definition of track may change as the bridge is made of only steel structures with no ballast and the rail is directly supported on the wooden sleepers that are riveted to stringers. Therefore the track does not consist of the ballast and subgrade material. According to Kargarnovin *et al* (2005), the track is modelled as a beam supported on two foundation layers representing the rail pad and ballast. The sleepers are represented as a continuous layer of mass and bridge which is modelled as beam and each coach considered with single degree of freedom considering the vertical motion of the vehicle. A similar approach is also presented by Goicolea and Gabaldon (2008) and Yang *et al* (2004).

The first step in analysing vehicle (train), track and bridge interaction is writing equations of motion of the train, track and bridge separately with their own parameters. The bridge parameters such as mass, stiffness and damping constant of the system is then written in a matrix form which will serve as an input to the equation of motion.

The vehicle equation considers the property of the coach body and wheel sets, including the primary and secondary suspension system shown in Figure 2.1. For instance, in order to determine the vertical displacement, an independent equation is written for vertical motion of the coach body, rear and front bogie and the rear and front wheel set as explained in Kargarnovin *et al* (2005). Only the vertical motion of the vehicle was considered in their derived equation. Each applied force to the system must be defined with a function.

Further important steps in this approach are writing track and bridge equation of motion which considers the property of rail and sleeper. Young's modulus, the shear modulus, density, stiffness and viscous damping of the pad, sleeper and ballast are important parameters included in both track and bridge equation of motion. According to the work of Kargarnovin *et al* (2005), three kinds of forces were used to write the track equation of motion. These are wheel-rail contact force; the rail-pad contact force and bridge-ballast contact force. The bridge-ballast contact force is the force that is also used in the bridge equation of motion. Since the number of degree of freedom is infinite, one must consider a limited number of bridge units that will sum up to form the entire bridge in order to find a closed form solution.

2.2.3 Dynamic factors

Dynamic factors such as the amplication factor (impact factor) mentioned in Goicolea and Gabaldon (2008) is one of the simplifying methodologies used in different references to compensate for the dynamic effect of a moving train on structures like bridges. Hamidi and Danshjoo (2010) also suggested the same factor to account for the dynamic effects of vehicle loads which is required to increase the static load generated from traffic load. In their work, Hamidi and Danshjoo (2010) suggest a method of calculating of impact factor based on static and dynamic deflection. According to their report, the impact factor obtained from deflection is higher than that obtained from other responses such as stress. One of the important preliminary concepts that one should keep in mind is that the dynamic response is higher than the static response of a structure.

Kassimali (2012) explained why a dynamic load should create a higher magnitude of response than static responses more specifically on stress response. This can be explained in terms of impact load as follows: When a load is applied rapidly to a structure, it causes larger stresses than those that would be produced if the same loads would have been applied gradually. The dynamic effect of the load that causes this increase in stress in the structure is referred to as impact. One example that can be cited for this is a work reported by Xia *et al* (2005). In this report, it is shown that dynamic deflection of the girder of the double-track pre-stressed concrete bridge subjected to a China-star train with a speed of 260km/h is higher than static deflection which is 0.87 mm and 0.718 mm respectively, which gives the maximum impact factor of 0.211. The formula for determining the impact factor is presented as below (Hamidi and Danshjoo, 2010).

$$I = \frac{D_{dyn} - D_{st}}{D_{st}} \qquad \text{Equation 2-1}$$

Where:

I = Impact factor

D_{dyn} = Dynamic deflection

D_{st} = Static deflection

This formula is used in Chapter 7 to determine the impact factor of a truss railway bridge based on static deflection obtained from FEM result and dynamic deflection obtained from mathematical and field measurement result. Rodrigues (2002) also proposed that dynamic amplification factors can be obtained by dividing the dynamic response by the static, such as measured maximum dynamic strain and maximum static strain.

Dynamic factors such as the impact factor are specified with different references. Table 2.1 below shows a comparison between these factors.

Table 2-1: Impact factors from different references and literatures

For	Formula	Code	Reference
All bridges L in m	$I = \frac{15.2}{L + 38.1} < 30\%$	AASHTO Manual	Hamidi and Danshjoo (2010), Yang *et al* (2004)
Steel railway bridges	$I = \begin{cases} 40 - \frac{3L^2}{148.6} \cdots L \le 24 \\ 16 + \frac{182.9}{L - 9.1} \cdots L \ge 24 \end{cases}$.	AREMA	Hamidi and Danshjoo (2010)
Steel railway bridges Where: f = natural frequency of bridge	$I = \begin{cases} 0.2 \cdots\cdots f < 1Hz \\ 0.2 < I < 0.4 \cdots\cdots 1 < f < 2.5Hz \\ 0.4 \cdots\cdots 2.5 < f < 4.5Hz \\ 0.4 > I > 0.25 \cdots\cdots 4.5 < f < 6Hz \\ 0.25 \cdots\cdots f > 6Hz \end{cases}$	OHBD (Canada)	Hamidi and Danshjoo (2010)

As indicated in Table 2.1, the impact factor is mainly a function of the span of the bridge as per American Association of State Highway and Transportation Officials (AASHTO) and American Railway Engineering and Maintenance-of-Way Association (AREMA). However other references such as Ontario Highway Bridge Design (OHBD) express the impact factor in terms of first natural frequency. In this research, the impact factor is calculated from mid-span deflection and result is compared with AASHTO, AREMA in Table 2.1 and also represented graphically in Figure 2.2.

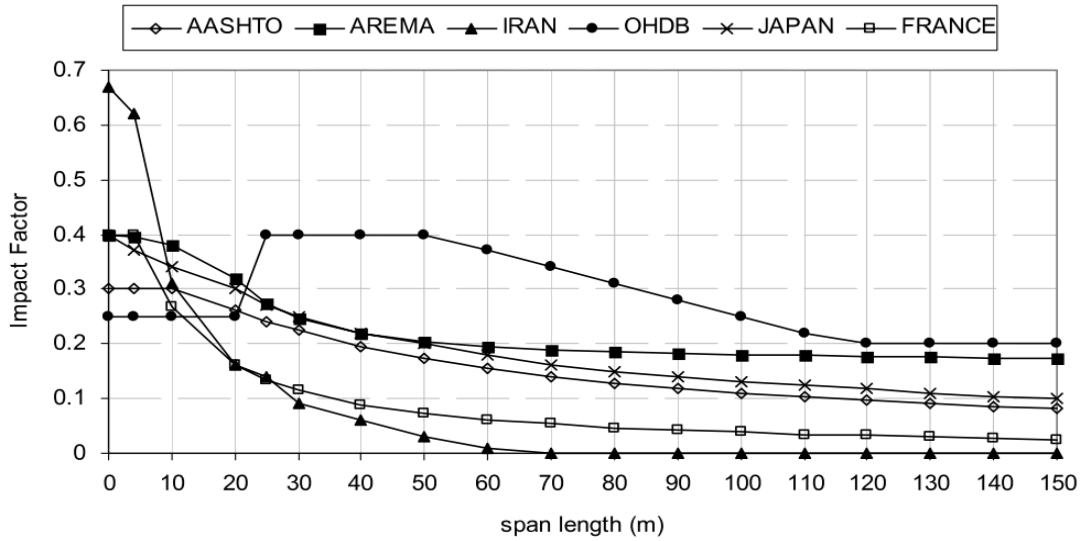

Figure 2.2: Impact factor based on various references (figure taken from Hamidi and Danshjoo, 2010)

2.2.4 Resonance and cancellation effect

Resonance and cancellation is one important dynamic effect one should consider during dynamic analysis. However, this research only briefly discusses this concept. There are certain train speeds that create a frequency much closer to the natural frequency. These are the kind of speeds that create resonance effect on the structure. A much larger response may be expected for short span bridges. A good explanation given for this by Goicolea and Gabaldon (2008) is that for bridges longer than the coach length, several axles will be on the bridge with different phases, thus cancelling the effects and impeding a clear resonance. According to Michaltsos *et al* (2010), a resonance type called impact load resonance is created when the train speed coincides with critical speed where there is rail discontinuity. In their work they also mention that a five times increase of response may be expected during resonance in the presence of the rail discontinuity.

In Chapter 6, observations on the different calculated train critical speeds that are expected to cause resonance on the selected steel truss railway bridge is presented. Michaltsos *et al* (2010) presented a formula for calculating critical speeds as follows:

$$V_{cr} = \frac{\omega_1 e}{2\pi}$$ Equation 2-2

Where:
ω_1 = Frequency of the first vertical mode of vibration of the bridge in rad/s
e = Axle spacing

This formula assumes that all wheel loads arrive on the structure at equal axle spacing. Another form of checking resonance speed is presented by Yang *et al* (2004). In order to identify the relationship between exciting frequency of the moving train and the fundamental frequency of the bridge, they defined a dimensionless parameter called speed parameter. Speed parameter is defined as the ratio of exciting frequency of the moving vehilce or train to the fundamental frequency of the beam or bridge. This is described as :

$$S = \frac{\pi V}{\omega L} \qquad \text{Equation 2-3}$$

Where:

ω = Fundamental frequency of the bridge in rad/s

V = Speed of the train

L = Span length of the bridge

According to this, a condition of resonance was formulated based on the term that maximizes the response from the equation of motion developed, which is similar to the displacement equation developed in this research in Chapter 5. This resonance conditions implies putting $\sin(\omega_1 d/2V) = 0$ in the equation of motion diminishes a denominator in their equation which indirectly maximises the response. This conditon is zero when $\omega_1 d/2V = i\pi$ where $i = 1,2,3,\ldots$Based on this condition, a critical length of train and speed parameter is calculated as follows

$$d = \frac{2i\pi V}{\omega_1} = 2iSL \qquad \text{Equation 2-4}$$

The above equation therefore gives a speed parameter formula which is dependent on the coach length and span length of the bridge as described with the formula below. Coach length,d, can be reviewed in Figure 5.2.

$$S = \frac{d}{2iL}, \qquad i = 1,2,3,\ldots$$

Where:

d = Coach length

L = Span length of the bridge

The speed parameters calculated are therefore 0.5d/L, 0.25d/L, 0.167d/L,0.125d/L… The speed that creates resonance based on this condition is classified to primary resonant speed and secondary resonant speed. Only the 0.5d/L creates primary resonant speed leaving the rest of secondary speeds reducing and diminishing at the end. The formula for determining primary resonance speed is similar to the critical speed formula developed by Michaltsos *et al* (2010), except that the latter uses axle spacing and that of Yang *et al* (2004) uses the coach length in their formula. These speeds are also discussed in Chapter 6.

The effect of cancellation might also occur when all the excitation effect from preceding wheel loads that have passed the bridge sum to zero resulting in no residual response. This occurs when a condition below is met as explained by Yang *et al* (2004).

$$\cos\frac{\omega_1 L}{2V} = 0$$

Where:

ω_1 = Frequency of the first vertical mode of vibration [rad/s]

L = Span length of the bridge

V = Speed of the train.

This condition essentially cancels out part of equation of motion when $t \geq L/V$. Please refer equation of motion in Chapter 5.

2.2.5 Fatigue

Fatigue is one of the major concerns that should be studied in depth as it may affect the long term structural integrity of a structure to the extent of its failure. The repetitive static and dynamic loading that is happening during the service life of structure may result into fatigue failure. As explained by Kassimali (2012) and Xia *et al* (2005), when a live load is rapidly applied to a structure, larger stresses are caused than those that would be produced if the same loads would have applied gradually. Therefore when more repetitive dynamic loading occurs in a structure, more repetitive increase in stress will be created which will result in fatigue. Due to the vast and complex nature of the subject, a detailed examination of this area was not included in the scope of this research project.

2.3 FINITE ELEMENT MODELLING (FEM)

The importance of Finite Element Modelling (FEM) for such a kind of exercise is to perform the common types of dynamic analysis namely modal analysis. From this modal analysis output, the natural properties of a structure such as its natural frequencies and mode shapes can be obtained. This has been exhaustively noted in the work done by Liu *et al* (2009), Ashebo *et al* (2007) and Kaliyaperumal *et al* (2008).

Some of the following points should be decided prior to each FEM in order to be able to model a closer representation of the real life situation:

a. Boundary Conditions
b. Meshing method
c. Addition of secondary elements
d. Connections
e. Modelling techniques

2.3.1 Boundary Conditions

Different types of models can be used to model the boundary condition of a structure, or in other words the support type. This is one of the conditions that should be taken into consideration during FEM. Different support modelling systems can be applied as shown in different research works. Bridge support can be modelled as simple pin-pin support; pin-roller support or bearing as shown in Figure 2.3, or as a spring model as shown below in Figure 2.4. It can also be simplified as that of the work done by Kaliyaperumal *et al* (2008) either as a simple or fixed support. The FEM in this research work also applies a simple pin-pin support for FEM using beam element as well as an approximate model similar to the actual support for all FEM using shell elements. A more detailed analysis is presented in Chapter 4. Nonetheless, one should be careful when performing static analysis such as checking stress at support or members nearby. This depth of detailing may be required during the initial design stage of the structure while selecting sections size or during structural analysis for structural rehabilitation or damage diagnosis.

If one is interested in using bearing as a support types, one can refer the work of Ashebo *et al* (2007) as classified as below. In their work they used three types of support to identify the possible degree of freedom of the support.

a. Fixed Bearing (no arrow implying no movement)
b. Four guided Bearing (two arrows in opposite directions)

c. Free Bearing (four arrows in four directions)

Each kind of bearing defines the type of restraints which are released to allow translational movement in the arrow direction. The guided support is similar to roller support which is free to move in one direction, such as parallel to traffic direction as shown in Figure 2.3. The fixed support is similar to pin support with no translation.

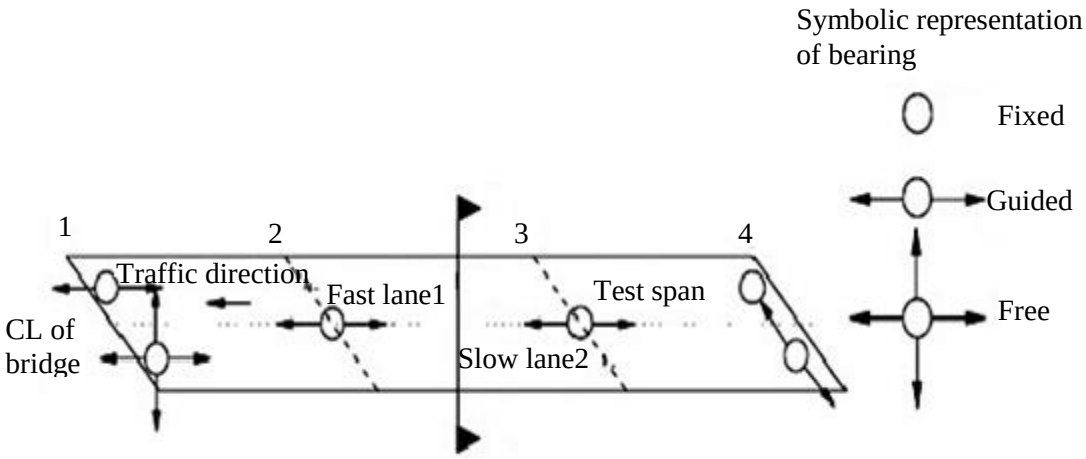

Figure 2.3: Symbolic representation of bearing type support (Ashebo *et al*, 2007)

Caglayan *et al* (2011) presented different approaches for modelling support and connections between elements in the model as shown in Figure 2.4. The connection between elements such as stringers and cross beam is simulated as rotary springs allowing flexibility to structure. Such depth of detailing were necessary since their work involved checking and verifying member sizes, checking load carrying capacity of members from stress response, lateral buckling load capacity of specific member such as compression flange of the main girders.

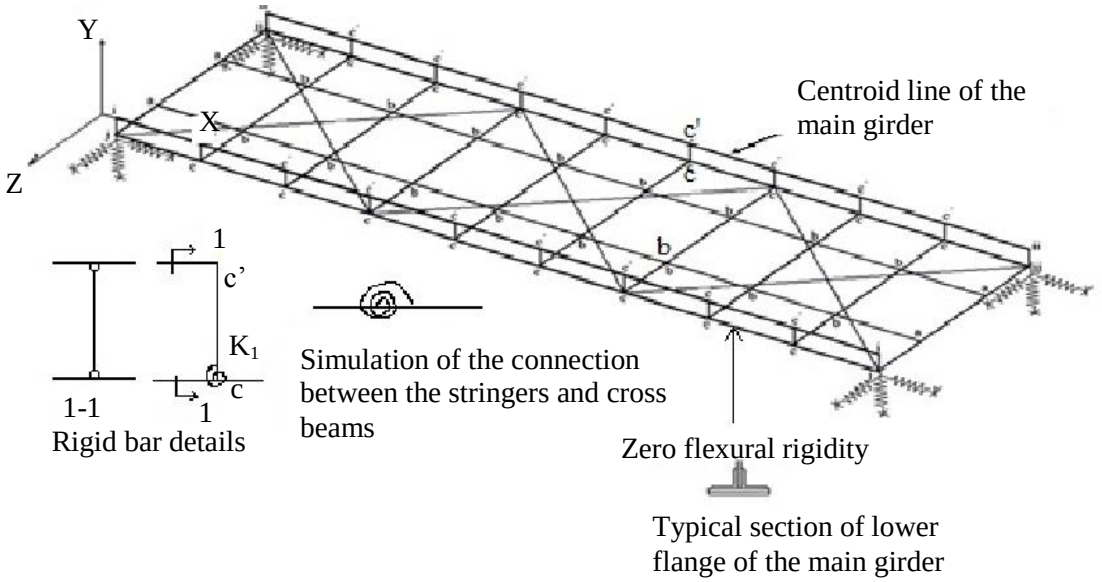

Figure 2.4: FEM of bridge with spring type support (Caglayan et al, 2011)

2.3.2 Meshing

Meshing of FEM should be done systematically to increase the visibility of results at the required location during analysing the FEM. However, different type of meshing can be used depending on the geometry of the structure. For instance the type of elements used by Kaliyaperumal *et al* (2008) for a continuous welded steel plate girder railway bridge is eight-noded, reduced integration shell element and three noded quadratic beam elements. In this research, only QUAD4 element of varying size is used for FEM with shell elements. The author understands the QUAD4 elements in GSA as the shell elements with four sides and four nodes.

2.3.3 Addition of a secondary element

The addition of a secondary element on FEM involves the inclusion of minor structural elements that are included in the structure to increase its stability or performance. Some of these elements which are considered in this research are: bracings, stiffener, rail or sleepers which alter the modal analysis result to a certain extent. This can be referred from the work of Kaliyaperumal *et al* (2008).

2.3.4 Connections

The connections between elements in the structure are also other parameters that may affect FEM result. Liu *et al* (2009) used a linear spring element to represent the headed shear

studs between the rail and sleeper. These elements can also be used to represent the connection between the concrete deck/slab and steel girder. Members can also be tied to each other assuming a rigid connection between them or their flexibility can be increased by using a spring connection between elements such as the works of Caglayan *et al* (2011).

2.3.5 Modelling types

FEM can be either modelled with all elements comprising of grillage, beam elements or shell elements. Kaliyaperumal *et al* (2008) proposed modelling as a combination of shell and beam model in one bridge by choosing one span of the bridge, where the result is required and modelling with the shell element. The shell element model is chosen over the beam element as it is the best way to capture the out-of-plane and torsional behaviour of main girders which leads to the development of fatigue cracks (Kaliyaperumal *et al*, 2008). Please refer Chapter 4 to observe the different types of elements used for FEM and how the results may vary.

2.4 FIELD MEASUREMENT

The field measurement is normally required to observe the extent of accuracy of the result obtained from mathematical approach and FEM for such type of an analysis. Taking the measurement usually requires an appropriate prior arrangement to get an effective and accurate result. In addition to this, the results obtained can be useful to study various structural characteristics of the bridge. This can be listed as follows (Ashebo *et al*, 2007):

a. Modal analysis
b. Seismic analysis and
c. Structural health monitoring

2.4.1 Identifying procedures for measurement

Some of the most important procedures that should be exercised before and during measurement are:

a. The calibration of the measuring instrument and loading parameters
b. Identifying the type of sensor required
c. Choosing the appropriate instrument setup location
d. Identifying the data required from the measurement
e. Identifying the type of loading
f. Estimate duration of measurement

g. Plan the data acquisition methodology
h. Choose the data analysis methodology

Calibration of the measuring instrument and loading is essential prior to field measurement for correct interpretation of results during field data analysis. Usually the calibration of the instrument is done by the manufacturing company. However, verification of pre-calibrated instrument may be done in the laboratory.

Calibration of the measuring instrument is performed to check the performance and accurateness of the instrument. For instance, the pre-calibrated USB accelerometer which was used in this research was tested in a laboratory with an industrial accelerometer fixed to a rotary machine with a known frequency. The detail test result can be referred to in Chapter 3. Additionally, pre-calibrated WA50 displacement transducers provided by the university laboratory were used.

Loading may represent the applied force, i.e. train or vehicle expressed as axle load for the dynamic analysis purpose of this study. Please refer to Chapter 6 for the magnitude of axle loads calculated based on the capacity and gross mass of the train. Calibrating the loading may involve the direct measurement of the loading parameters and comparing it with known parameters. The parameters involved for train loading for instance are: gross mass, distance between the left and right wheels, axle load and axle spacing. The axle load for instance, can be measured using the axle sensor explained in the section below. A measuring tape can be used to measure the axle spacing. Work by Ashebo *et al* (2007) can be referenced to understand how this axle load is calibrated. In this research, the loading parameters were taken directly from the train configuration manual provided by PRASA as explained in Chapter 3.

The type of sensor that can be used for field measurement depends on the type of response required. Some of the common instruments used for dynamic analysis are:

a. Accelerometer
b. Displacement transducer
c. Strain gauges
d. Axle sensor

The accelerometer measures acceleration of structure when subjected to dynamic force. This has been used by Liu *et al* (2009), Ashebo *et al* (2007), Kaliyaperumal *et al* (2008),

Rodrigues (2002), and Xia *et al* (2005). There are different types of acceleration sensors. Some only measure acceleration in one direction such as the Kinemetrics Uniaxial Episensor (ES-U) accelerometers with power supply condition units used by Rodrigues (2002). Other accelerometers can measure acceleration in more than one direction such as the USB X16-1C accelerometer used in this study.

The result obtained from the accelerometer is used for determining:

a. Natural frequency
b. Mode shapes (only briefly discussed in the scope of this research)
c. Damping constants of bridge (not considered in the scope of this research)

The acceleration data collected may require further processing. Depending on the type of data collected, one may need to filter the data to remove unnecessary noise that may impede the dominant frequency from being observed clearly in the power spectral density plot. For instance, Low pass filtering technique is used by Liu *et al* (2009) for 30Hz. This is briefly discussed in Chapter 3.

Pre-processing measured data may involve trend removal, high-pass and low-pass filtering using Butterworth filter or similar filter, decimation of signals from sampling frequency such as 200Hz to the required frequency limit 50Hz as exercised by Rodrigues (2002). The frequency resolution can be calculated by dividing the sampling frequency to number of sample taken. This filtering exercise is also done by Xia *et al* (2005) at 40Hz low pass filtering. Different types of filtering can be used before the auto spectra or power spectra are plotted, such as Hanning window (Rodrigues, 2002). The data can be averaged and normalized before the power spectral density is plotted (Rodrigues, 2002).

The LVDT stands for linear variable differential transformers. In this study it is used to measure the displacement of the bridge as explained in Chapter 3. Successful results using LVDT were observed from the work of Liu *et al* (2009). However the term displacement transducer is preferred to be used in the rest of this report.

The strain is measured with different types of strain gauges. Strain gauges have been used by different research works such as Liu *et al* (2009), Ashebo *et al* (2007), Kaliyaperumal *et al* (2008), Rodrigues (2002). For instance, four 740A02 pezoelectric ICP strain sensors from PCB is used by Rodrigues (2002). According to Asheboro *et al (*2007), the results obtained from the strain gauge is also used for moving force identification or evaluation of

dynamic load factors. These factors are not included in the scope of this study and will not be discussed further.

In this study all procedures that may require any sort of destruction on the existing structure including removal of paint were avoided. Therefore, strain gauges were not used in this research since the available type of sensor requires removal of paint of the bridge steel structure to get accurate readings. If a fibre optic sensor is available, it could be used to measure the strain gauges without having any contact to the structure, as suggested by Liu *et al* (2009) to measure the strains in the longitudinal directions.

The axle sensor can be used for the following purpose as described by Ashebo *et al* (2007), to:

a. Trigger the data acquisition system
b. Locate the position of the axle on the top of the bridge
c. Measure the speed of in-service vehicles.

Besides the unavailability of the sensor during this research, the way the USB accelerometer works which is discussed in Chapter 3 does not allow synchronizing of the sensor data and the data is acquired automatically. Therefore it was imperative to take the necessary data as mentioned above manually. Please refer to Chapter 3 for a more detailed discussion.

Choosing instrument set up location

For a single span bridge such as the one analysed in this research, taking acceleration readings at different parts and various locations on the structure is believed to provide an understanding of the dynamic response at different parts of the structure. While dealing with a continuous span, it may be necessary to understand the dynamic coupling between neighbouring spans (Liu *et al*, 2009). In such cases, the instrument set up must be done at different points or different spans of the bridge. Setting up the measuring instrument involves choosing an appropriate method of fixing the instruments; proper configuration of instruments as discussed in Chapter 3 and choosing the right measurement location on the structure.

Sectioning or phasing may be necessary when dealing with multi-span bridges such as that of a seven span bridge studied by Liu *et al* (2009). By phasing is meant taking a small portion of the bridge only for analysis purposes. This exercise is not done in this research as

the bridge selected is only a single span bridge, which makes it easier to complete the field measurement at once. The most common location of fixing the instrument such as an accelerometer is on the main structure such as the girder (Xia *et al*, 2005).

Method of fixing

Gluing is the most common method of fixing accelerometer which is used by different research works. The type of glue used is however are not specified by many research works. Refer for instance the work of Ashebo *et al* (2007). It is important to check the accuracy of different possible fixing methods before using them. In this study, bee wax, super glue, double sided tape and screws were tested and compared in the laboratory to check the accuracy of the result obtained using each fixing methods. The lab result is discussed in Chapter 3. For the purpose of this research, due to the ease of use, relative accurateness and low cost of installation, double sided tape was preferred.

Strain is not measured in this research. However, glue can also be recommended as a common fixing mechanism for strain gages. For instance, glue is used by Xia *et al* (2005). A displacement transducer can be fixed using a clamp fixed to a stationary structure. In this study, the adjacent bridge was used as a relatively stationary reference point to fix the accelerometers using self-designed mounting section as explained in Chapter 3.

Configuration

The sampling rate or frequency is one important configuration that needs to be set up prior to taking the measurements. First, an initial estimate of the actual frequency of the structure should be obtained either from the FEM result, previous knowledge or based on the results reported on previous research works. Then, based on the estimate, a sample rate required for measurement is selected. The higher the sample rates the higher the accuracy of the reading is. This is further explained in Chapter 7. The sample rate selected determines the maximum frequency that can be measured using the instrument. Usually, one may take at least to 2-10 times the required frequency. This may not give a frequency above half of the sample rate. For instance, Rodrigues (2002) has used 200Hz sampling frequency for vibration measurements on a truss railway bridge subjected to active tilting train. Xia *et al* (2005) has recorded a data at 5000Hz sampling frequency while 64 trains crossing the bridge. In this study, 400Hz and 1200Hz sample rates were selected for accelerometer and displacement transducer respectively. The sample rate used for the accelerometer was lower than that of used for the displacement transducer. This was solely due to the maximum

sample rate limit that can be taken by the specific USB accelerometer was 400Hz. This is briefly discussed in Chapter 3.

Identify the data required from measurement

The data that is measured can be classified as free and forced vibration data and is explained below:

a. Free vibration data

This is a portion of data that shows a response immediately after the train leaves the bridge (Liu *et al*, 2009). This data can be used to extract the natural frequency of the bridge. Xia *et al* (2005) also extracted frequencies and damping ratios from this free vibration data. Extracting the required data from the measured data is one of the challenging tasks during data analysis. According to Caglayan *et al* (2011), raw acceleration data measured is not good enough to provide the dynamic characteristics of the bridge, which therefore requires pre-processing prior to identification of the responses. This is explained further in Chapter 3. This may involve the removal of the mean, existing trends, noise contaminations and outliers, filtering, decimation and synchronisation of the collected data.

b. Forced vibration data

This is a portion of data that shows a response while the train is still crossing the bridge. This can be referred from the work of Liu *et al* (2009) and Ashebo *et al* (2007) where controlled traffic and normal traffic used to obtain the second and third modal frequency is obtained. Controlled traffic in this instance indicates a calibrated truck with known parameters such as weight and speed of the truck.

Identify type of loading

The train axle load can be represented as moving loads. Table 2.2 indicates an example of train configurations which are basically similar to the one that is used in this research. Please refer to Chapter 6 for a detailed comparison. The terms locomotive and passenger coach referred from previous research work as shown in Table 2.2 which is similar to motor and trailer coach respectively are presented in Table 6.4.

Table 2-2: Example of Train loads and configurations

Train type	Axle load[kN]		Length[m]		No. of coaches	Reference
	L	P	L	P		
Italian ETR500Y	176.4	112.9	19.7	26.1		Liu *et al* (2009)
China-star	195	142	21.29	25.50	9 coaches(22 bogies or 44 wheel sets)	Xia *et al* (2005)

N.B: In the above table, 'L' stands for locomotive and 'P' stands for passenger coach

Duration of measurement is one of the important points to be decided before field measurement as it will affect the amount of data collected. It is usually important to get the maximum amount data required to get more valuable result out of it. However one must make sure the amount of data is collected in a planned manner to avoid confusion during the data analysis stage. A good example of a well-planned data recording method can be referred to from the work of Ashebo *et al* (2007), during which the data was collected for five consecutive days. Xia *et al* (2005) has taken seven days' measurements. In this research, the measurement is done in two days where the measuring instrument is first properly calibrated in the lab to check its accuracy of measurement, as elaborated in Chapter 3.

The selection of the time of testing in a single day is also one of the most important things to consider in bridges subjected to extremely heavy traffic. Ashebo *et al* (2007) presented their approach as follows:

a. The first portion of data should be collected when the traffic flow is low in order to get data closer to the free vibration for first modal analysis.
b. The second and third modal test must be done preferably while in-service or normal traffic is experienced. This is beyond the scope of this study.

Data acquisition

Instruments such as displacement transducers used in this study need special software for data acquisition systems. One example of software that can aid with data acquisition is LabView 7.0 software from National Instrument used by Ashebo *et al* (2007) and Rodrigues (2002). The signal should pass through different modules and signal conditioner before reaching the computer, unlike the USB accelerometer which uses a direct acquisition of the data collected. However, the type of accelerometer used for this research records the data automatically, therefore no special data acquisition system is required.

Depending on the type of availability of measured data; either acceleration readings or strain reading, the natural frequency of the bridge can be read from different frequency range. For instance acceleration response is sensitive in relatively higher frequency range and strain responses are sensitive in lower frequency range (Ashebo *et al*, 2007). This is best represented by graphs illustrating this as follows:

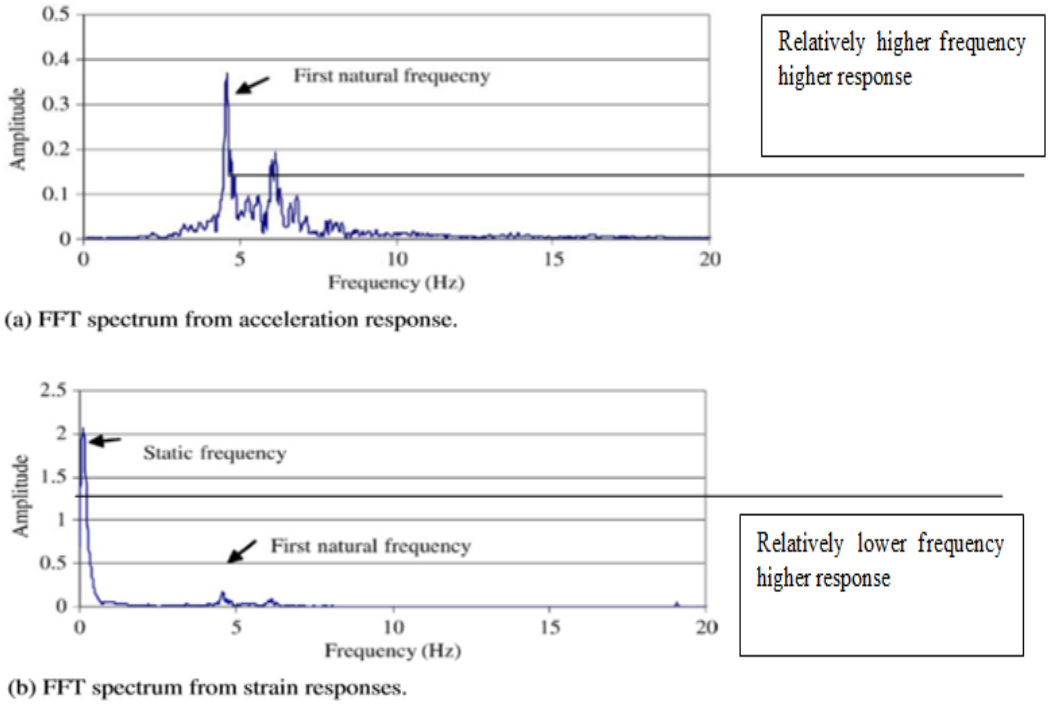

Figure 2.5: FFT spectrum from acceleration and strain responses (Ashebo *et al,* 2007)

Data analysis

In this section, the different practices for extracting dynamic response from FEM and field measurement data, namely mainly the modal analysis result are discussed. The modal analysis consists of identification of modal shapes and frequencies of the structure. To identify the data analysis methodology, it is important to decide which data is required. The data required may be modal frequency of either vertical, lateral or torsional modes or the respective mode shapes. Different methodologies were utilized by different research works. For instance, Liu *et al* (2009) used a stochastic subspace identification (SSI) method for identifying modal responses directly from the free and forced vibration field measured data as mentioned in the previous section. Kargarnovin *et al* (2005) used Galerkin's method, which is a time stepping method used in the time domain analysis after modal analysis is computed. The SSI method and Galerkin's method fall outside the scope of this study and will not be discussed further. Identification of modal shapes from field measured data is

also not included in this research, but rather the identification is made using the FEM package which is further discussed in Chapter 4.

Data analysis to determine higher mode responses such as vertical, lateral or torsional mode response may involve choosing the right data from the raw measurement data. All modes may not be identified at the same time from all kinds of data (Liu *et al*, 2009). One may expect to see the first and second vertical bending modes from the free and forced vibration. However, one may not observe torsional modes from the forced vibration. The results obtained by Liu *et al* (2009) shows the free vibration may at least indicate the first torsional vibration mode, in addition to the first and second vertical bending modes. Frequency domain method applied to vibration test data and Ibrahim time domain method applied to free decay responses measured immediately after the train crossed the bridge are the methodology used for modal identification by Rodrigues (2002). In this study, only the first mode of vibration was analysed as it is the only mode experienced by the bridge while the train crosses the bridge once, as shown from the results presented in Chapter 3.

2.4.2 Parameters

Some of the basic parameters that easily influence the magnitude of dynamic responses of the bridge are: span length of the bridge, stiffness of the bridge expressed in terms of flexural rigidity, mass per length of the bridge, natural frequency of the bridge, speed of train, axle load and support or boundary condition. The ground condition also affects the dynamic behaviour of railway lines which is beyond the scope of this study. However, one may refer the work of Madshus and Kaynia (2000) to observe a study that has been conducted for railway lines on soft ground.

The only parameter that one can manipulate during field measurement is the train speed as the remaining parameters are relatively constant for a specific type of train and bridge. The speed of the train has a tremendous amount of impact on the structure responses. This is briefly discussed from mathematical point of view in Chapters 8 and 9. Both magnitude and pattern of response may alter as speed changes.

2.5 LIMITING VALUES FOR DYNAMIC RESPONSES

In modern times, the dynamic responses are considered during design as recent references already put an allowance for vertical and lateral displacement and lateral and vertical acceleration which aids the structural designer. For a detailed analysis, one may need to go

through the methodology presented in this study and then compare with the available references.

Table 2.3 presents the maximum acceleration allowance by different references. For instance the field measurement result presented by Xia *et al* (2005) shows a typical vertical acceleration of girder increases as the train speed is increases. The maximum measured value for vertical acceleration was 1.90m/s^2 for speed of 307km/h, which is below the limit. For the same bridge a lateral acceleration of the girder was 1.40m/s^2 which is still within the limit. However, there are certain critical speeds that must be considered during design as discussed in Section 2.2 and Chapters 7 and 8 where there is a possibility of the response crossing this allowance.

Table 2-3: Maximum acceleration allowance for bridge and vehicles in m/s^2

Vertical acceleration	Lateral Acceleration	Responses of	Code	Reference
2.25	1.75	Locomotive & passenger coach	Safety and serviceability standards of bridges	Xia *et al* (2005)
3.5	1.5	Bridge response	Safety and serviceability standards of bridges	Xia *et al* (2005)

The vertical acceleration response of train itself is studied by Kargarnovin *et al* (2005) which is not measured in this study. A limit of 1m/s^2 to maximum acceleration of a train for various train speeds for different suspension systems of the train is also presented by Kargarnovin *et al* (2005). A train passing on a perfectly smooth track or travelling with lower speed (less than 125km/h) responds within the limit specified above. However, higher speeds may force the structure and the train to behave above the allowance. The work of Kargarnovin *et al* (2005) explains this. Figure 2.6 shows a comparison of maximum acceleration response of train travelling at different speeds and on different level of quality tracks. In this figure the limit set by Eurocode and SNCF are also indicated.

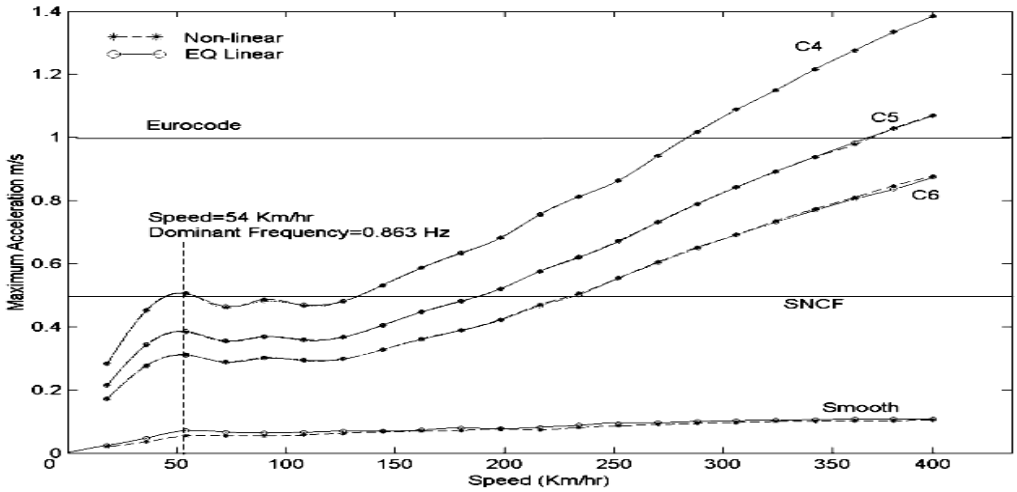

Figure 2.6: Maximum acceleration of train under various speed (Kargarnovin *et al*, 2005)

The different quality of tracks utilized to plot Figure 2.6 are smooth, C6, C5 and C4. These terms indicate the level of quality of track where smooth indicates the best quality and C4 is the relatively poorer quality of the track. Observation of results presented in Figure 2.6 shows that for some relatively best quality tracks, one can expect the response to be within Eurocode limit ($1m/s^2$) up to 400km/h. For relatively poor quality track, both limits set by Eurocode and SNCF are easily bypassed at 275km/h and 140km/h respectively. However, when referring to a conservative limit as presented by the safety and serviceability standards of bridges presented in Table 2.3, the results observed by Kargarnovin *et al* (2005) may fall in the limit for all type of train on different type of tracks considered.

Similarly, the displacement response must be checked with the available references. The maximum deflection allowance for a bridge from safety and serviceability standards of bridges shows a limit of 1.6mm for vertical deflection of a girder and 0.92 and 0.30 mm for lateral deflection of a girder and pier respectively (taken from Xia *et al* 2005). For instance, Xia *et al* (2005) measured values of 0.87mm, 0.33mm and 0.19mm for the vertical deflection of bridge girder, lateral displacement of the bridge girder and lateral displacement of the pier respectively, which are below the limiting values given.

According to Bates (1991), the steel that is used for construction of bridges that are built 79 years ago has an ultimate tensile strength between 386MPa to 455MPa. The reader can check the maximum tensile stress obtained at the mid span of the bottom chord of the bridge with the specified ultimate strength of the steel. When the bridge is loaded with the train the bottom chord stays in tension and the maximum tensile stress is expected at mid

span. This ultimate tensile is the maximum stress that a material can withstand while being stretched or pulled before failing or breaking.

2.5.1 Previous Study Results

It would be difficult to directly compare dynamic responses of bridges obtained by different research works as the type of bridge or the train they are exposed to differ. This section will discuss the general sense of magnitude of the responses for different type of bridges.

Displacement

Responses for different kinds of bridges such as composite bridges or pre-stressed box girder bridge are presented in Table 2-4. The work of Michaltsos *et al* (2010) in Table 2-4 indicates that the influence of speed on magnitude of vertical deflection is inversely proportional to span length of the bridge and speed of the bridge. In other words, short span bridge responds less to higher speed than long span bridge. Another observation made in this work is that the magnitude of a response is maximized when the train speed is close to the corresponding critical speed in longer span but the opposite happens on shorter span bridges.

Table 2-4: Overview of dynamic displacement from previous research works

Description	Speed[km/h]	Maximum[mm]	Reference
Composite bridge	288	1,9	Liu *et al*(2009)
Pre-stressed box girder bridge			Xia *et al* (2005)
Vertical	260	0.87 or (1/27000L)	Xia *et al* (2005)
Lateral(of girder)	230	0.33 or (1/72000L)	Xia *et al* (2005)
Lateral(of pier top)	307	0.12	Xia *et al* (2005)
For any bridge type (Numerical Analysis)			Michaltsos *et al*(2010)
30m span	72-180	10-14	Michaltsos *et al*(2010)
70m span	72-180	15-20	Michaltsos *et al*(2010)

Acceleration

Xia *et al* (2005) measurement result shows that the magnitude of acceleration may vary depending on the sampling frequency and the applied filtering for pre-processing the measured data. A maximum acceleration of 1.9m/s^2 and 1.4m/s^2 is measured in their work. However, this result is specific to one project and cannot be generally applied to other studies.

Frequency

The results obtained by Rodrigues (2002) shows the comparison of field measurement with FEM and this comparison is successful for up to the fourth natural frequencies. Sometimes the natural frequency of the train, frequency of passing bogies and dominant frequency of the bridge coincide as explained by Kargarnovin *et al* (2005). This could result in resonance of the bridge. Rodrigues (2002) indicates that resonance occurs if the relationship between train speed and uniform axle spacing equals a natural frequency of the bridge. In other words a resonance occurs when the excitation frequency equals natural frequency where the excitation frequency is calculated by deviding the train speed with uniform axle spacing. This formula is also discussed in Sectoin 2.2.4. Other parameters affecting the natural frequency of the bridge, such as span length and mass for constant stiffness of the bridge, are discussed in this study in Chapter 6.

The excitation frequency (ω) is a function of span length of the bridge and the velocity of the travelling train. That is calculated as:

$$\omega = \frac{\pi}{t_d}$$ (Chopra, 2007) and (Yang *et al*, 2004)

Equation 2-5

Kaliyaperumal *et al* (2008) presented first natural frequency calculated using different empirical formulas from different references as shown in Table 2-5. In their report all the values obtained from their FEM using shell and beam elements on simple and fixed support bridge fall within the boundary of the calculated natural period as presented in Table 2-5.

Table 2-5: Empirical formula for first natural frequency (all quoted by Kaliyaperumal *et al*, 2008)

Type of bridges	**Empirical formula [Hz]**
Railway bridges of all types, materials and structural system (Fryba)	$133 * l^{-0.9}$
Steel plate girder bridge without ballast (Fryba)	$208 * l^{-1}$
Unloaded railway bridges of all types and materials UIC & BS EN 1991-2	
lower limit ($20 \le l \le 100m$)	$23.58 * l^{-0.592}$
upper limit ($4 \le l \le 100m$)	$94.76 * l^{-0.748}$

The mass of the train and train-bridge interaction may have a significant influence on the frequency response of the bridge. This can be inferred from the results obtained by Liu *et al* (2009). This is especially important when the mass of the train is much higher than the mass of bridge, as the interaction between the train and bridge becomes more evident.

The type of model used for modal analysis may also affect the magnitude of frequency obtained. Table 2-6 presents an exercise performed by Kaliyaperumal *et al* (2008) for comparing the different possible model types that can be applied during FEM. Their models consisted of six span continuous welded plate girder railway bridge which varied by adding and removing some elements, support condition and number of spans from the FEM. This exercise is also performed in this study as included in Chapter 4.

Table 2-6: Comparison of natural period for FEM types (Kaliyaperumal *et al*, 2008)

No. of spans	Single –span				Three –span				Six span
Model	Shell element		Beam element		Shell element		Beam element		Beam - shell
Boundary Conditions	SS	Fixed	SS	Fixed	SS	Fixed	SS	Fixed	SS
T1	0.182	0.123	0.176	0.114	0.181	0.151	0.178	0.142	0.208
T2	0.156	0.086	0.148	0.114	0.161	0.148	0.152	0.137	0.164
T3	0.110	0.066	0.115	0.114	0.146	0.131	0.14	0.116	0.145

NB: 'SS' indicate Simply supported bridge where the support translations are restricted in X, Y and Z direction and 'Fixed' implies fixed support where the translations and rotations of the supports are restricted in X, Y and Z direction. The terms T1, T2 and T3 represent the first three natural periods of the bridge.

From Table 2-6 we can observe that the type of elements used in FEM can significantly change the magnitude of frequency in both simply supported and fixed support bridge. All beam elements provide a higher frequency magnitude as compared to shell element FEM result. The number of spans considered affects the magnitude of the frequency to a certain extent only as shown in comparison made between single and three span bridge. However, the results obtained from the six span bridge is higher than the two cases which indicates that for a bridge with many number of spans, it is important to model the bridge as a whole. A combination of beam-shell elements can be applied to minimize modelling and analysis time if necessary. It is always good to refer to previous works to understand the extent of variation of results from field measurement and that obtained from FEM as presented in Table 2-7.

Table 2-7: Natural Frequency - considering vertical bending of bridge only

Vertical Bending mode	Liu *et al*(2009) Frequency [Hz]			Ashebo *et al*(2007) Frequency [Hz]			Rodrigues(2002) Frequency [Hz]			Xia *et al* (2005) Frequency [Hz]		
	M	F	C	M	F	C	M	F	C	M	F	C
1st mode	3.90	NA	NA	4.58-4.67	4.54	NA	6.88-7.01	NA	6.95	7.70	NA	NA
2nd mode	10.41	NA	NA	NE	4.79	NA	15.77	NA				
3rd mode				6.22-6.39	6.70	NA						
4th mode				7.73-7.81	7.53	NA						
5th mode				NE	10.40	NA						
6th mode				10.81-11.11	10.66	NA						
7th mode				13.30-13.67	14.72	NA						
8th mode				15.73-15.74	16.34	NA						

Note: 'NE' and 'NA' indicates not extracted from measured data and not available respectively

The abbreviation 'M', 'F' and 'C' indicates the measured, FEM, Calculated data respectively.

Liu *et al* (2009) analysed a composite bridge with steel double box section, girder and concrete deck

Ashebo *et al* (2007) analysed a concrete bridge with double box girder cross section

Rodrigues (2002) analysed a Steel Truss Railway bridge

Xia *et al* (2005) analysed a double track prestressed concrete bridge

Following the work of Ashebo *et al* (2007) and Rodrigues (2002) presented in Table 2-7, we can observe that field measured frequency gives similar result with calculated and FEM frequency. Comparison between different types Table 2-7 of bridges shall not be made as the parameters of each bridge varies. For instance, a double track prestressed concrete bridge studied by Xia *et al* (2005) and truss bridge by Rodrigues (2002) shows similarity on the first frequency of the vertical vibration mode. However, this does not indicate a similarity or difference between the two bridges. In Table 2-8, it is shown that Rodrigues (2002) used two methods of calculating the frequency: frequency domain method (calculation 1) and Ibrahim time method (calculation 2). The result does not show a significant difference. In this study therefore only the frequency domain method was applied to identify frequency. A Fourier transform is performed to get the dominant frequency of the bridge. A software named Matlab is used to perform a Fourier transform sing which the time domain acceleration readings is converted to frequency domain data. In

other words the acceleration data which was read as a function of time is converted to data as a function of frequency using Fourier transform.

Table 2-8: Natural Frequency -considering vertical bending mode

Vertical Bending mode	Rodrigues(2002) Calculation 1 [Hz]	Calculation 2 [Hz]
1st mode	6.88	6.95
2nd mode	15.77	

2.6 EXCLUDED ITEMS

The following are some of the important points that may significantly affect the dynamic response of a structure. However these are not included in the scope of the research presented here:

a. Railway track irregularity, roughness and rail discontinuity
b. Effect of damping
c. Skewness of the bridge

2.6.1 Railway track irregularity, roughness and rail discontinuity

Railway track irregularity and roughness might be caused by wear and tear, clearances, subsidence or inadequate maintenance as described by Goicolea and Gabaldon (2008). Kargarnovin *et al* (2005) expresses the track irregularity as a function of spatial frequency or wave number (rad/m) noted by:

$$\Omega = \frac{2\pi}{\lambda}$$

Equation 2-6

Where:

Ω = Track irregularity

(λ) = wavelength of irregularity.

Kargarnovin *et al* (2005) showed that irregularity with shorter wave length between 0.03m-30m affects the ride comfort of the train significantly. They concluded that track irregularity is the dominant factor affecting the ride comfort as compared to other causes of vibration such as vibration due to train passing on the bridge or sleeper. Rodrigues (2002) proposed the application of a factor from EC1 code to a function developed after measuring the structural response at various speed in order to compensate for wheel defects and track irregularities.

Rail discontinuity can occur as a result of existing construction joint while joining two rail segments. According to results obtained by Michaltsos *et al* (2010), the deflection amplitude increases by the order of 20% to 150% during the presence of rail discontinuity due to imposed impact loading.

2.6.2 Effect of damping

Damping of the structure may exist due to various immeasurable reasons. However, one can estimate the effect directly from the field measured data. The works of Liu *et al* (2009), Rodrigues (2002) or Chopra (2004) are relevant to estimate the damping of structures from field measured data.

2.6.3 Effect of skewness of the bridge

Ashebo *et al* (2007) conducted a field a modal analysis on evaluation of dynamic loads on skew box girder continuous bridge. However, the main intent of their research was to observe the impact of skewness of bridge on the dynamic response which they have concluded that 0^0-30^0 skew angle has no influence on both static and dynamic characteristics of the bridge.

2.7 SUMMARY

2.7.1 Summary of literature review

Each paragraph in this section provides a brief description of the different literatures referenced for this study. The description includes the type of bridge on which the study is conducted, the type of responses of the bridge studied and the type of methodology used to extract these responses.

Ashebo *et al* (2007) studied the effect of the skewness of a skew box girder three spans bridge in Hong Kong having a total length of 73m and 10.58m wide when subjected to truck loads. Natural frequency is observed using FEM using SAP2000 software and field measured acceleration of bridge.

Caglayan *et al* (2011) performed a dynamic and seismic assessment of four span double track railway bridges with riveted steel plate girders and open decks each spanning 13.5m.

Natural frequency from measured acceleration data and stress from measured strain data was reported. A single span model using FEM software COSMOS is also included.

Mathematical approach is presented by Hamidi and Danshjoo (2010) to determine the impact factor for steel railway bridges considering simultaneous effects of vehicle speed and axle distance to span length ratio.

Kaliyaperumal *et al* (2008) performed dynamic analysis on six-span continuous welded plate girder railway bridge of a total length of 189m with a skew angle of 80 degrees located in Stockholm subjected to train loads. Natural frequency was calculated from acceleration data and stress from strain data and FEM using ABAQUS.

A 30m span concrete railway bridge subjected to high speed rail in Taiwan is studied by Kargarnovin *et al* (2005). The effect of track, irregularity, train speed, damping and stiffness of suspension system, ballast stiffness on comfort indicator is observed. Mathematical model using equation of motion of vehicle tack and bridge, field measurement.

Liu *et al* (2009) studied a composite bridge with girder and double box section of seven spans Italian high sped railway line between Torino and Milano. Each span is 73m and total length of 322m and 13.6m. Natural frequency obtained for vertical bending and torsion of the bridge from acceleration data and stress from strain data. Field measurement and numerical methodes (the numerical methods are not described in the literature).

Madshus and Kaynia (2000) observed the dynamic amplification on the rail/embankment/ground system as train speed approaches its critical value. The railway line is located in Sweden subjected to X-2000 high speed train travelling at 200km/h Displacement at various depths up to 12m below ground using electronic displacement sensor, vertical and horizontal acceleration at top of embankment and till depth of 7.4m, particle velocity using seismometers up to depth of 6.9m were reported. The influence of train speed on the dynamic behaviour of light weight steel bridges was investigated.

Michaltsos *et al* (2010) analysed the influence of train speed on the dynamic behaviour of light weight steel bridges. A theoretical approach using single span equation of motion

using Dirac delta function and Heaviside's unit step function was used. Mid span deflection at different speeds and at different values of rail discontinuity were analysed.

Rodrigues (2002) evaluated steel a truss railway bridge subjected to an active tilting train with a speed of 200km/h using field measurement, modal identification (basic frequency domain method and Ibrahim time domain method. A single span truss railway bridge crossing the Trancao river of span length 31.4m and width of 3.14m was investigated. Acceleration data for locomotive hauled, electric triple and active tilting train at different speeds) using ES-U (Episensor accelerometers) and piezoelectric strain sensors was reported.

Xia *et al (*2005) presented the experimental results of a bridge under China-star high-speed train loads. Vertical deflection, vertical and lateral acceleration, lateral and longitudinal strains, vertical and longitudinal rail forces, lateral and vertical frequency and damping were reported. The bridge was double track prestressed concrete with girder and box section railway bridge of 28 spans subjected to Qun-Shen high speed passenger rail at speed of 270 and 321.5km/h.

Chopra (2007) and Yang *et al (*2004) provides a depth theory and wide range of applications of dynamic analysis of structures including bridges with practical example of results such as natural frequency.

2.7.2 Conclusion from literature review

The following conclusions are made based on the literature study:

- ✓ The mathematical approaches discussed in Chapter 5 are based on the theory referred from the literature discussed in Section 2.7.1. These theories are applied during the derivation of equation of motions presented in the mathematical approach in Chapter 5. The approach by Michaltsos *et al* (2010) gave a guide while developing a forcing function from the Dirac delta function and Heaviside's unit step function as discussed in Section 5.4. The formula for calculating the impact factor is referred from Hamidi and Danshjoo (2010). The concepts of the derivation of equations of motion are referred from Chopra (2007) and Yang *et al (*2004).

- ✓ Indications of the types of field measured bridge responses and types of instrument used for conducting field measurement are referred from Ashebo *et al* (2007), Caglayan *et al* (2011), Kaliyaperumal *et al* (2008), Kargarnovin *et al* (2005), Liu *et al* (2009), Madshus and Kaynia (2000), Michaltsos *et al* (2010), Rodrigues (2002) and Xia *et al (*2005). These references assisted in understanding of the calibration of the measuring instrument and loading parameters, identifying the type of sensor required, choosing the appropriate instrument setup location, identifying the data required from the measurement, identifying the type of loading, estimating duration of measurement, planning the data acquisition methodology and choosing the data analysis methodology. However the actual application of the methodology for conducting field measurement, field data gathering and analysis are referred from the instrument manual and specification.
- ✓ The FEM for this study is performed using OaSYS GSA software. This software is not used by any of the literature reviewed. However the approaches are compared with Ashebo *et al* (2007), Caglayan *et al* (2011) and Kaliyaperumal *et al* (2008). Some of the approaches referred to are the boundary conditions, meshing in FEM, addition of secondary elements such as bracings, stiffener, rail or sleepers which alter the modal analysis result to a certain extent, connections between structural elements and modelling types. These are discussed in Section 2.3.
- ✓ The equation of motion of the bridge and train system is derived based on the assumption that the system is generalized and simplified as discussed in Chopra (2007) and Yang *et al (*2004).
- ✓ Dynamic factors such as the amplication factor (impact factor) mentioned are one of the simplifying methodologies used in different references to compensate for the dynamic effect of a moving train on structures like bridges. Formulas and approach to determine these factors are discussed in Goicolea and Gabaldon (2008), Hamidi and Danshjoo (2010), Chopra (2007) and Yang *et al (*2004).
- ✓ Resonance and cancellation is one important dynamic effect one should consider during dynamic analysis.
- ✓ The following are some of the important points that may significantly affect the dynamics response of a structure. However these are not included in the scope of the research presented here. These items are: railway track irregularity, roughness and rail discontinuity, effect of damping and skewness of the bridge.

3 FIELD MEASUREMENT AND ANALYSIS OF RESULTS

3.1 INTRODUCTION

In this chapter, a brief description of field measurements taken on an actual selected single span simply supported steel truss railway bridge is discussed. The aim of these field measurements was to determine the dynamic response of the structure from the acceleration and displacement data using an accelerometer and displacement transducer respectively. The measured acceleration data was then converted to frequency data in order to compare the results obtained from FEM and a mathematical approach as described in Chapters 4 to 7. Similarly, the displacement data obtained from different locations along the mid span and at different train speeds was compared with the results obtained when following alternative methodologies. This comparison is included in Chapter 7 of this research report. Dimension measurement was taken from the actual bridge to draw the As-Built drawing from scratch from which the FEM discussed in Chapter 4 was accordingly developed. The type of instrument used and the manner in which it was verified in the laboratory to check its performance and accuracy is also explained in this section of this report. The results from the laboratory and field measurements will be analysed and discussed in the following chapter.

3.2 DESCRIPTION OF SELECTED BRIDGE

The specific bridge discussed in this research report is located in between an urban and rural area along the M18, in Irene, Centurion in the Gauteng province of South Africa and is owned by Passenger Rail Agency of South Africa (PRASA). The bridge is built above the Hennops river, a river that joins Olifantspruit and the Sesmylspruit river as shown in Figure 3.1. The bridge consists of two independent single span simply supported truss bridges as indicated in Figure 3.2, where each truss was made in the form of a common type of truss called a Pratt truss (Kassimali, 2011). Each independent bridge services the trains coming to and from Johannesburg to Pretoria. It is exposed to a relatively heavy traffic of passenger metrorails where a train passes every 10 to 15 minutes during peak hours and every 30 to 40 minutes during off-peak hours. The train consists of twelve coaches with three motor coaches and nine trailer coaches. The bridge is also exposed to trains that carry goods which have 1 up to 50 coaches. The gross mass and capacity of each coach are briefly included in Chapter 6. The rail line uses an electrified system as shown in Figure 3.2 and Figure 3.3. The maximum speed limit on the bridge is 90km/h. A narrow gauge type track with a width of 1067 mm is used, as per Figure 3.4. A visualization is included in Chapter 4. The bridge

is made up of various built-up sections which consists of cross beams, stringers, bracings, wooden sleepers and rails, but with no ballast or deck as shown in Figure 3.4 to Figure 3.10.

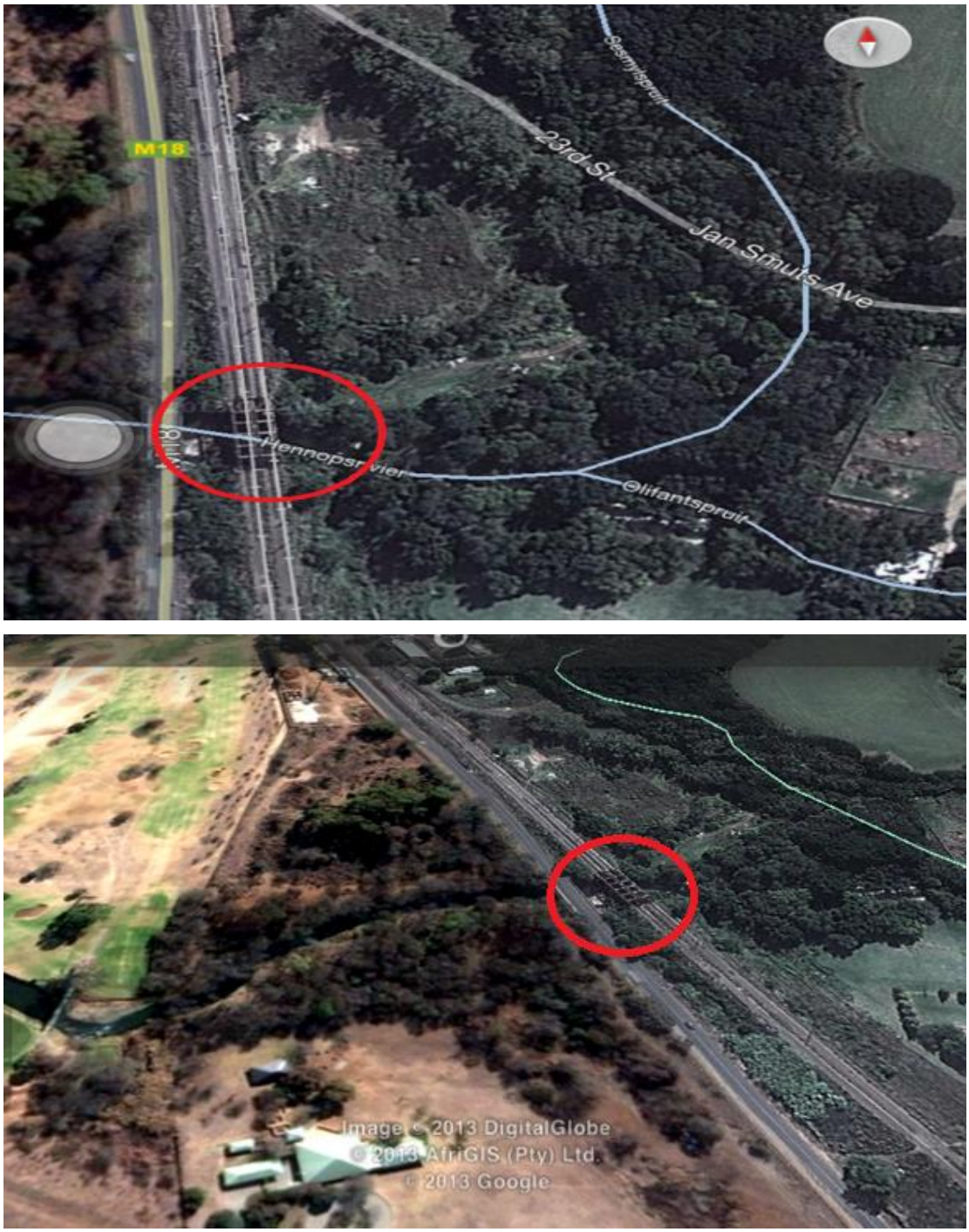

Figure 3.1: Satellite view of the bridge at Irene, Centurion, South Africa

Figure 3.2: Front view of steel truss railway bridge at Irene and estimated year of construction

Figure 3.3: Side view of steel truss railway bridge at Irene, Centurion, South Africa

The stringers and cross beams are made of 700 x 270mm plate girders with a thickness of 10mm as shown in Figure 3.4 to Figure 3.6. The bottom chords and top chords are constructed with a 400 x 100mm folded C-channels with a thickness of 10mm placed back to back and connected with plates measuring 10mm thick to form an open box-like beam measuring 600mm from edge to edge. A typical section is included in to Figure 3.6.

Figure 3.4: Section of bridge showing sleeper, cross beam, bottom chord and walkway

Figure 3.5: Section of bridge showing top chord, top and side bracing

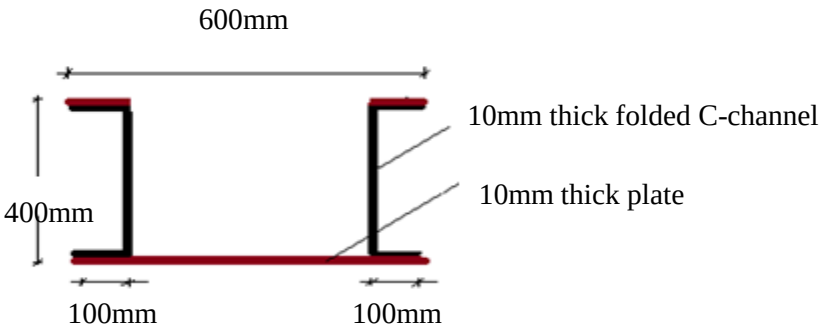

Figure 3.6: Typical section for top chord and bottom chord

All vertical web members are also constructed from built up sections to form an I section. They consist of four angle irons measuring 100 x 100mm with a thickness of 10mm, forming two pairs of T-sections facing back to back and connected by plates 65mm wide of 10mm thickness. These plates are riveted down in a zigzag shape in between the pairs of T-sections, as shown in Figure 3.7 and Figure 3.8.

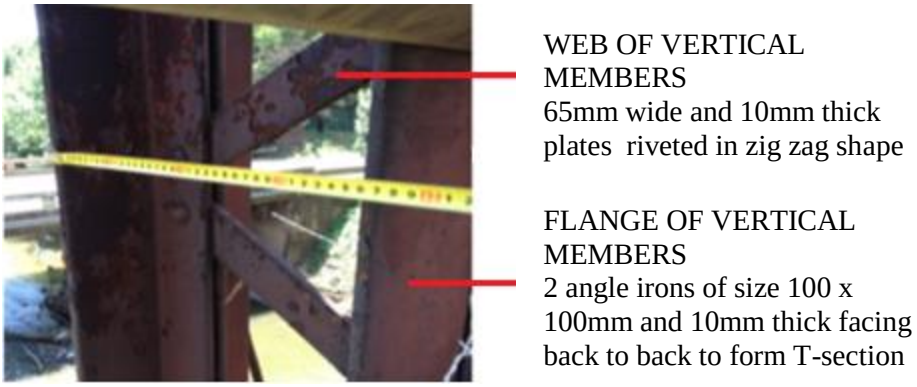

Figure 3.7: Vertical members

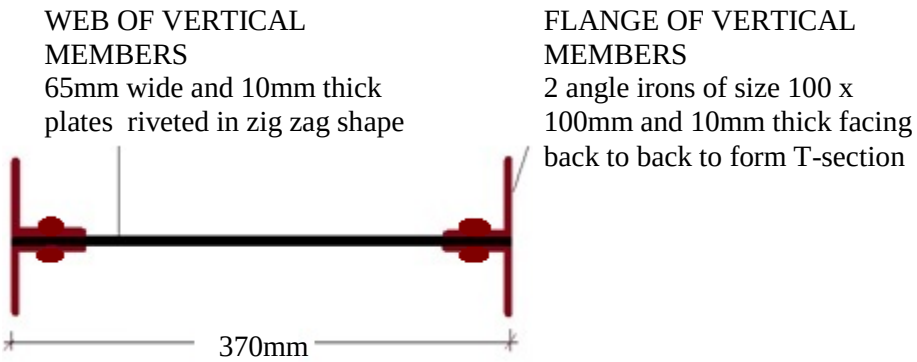

Figure 3.8: Section of typical vertical members

The wooden sleeper shown in Figure 3.9 measures 240 x 195 x 2200mm and is placed at an average spacing of 380 to 470mm.The span length of the bridge is 32543mm with a total width of 5400mm when measured from external edge to edge. The bottom bracing is shown in Figure 3.10.

Figure 3.9: Section showing stringer and cross beam

Figure 3.10: Section showing bottom bracing

3.3 REASON FOR SELECTION OF THE BRIDGE

Existing research works commonly focus on the response of composite railway bridges, as referred to in Chapter 2. In this research work, an analysis is conducted on a steel truss railway bridge. The study aims to provide valuable input in terms of providing knowledge and experience in dealing with a dynamic analysis of bridges with different parameters. This becomes prudent when the need arises to upgrade existing bridges to accommodate more rapid trains, lighter or heavier trains and bigger or smaller trains. Furthermore, the specific bridge under discussion was the only steel railway bridge available in Gauteng which falls under the auspices of PRASA. In addition to this, the structural details of the

selected bridge are believed to provide sufficient opportunity to exercise different FEM as indicated in Chapter 4.

3.4 TRAIN CONFIGURATION

General view of the train is shown in Figure 3.11. The train consist of 12 coaches out of which the three coaches are the motor coaches and the remaining nine coaches are trailer coaches. Each coach consists of four axle loads.

Figure 3.11: A general view of the train

3.5 BRIEF DESCRIPTION OF INSTRUMENT

Field measurement is conducted using four HBM's WA50 displacement transducers from Hottinger Baldwin Messtechnik GmbH (HBM) and seven Universal Serial Bus (USB) accelerometers of each model X16-1C. For a better visualization refer the set up done in laboratory in Figure 3.14 and Figure 3.15. The displacement transducer is a product of a company called Hottinger Baldwin Messtechnik GmbH (HBM) which is expected to give reasonable results based on results obtained from previous research works. The accelerometer is a product of a company called Gulf Coast Data Concept (GCDC) which is mainly selected due to its availability and the ease of setup in the field.

The instrument that was used for displacement measurement is a displacement transducer where its model is described above as HBM's WA50 displacement transducer with a nominal sensitivity 80mV/V±1%. It was utilized in this study to measure the displacement of the bridge at the mid span of the bridge. As shown in Figure 3.12, the displacement

transducer consists of a transformer housed in a metal case with a ferromagnetic core which can be attached to an extension rod. The core slides through a built-in transformer with primary and secondary windings. Therefore, when the structure is displaced, the core also slides, creating a magnetic difference between these windings. This creates voltage which is convertible to any linear variable such as displacement using a predetermined calibration factor.

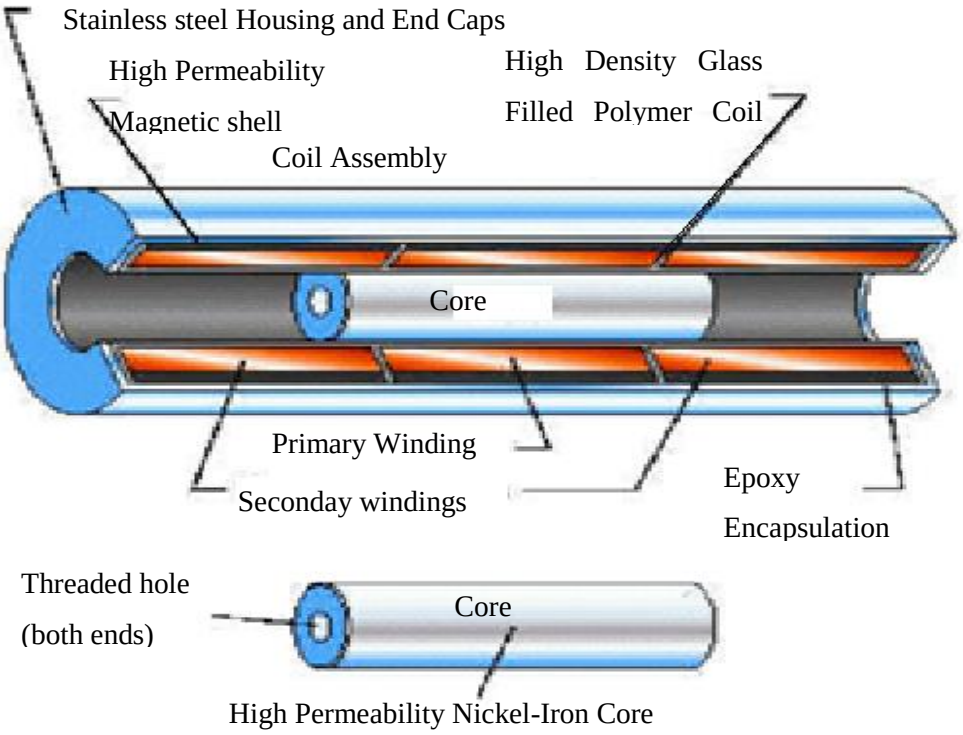

Figure 3.12: Section view of displacement transducer (Penny & Giles, 2009).

The other type of instrument that was used for measurement is accelerometer which is a Micro Electromechanical Systems (MEMS) type of sensor made up analog devices of model ADL345. It is capable of measuring acceleration in three directions: lateral, longitudinal and vertical directions. However, in this study only the vertical portion of the data is discussed as it is the dominant response specific to the type of load considered. The industrial instrument shown in Figure 3.16 is used as a reference instrument in the laboratory during test of the USB accelerometer.

As shown in Figure 3.13 which is taken from GCDC, the accelerometer consists of differential capacitor unit cells where each cell is composed of fixed plates attached to substrate and movable plates attached to the frame. When acceleration force applied on the

sensor a capacitance difference is recorded. This data is then converted to raw data in the form of digital count using an inbuilt analog to digital converter.

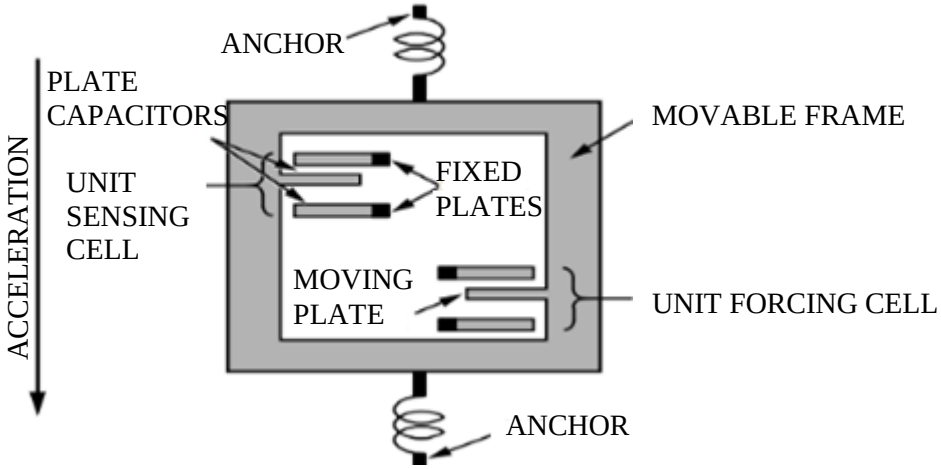

Figure 3.13: Simplified view of sensor under acceleration (GCDC)

3.6 ACCURACY OF THE INSTRUMENT

The accuracy of instrument was studied by performing tests in the lab to verify the manufacturer calibration. Both WA50 displacement transducers and accelerometers were pre-calibrated by the manufacturer and only a verification of the results was performed in the laboratory. Nonetheless, the following procedure was followed to further check the level of accuracy of the accelerometers as compared to Integrated Circuit Piezoelectric (ICP) industrial accelerometers:

a) Checking the performance and accuracy of the instrument.
Three accelerometers fixed with different techniques and a standard industrial accelerometer screwed to rotary machine is shown in Figure 3.14 and Figure 3.15. Section 3.10 includes plots for comparison between the USB and industrial accelerometer.

b) Checking suitable fixing techniques within an acceptable level of accuracy. The selected fixing methods are: wax, screw and double sided tape. The idea of using screws or glue for fix the instrument was rejected to avoid minor and major damage to the bridge during fixing or removing the instrument. However, the final selection is made based on the comparison result presented in Section 3.10, which is obtained

from acceleration data measured in the laboratory using these aforementioned methods.

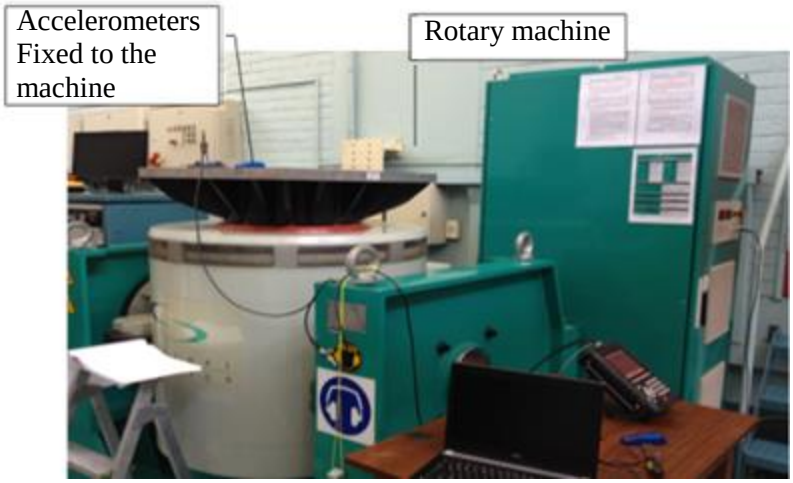

Figure 3.14: Set up of accelerometers in the laboratory

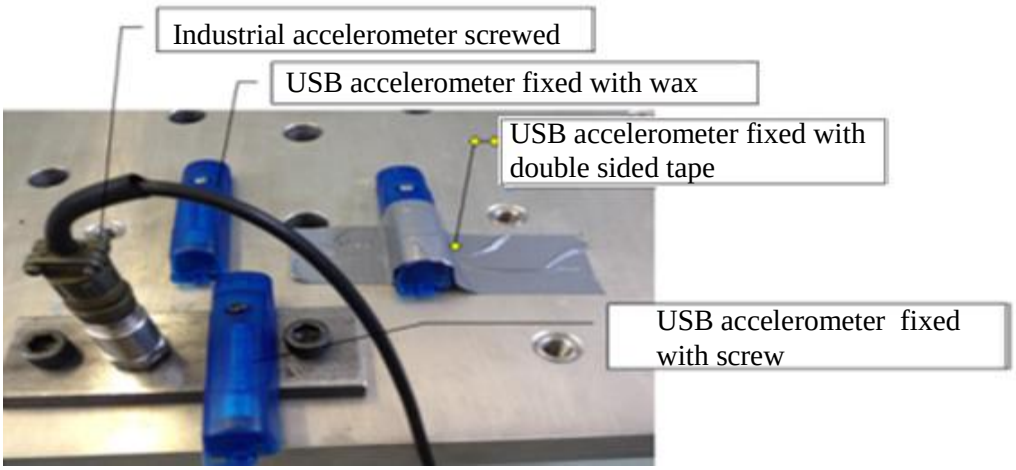

Figure 3.15: USB with three fixing techniques vs. industrial accelerometer

Figure 3.16: Closer view of USB and industrial accelerometer

3.7 INSTRUMENT SETUP

Four displacement transducers and seven accelerometers were used during field measurement located as shown in Figure 3.17. The instrument set up location is selected based on the location of maximum static response of the structure, mainly deflection obtained using FEM and hand calculation. Measurements taken at these locations were assumed to give sufficient information on the dynamic response of the structure. All accelerometers were placed horizontally down on the bridge facing in the direction of Pretoria. The measurement was performed over two days. On the first day, only four accelerometers were used at selected locations. On the second day, the remaining three accelerometers with four displacement transducer were set up. The specific locations were presented in Table 3-1 to Table 3-2 and also shown in Figure 3.19 to Figure 3.22. However it was possible to perform all measurement in one day.

Table 3-1: Accelerometer setup locations

Day1		**Day2**	
Location ID	**Location**	**Location ID**	**Location**
1	mid span left cross beam	5	mid span right cross beam
2	mid span left rail	6	mid span right stringer
3	¾ span left stringer	7	mid span right rail
4	¾ span left top of the bottom chord		

Table 3-2: Displacement transducers setup locations

Day 2	
Location ID	**Location**
A	mid span right bottom chord
B	mid span right cross beam
C	mid span intersection of right stringer and cross beam
D	mid span right rail

The displacement transducer is fixed to adjacent bridge at mid span using a self-designed mounting section as shown in Figure 3.20 and Figure 3.21. The mounting sections consist of a 50x50x2mm RHS section pieces welded together to reach the bridge measurement is taken from the adjacent bridge. The section at point ‘a’ is clamped to the flange of bottom chord of the adjacent bridge. The section at point ‘b’ and ‘c’ are fixed on a section which is

clamped to the web member and also tied with 6mm size wire cable to additionally support the section as shown in Figure 3.21.

The plungers of the displacement transducers were fixed at their mid length to allow both upward and downward movement of the plunger resulted from displacement of structure. The displacement transducer at point ‘a’, ‘b’ and ‘c’ were setup vertically downward touching the structure from the top. Any downward movement is therefore recorded as negative value as the core is moving away from the displacement transducer. In actual fact the displacement is positive downward. The displacement transducer that was fixed at point ‘d’ touches the structure from the bottom. Therefore the reading for downward movement is positive as shown in Figure 3.25.

The method which was used for fixing the accelerometer was double-sided tape measuring 12mm wide and 0.8mm thick. The tape is called auto trim repair tape. In addition to this tape a duct tape was used to give additional tightness as shown in Figure 3.19. The double sided tape reaches its maximum curing stage 24 hours after fixing, which makes it easier to fix and remove without affecting the paint of the structure. One of the reasons for choosing this method was due to the simplicity in thus affixing the accelerometer. The bridge is built roughly 8m high above the river and minimizes the risk of personal injury or loss of the measuring tool. The straightness of the fixing location on the structure is checked using the spirit level before fixing the accelerometer so that the acceleration measured will match the global X, Y and Z axis.

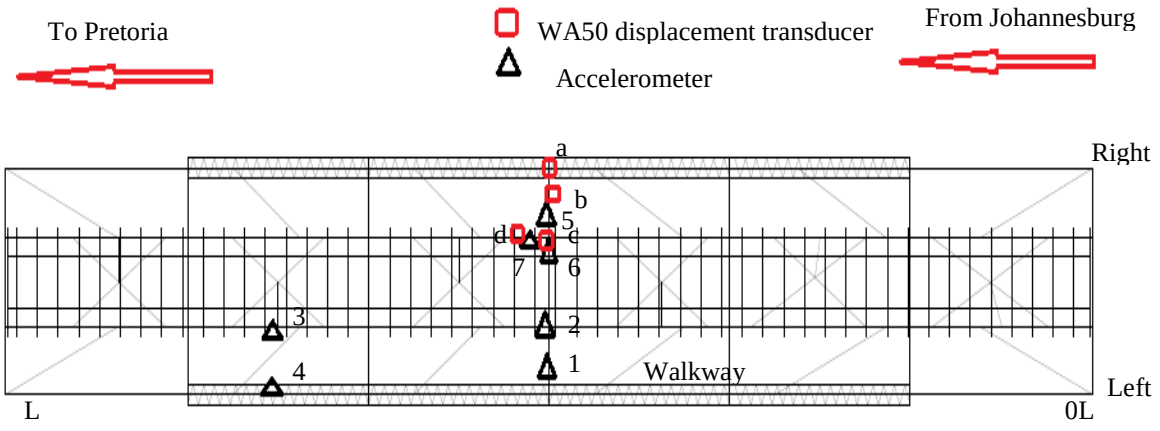

Figure 3.17: Measurement Locations

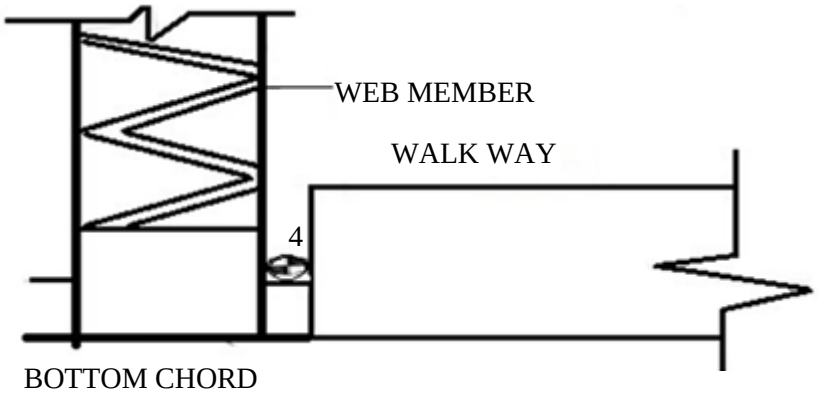

Figure 3.18: Accelerometer fixed at point '4'

Figure 3.19: Accelerometer fixed at point '7'

Figure 3.20: Displacement transducer fixed at point 'a'

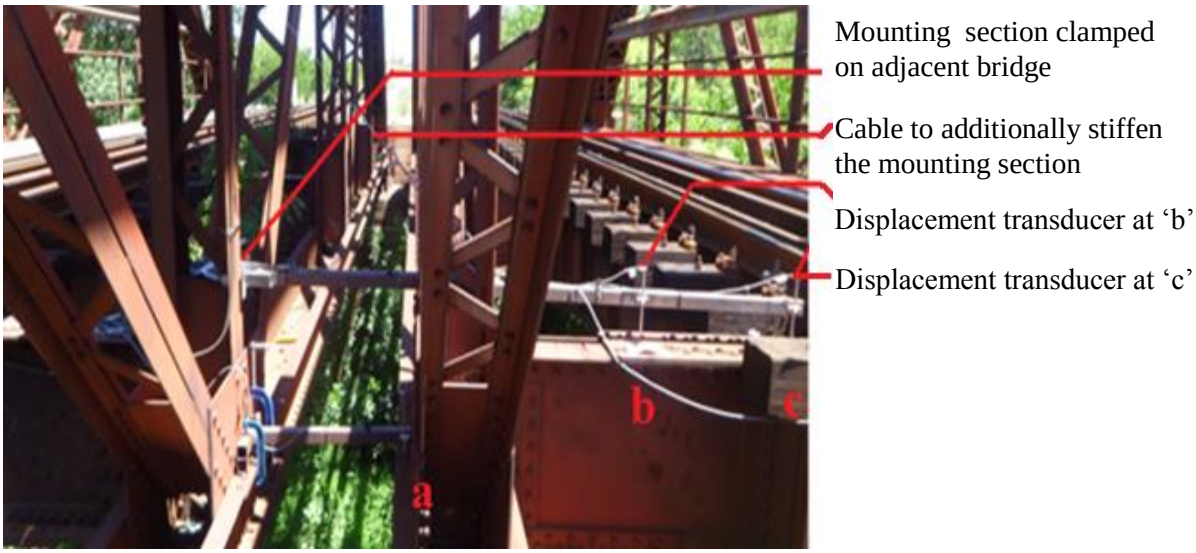

Figure 3.21: Displacement transducer fixed at point 'a', 'b' and 'c'

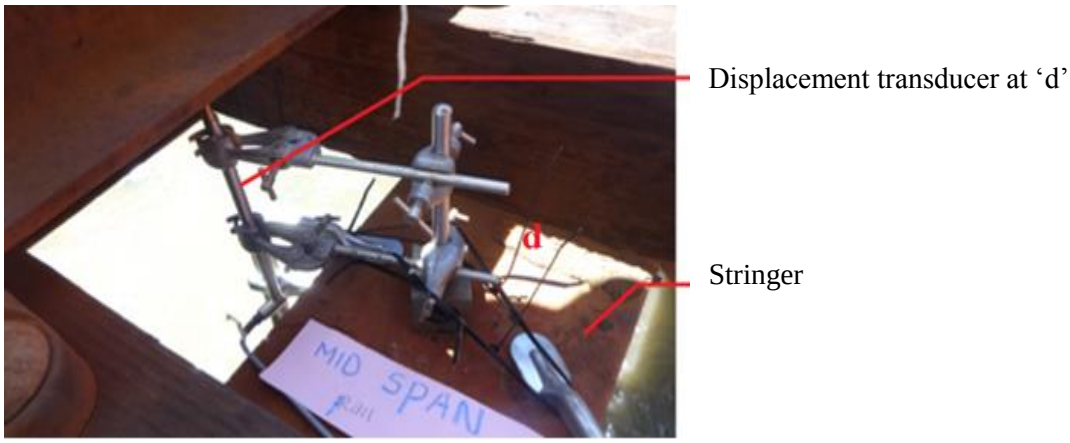

Figure 3.22: Displacement transducer fixed at point 'd'

All accelerometers that were used for measurement are X16-1C models and were manually configured to record data at 400Hz sample rate. Similarly, each WA50 transducer was adjusted to record at 1200Hz sample rate.

3.8 DATA GATHERING AND ANALYSIS

The data is automatically recorded in the microSD memory storage of the accelerometer. The data is recorded in four columns where time and raw accelerometer sensor readings from the X, Y, and Z axis are represented in each column. Time is measured in seconds, starting from the time of configuration. The acceleration is measured as a raw data which is converted to g-force using a conversion unit of 1024 that is referred from the

manufacturer's manual for this specific accelerometer model. Typical field measured acceleration data is presented in Appendix C2.

The only data that needed manual recording was the speed of train, and the location and orientation of the instrument. A Video was recorded at the same time to capture all information and calculate the speed to be utilized in Chapter 6. It is assumed that the bridge has no longitudinal slope, meaning that the two ends of the bridge have the same vertical elevations. This implies that the acceleration data recorded in the z direction was assumed to represent the vertical acceleration of the bridge in the global direction where the accelerometer is located.

The data from the displacement transducer is already converted to mm using the calibration factor set internally by the manufacturer. Typical field measured displacement data is presented in Appendix C1. In both instruments, time is not synchronized with actual time, only computer time which implies the approximation of the time of arrival of the train is made.

Measured data can be analysed after pre-processing taken place. The following pre-preprocessing methods were reported by Caglayan *et al* (2011). These are:

a) Synchronizing the time and acceleration data
b) Removing outliers and existing trends
c) Filtering

However in this research the pre-processing methods which were found applicable were; Synchronizing and de-trending after applying the necessary conversion units as discussed in Section 3.8. This is further discussed in Appendix B3.

Synchronizing of the data involves making sure all signal starts at the same time. For instance if we have a 1 sec signal and we took two readings of this signal for a duration of 3 & 4 sec respectively. These durations shows the data includes additional data before the start and end of the signal. Let us say the signal on the first and second data starts at the first and third sec respectively. During synchronizating of the two data we will make sure the starting data for the first data is the 1st data on the 1st sec where as the starting data for the second data is the data on the 3rd sec at which the actual signal starts.

De-trending involves removing the mean value from the entire signal to make sure we achieve the net signal. For instance the acceleration data automatically measures the acceleration of gravity as a constant value of 9.81m/s^2 before the train arrives on the bridge. By the time the train arrive a signal starts to read a value ±9.81m/s^2. Removing the gravity by deducting value equal to gravity or 9.81m/s^2 will give us the net acceleration signal on the bridge. The removal of a constant value of 9.81m/s^2 is called de-trending.

3.9 BRIDGE DISPLACEMENT RESULTS

This section presents the results obtained from displacement transducers fixed at the mid span and an accelerometer fixed at different parts of the bridge while the train is travelling at different speeds, as shown in Figure 3.17.

Displacement was measured at different locations along the mid span of the bridge relative to an adjacent bridge. That implies the actual displacement of a bridge to be measured is equal to the sum of the measured relative displacement of the bridge with respect to an adjacent bridge and the displacement of the adjacent bridge.

Four locations were selected to collect displacement data as shown in Figure 3.17 and presented in Table 3-2. The displacements measured at different locations (a, b, c) along mid span while the train is travelling at a speed of 38.3km/h are shown in Figure 3.23. A comparison of the results obtained at different speeds at mid span, are presented in Figure 3.24. Data was collected at 38.3km/h, 63.5km/h and 91.8km/h.

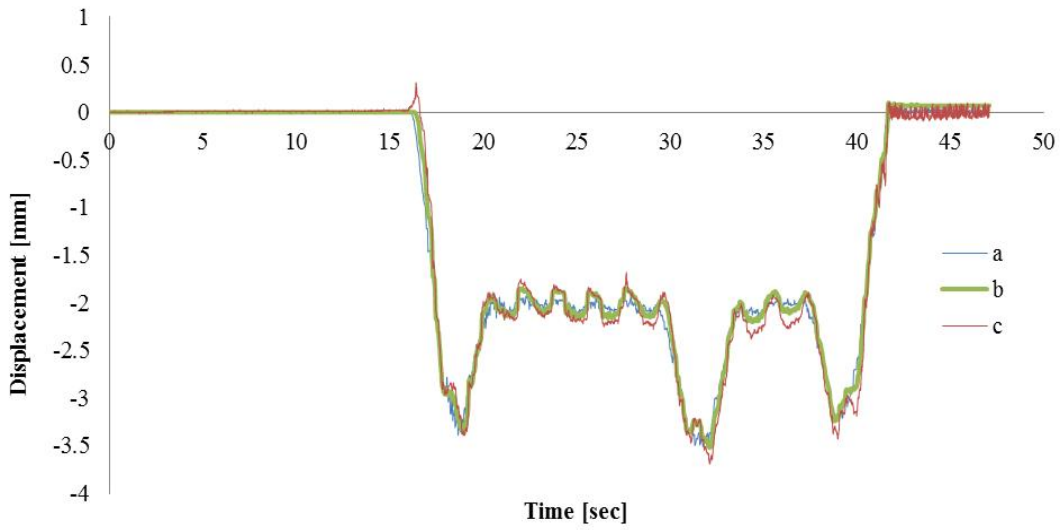

Figure 3.23: Displacement vs. time at different locations at a train speed of 38.3km/h

The result from Figure 3.23 shows a very close result giving a maximum of 3.69mm at the intersection of the stringer and cross beam. The displacement transducer that was set on the 'a' and 'b' gave readings of 4.88% and 4.61% lower than point 'c'. This shows that there is only a negligible difference between different locations at the mid span.

The train set arrangement is 1MC+3TC+1MC+6TC+1MC. Comparison of capacity of each type of coach in Table 6-4 indicates that the motor coach (MC) is heavier than the trailer coach (TC). This can be evidenced from Figure 3.23 and Figure 3.24. This arrangement may change to 1MC+6TC+1MC+3TC+1MC if the approaching training is facing opposite to the train with different train set arrangement. The difference in displacement pattern shown in Figure 3.23 and Figure 3.24 indicates the difference in the two set of arrangements for the two trains travelling at different speeds where one pattern is a mirror view of the other. To avoid confusion therefore, the author decided to plot the two graphs separately.

The displacement pattern is slightly affected with the train speed. The result presented in Figure 3.23 shows a maximum displacement of 3.69mm while the train was travelling at speeds of 38.3km/h. The result presented Figure 3.24 shows a maximum displacement of 4.02 and 4.29mm while the train was travelling at speeds of 63.5km/h and 91.8km/h respectively. Comparisons of all these speeds with the mathematical results are presented in Chapter 6.

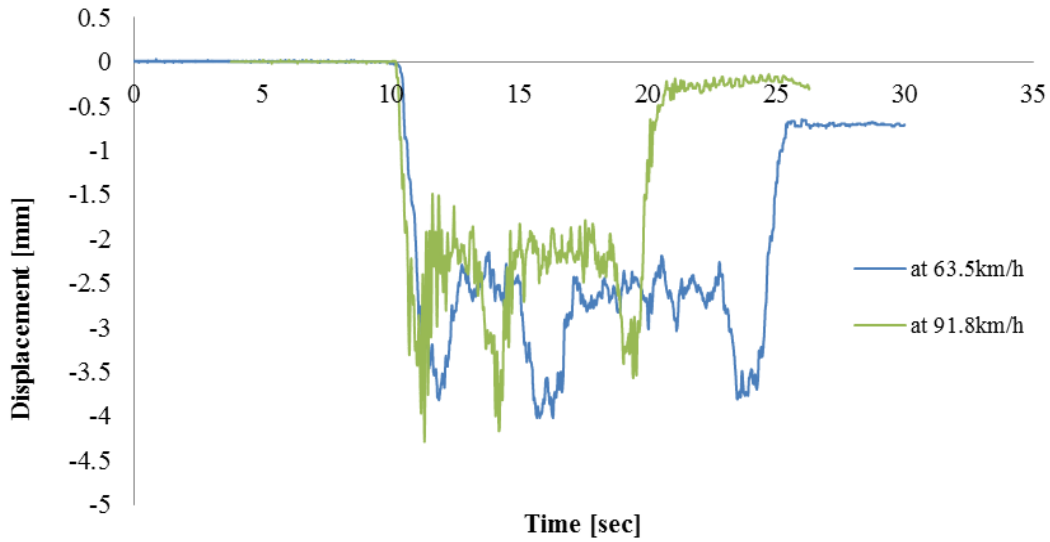

Figure 3.24: Displacement vs. time at point 'c' for two different train speeds

The measurements taken on the rail relative to the stringer which is taken from point ‘d’ does not represent the magnitude of the response of the bridge as shown in Figure 3.25. However, it may indicate the duration of the train on the bridge. In addition to that the front and back wheel of each coach can be traced from this measurement. The displacement pattern at point ‘d’ remains unchanged for two different speeds as shown in Figure 3.26.

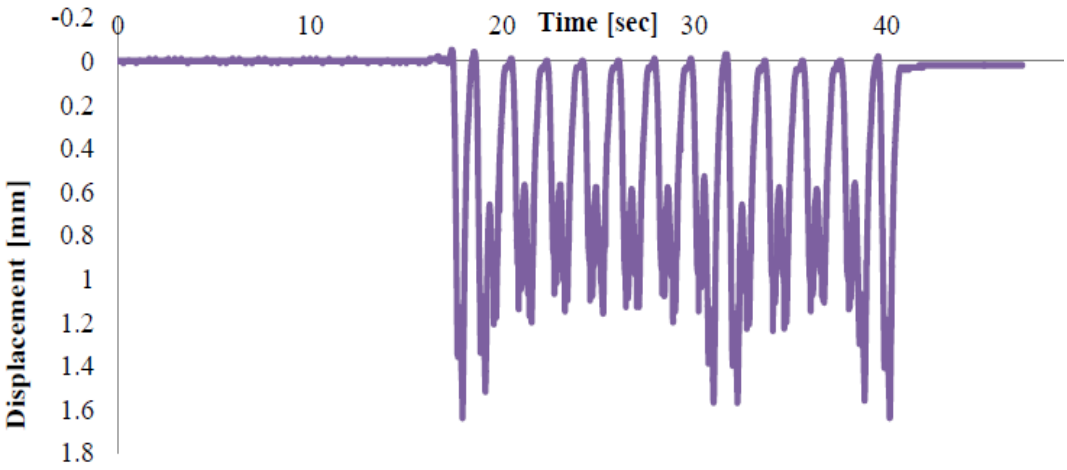

Figure 3.25: Displacement vs. time at point ‘d’

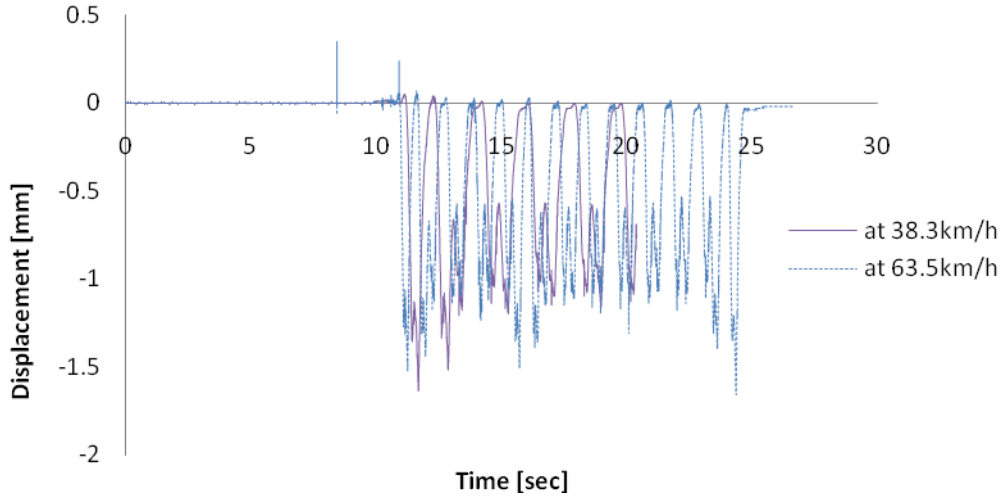

Figure 3.26 : Displacement vs. time at point ‘d’ for two different train speeds

The maximum displacements and accelerations that were measured for different train speeds at point ‘c’ were summarized in Figure 3.27 and Figure 3.33 respectively. The measured results indicate that displacement values increase as train speed increases.

Similarly, the maximum acceleration obtained from point '5' in Figure 3.17 is plotted as a function of train speed in Figure 3.33.

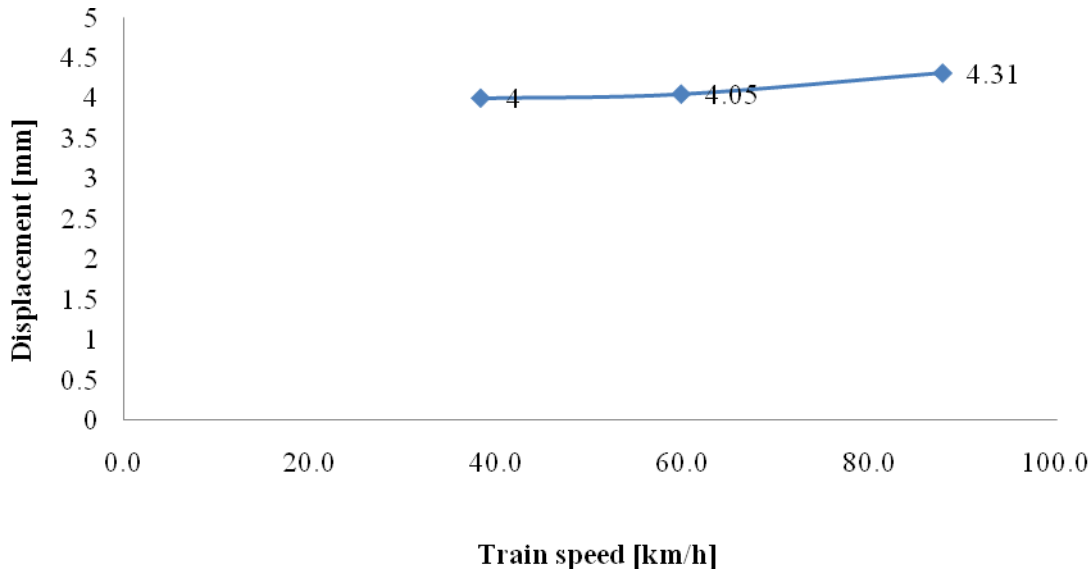

Figure 3.27: Effect of speed on bridge displacement on displacement transducer at point 'c'

3.10 BRIDGE ACCELERATION RESULTS

In this section, a discussion is made based on the few plots extracted from tests in the laboratory and an actual field measurement data obtained using accelerometers.

Laboratory test using different accelerometers

The results obtained from the laboratory test on USB accelerometers are shown in Figure 3.28 and Figure 3.29. In Figure 3.28, the three lines illustrate responses obtained using USB accelerometer fixed using three fixing materials, namely: screws, wax and double-sided tape. The fourth line is an industrial accelerometer screwed directly on the rotary machine. All accelerometers were supplied with constantly varying force which gives constantly varying acceleration data. The frequencies of each response extracted from the USB and industrial accelerometer readings fixed with double sided tape and with screw respectively are shown in Figure 3.29.

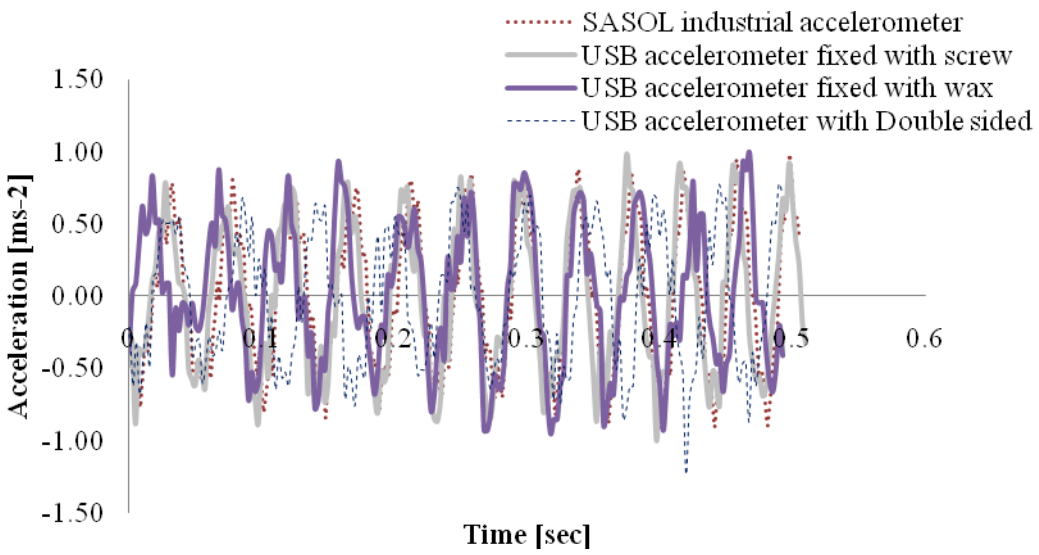

Figure 3.28: Acceleration vs. time plot from pre-processed data from different type of accelerometers

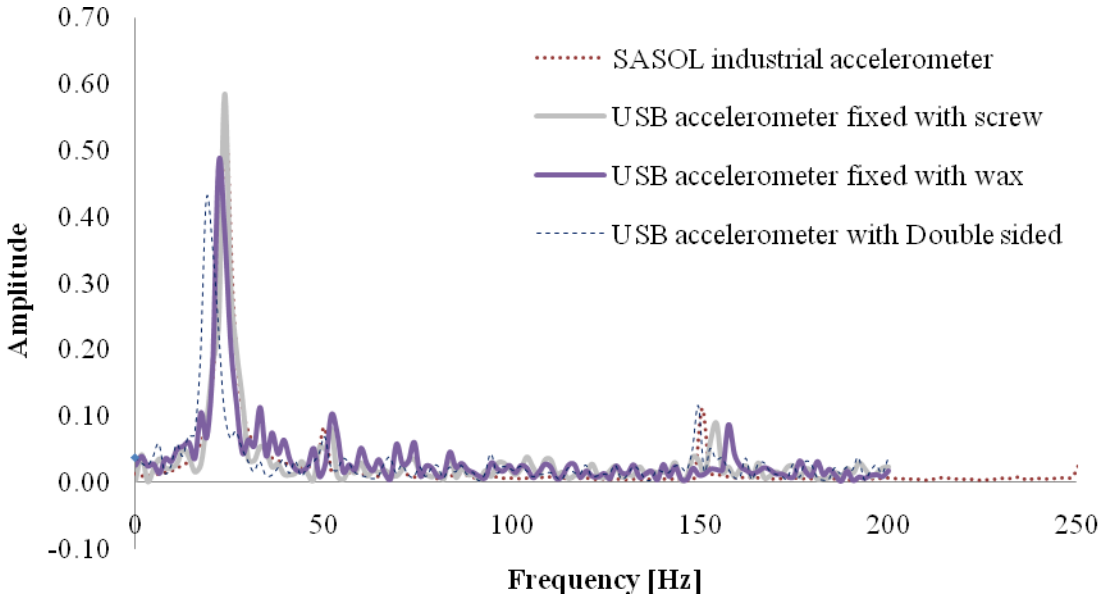

Figure 3.29: Amplitude vs. Frequency plot from different type of accelerometers

Acceleration taken from field measurement

The collected acceleration data was pre-processed before examining the data. The pre-processing methods which were found applicable were; Synchronizing and de-trending after applying the necessary conversion units as discussed in Section 3.8. A conversion unit of

1024 is used to convert the raw data to g-force and multiplied by 9.81 to convert the g-force to m/s^2 in all acceleration readings.

The acceleration data is divided in to forced and free vibration data to further observe the frequency content of the signal. The results plotted in Figure 3.30 to Figure 3.33 show a comparison between free and forced vibration data. In Figure 3.30, the black line that extends from point A to point E represents the acceleration data for the entire length of a signal for the accelerometer located at point '1' which is fixed at the left side of cross beam at mid span. The green line starting from B to C implies the portion of the data taken as a sample of forced vibration, which is assumed to be sufficient enough to obtain the required information. The last line indicates the free vibration portion of the signal extends from D to E. The points from A to B and C to D are part of the forced vibration data which is left out from discussion.

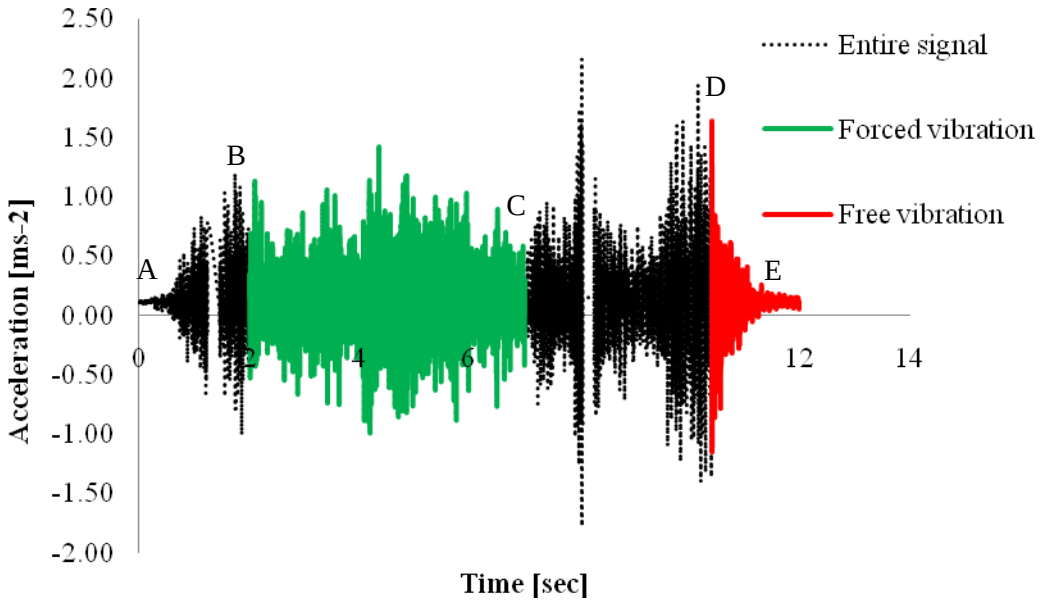

Figure 3.30: Comparison of acceleration vs. time plots for free and forced vibration data at point '1'

The frequencies shown in Figure 3.31 and Figure 3.32 are obtained from acceleration data using FFT. One can observe that both free and forced vibration data gives a better indication of the magnitude of the frequency unlike the entire signal taken as it is shown in Figure 3.31. Comparisons of this result with the one obtained from the FEM discussed in Chapter 4 shows that the free vibration data gives closer results to the FEM result.

However, the frequency and acceleration obtained from displacement data was not satisfactory and left out from discussion in this report.

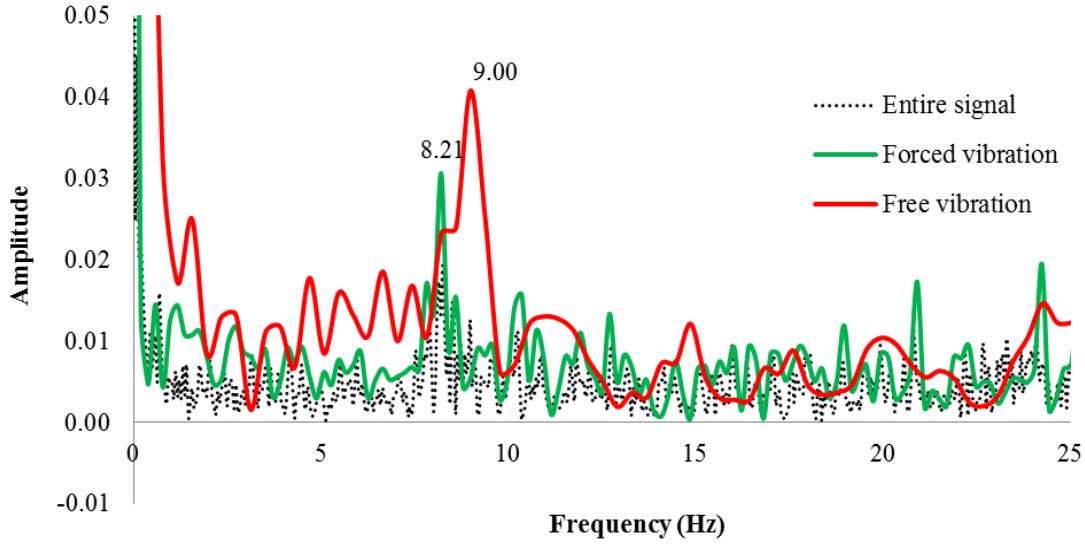

Figure 3.31: Comparison of amplitude vs. frequency plots using pre-processed data at point '1'

Based on observation made from Figure 3.31, it was decided to use free vibration data to compare the results obtained from the accelerometers placed at different locations. Figure 3.30 to Figure 3.32 use the free vibration data. The pre-processing methods which were found applicable were; Synchronizing and de-trending after applying the necessary conversion units as discussed in Section 3.8.

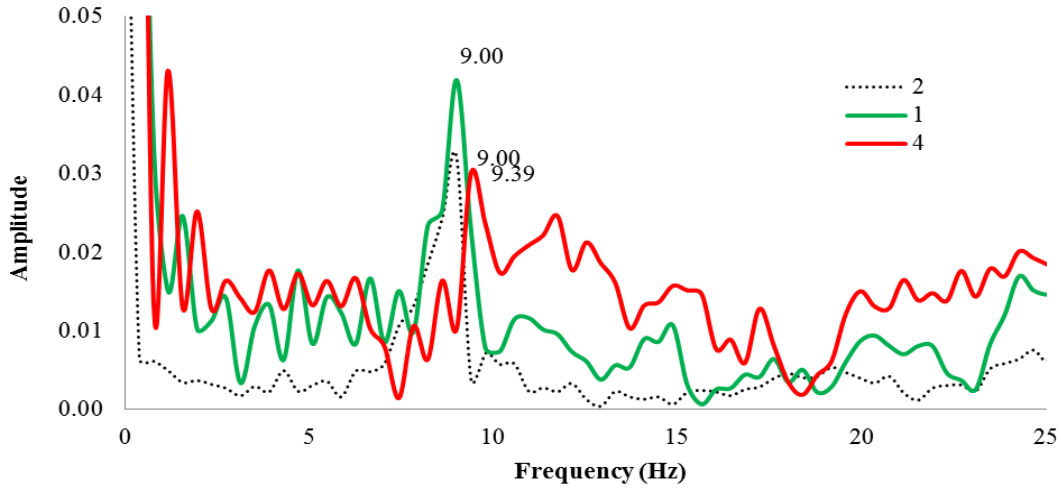

Figure 3.32: Amplitude vs. frequency plot using free vibration data at different locations

The frequency domain plot shown in Figure 3.32 indicates a dominant frequency between 9.0 to 9.4Hz for all accelerometers compared. The accelerometer at point ‘1 give a distinct dominant frequency as compared to the other location. The other observation that can be made from Figure 3.32 is that the two accelerometers fixed at mid span give similar frequency which is different from the one at ¾ of span. This magnitude is very close to the results obtained both from FEM and the mathematical approach. Therefore it is advised to take measurements from the mid span. The amplitude of the acceleration result however is unreasonably high which is discussed further in Chapter 6. The magnitude of maximum acceleration for different train speeds are compared in Figure 3.33. The result show that acceleration also increases as train speed increases. However a slightly different relationship between speed and displacement or acceleration is observed from comparison made with the mathematical results in Chapter 7.

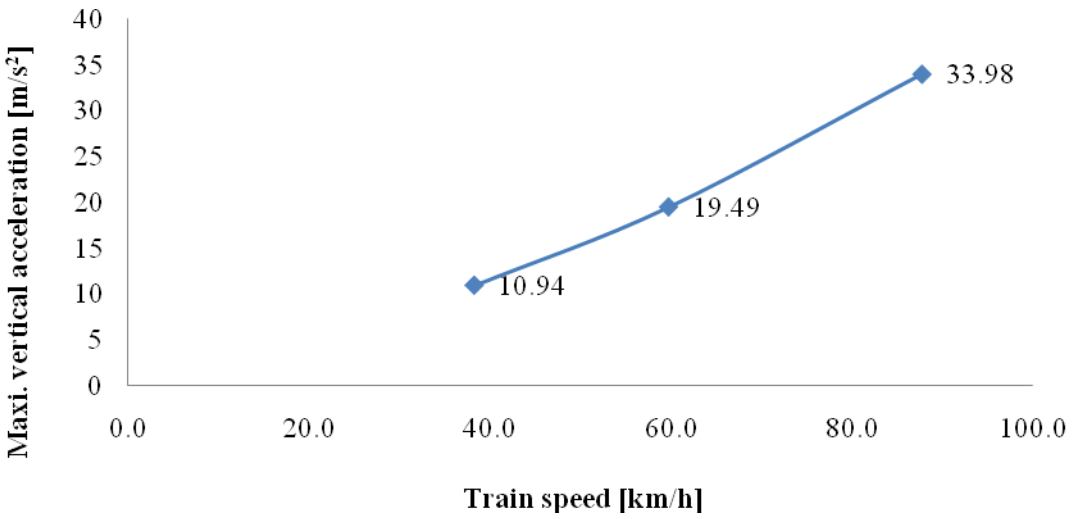

Figure 3.33: Effect of speed on bridge acceleration on accelerometer at point ‘5’

3.11 SUMMARY

In this chapter, the field measurements that were taken on the selected single span simply supported steel truss railway bridge are discussed. The type of bridge and train from which the data is measured is briefly described in order to make referencing easier during FEM and Mathematical approach discussed in Chapter 4 and 5 respectively.

The field measuring instruments used are accelerometers and displacement transducers from which the dynamic responses of the structure are obtained. The principles and the methodology in which these measuring instruments operate are also briefly explained in Section 3.5. The accelerometers were tested at the laboratory as discussed in Section 3.6 and Section 3.10. Matlab software is used to do analysis on the measured data more specifically during the conversion of the acceleration data to frequency domain data from which frequency of the bridge is determined. The instruments are set up at mid span and $3/4^{th}$ of span on selected members of the bridge such as Cross beam, Stringer, Bottom chord and Rail. The displacement transducers are fixed to the adjacent structure using self-built section and double sided tape is used for the accelerometers. These are discussed in Section 3.7. The methodology used for the analysis and interpreting of the measured data is explained in Section 3.8.

Data was collected when the train is travelling at a speed of 38.3km/h, 63.5km/h and 91.8km/h. The displacement results which are discussed in Section 3.8 show very close result giving a maximum of 3.69mm, 4.02mm & 4.28mm for speed of 38.1km/h, 63.5km/h & 98.1km/h respectively at the intersection of the stringer and cross beam. The measured results indicate that both displacement and acceleration values increase as train speed increases. However the maximum speed allowed for the train travelling on the measured bridge is 90km/h. Therefore it was not possible to measure bridge responses while the train is travelling at a higher speed such as 100 or 200km/h. The pattern and amplitude of acceleration data is similar at different part of the bridge at a particular train speed. The frequency extracted from this acceleration at different part of the bridge is also similar.

4 FINITE ELEMENT MODELLING OF STEEL TRUSS RAILWAY BRIDGE

4.1 INTRODUCTION

The objective of the following chapter is to present a three-dimensional FEM of the bridge which was utilized to determine the modal frequency and mode shapes using modal analysis. The specific structure under consideration is the single span simply supported steel truss railway bridge from Chapter 3; subjected to different load cases, as will be defined in more detail later in this chapter. The relevant boundary conditions are likewise discussed more in Section 4.6.

In order to accomplish the objective as stated above, two kinds of FEM types were utilized. These were modelling the bridge using grillage (beam) elements, and using shell elements. Kaliyaperumal *et al* (2008) reported that a combination of these two model types has been selected as the most economical way of modelling. However, non-structural parts such as the rail pad and rail track (please refer to Chapter 2) in the FEM were not studied, but were omitted in the aforementioned research work. Therefore, this research report attempted to repeat all the existing modelling types but in addition more detail is added to each type of model such as the non-structural parts of the bridge such as rail, sleeper and stiffeners which were not included in other similar research works. A detailed description of OaSYS GSA, which is a FEM package utilised for this research report, is discussed in the remainder of this chapter.

The results obtained from the different FEM include the first vertical vibration mode shape and frequency. The bridge is believed to experience only the first mode while the train crosses the bridge. This is due to the fact that the calculated excitation frequencies for different train speeds are low as compared to the calculated natural frequency of the bridge as presented in Table 6-7 and Table 6-6 respectively. As a result higher modes of the bridge are not expected to be excited. This is comfirmed from the results shown in Figure 3.31. Therefore, higher modes were not discussed in this research. Modal analysis was also performed by considering only the self weight the bridge without any applied load in order to be able to compare this with the free vibration response of the bridge from field measured data. By unloaded bridge, it was meant in this study that only the self-weight of the structure was considered during the analysis. The first mode shapes and frequencies for each type of model can be seen in the FEM.

4.2 ABOUT THE FEM SOFTWARE PACKAGE

OaSYS GSA (GSA) is a commercially used software package with the capacity of designing and analysing a wide range of structures. To demonstrate the confidence in the package both static and modal analysis on a simply supported beam with known physical property such as dimension and moment of inertia is analysed and accurate results were obtained. For the purpose of this research, only modal analysis was performed using the student version of GSA. It uses eigenvalue analysis to calculate the dynamic natural frequencies and mode shapes. The modal analysis results are summarized in Chapter 5.

4.3 DESCRIPTION OF THE FEM

The type of bridge used to develop the FEM is the same bridge where the field measurements were taken. A detailed description of the bridge under discussion is included in Chapter 3. The modelling types used in this research report are classified as: Bridge FEM using beam elements and Bridge FEM using shell elements.

4.3.1 Bridge FEM using Beam Elements

In this type of model, each member of the structure is modelled as a beam element. The beam elements were used to create built-up sections to match the actual bridge. Elements were connected to each other at one node. During exercising the two FEM types, it was found that this method of modelling is easier to model the structure and extract static and dynamic responses as compared with the second type discussed in Section 4.3.2. Figure 4.1 & Figure 4.2 shows the FEM with beam elements with all the elements included.

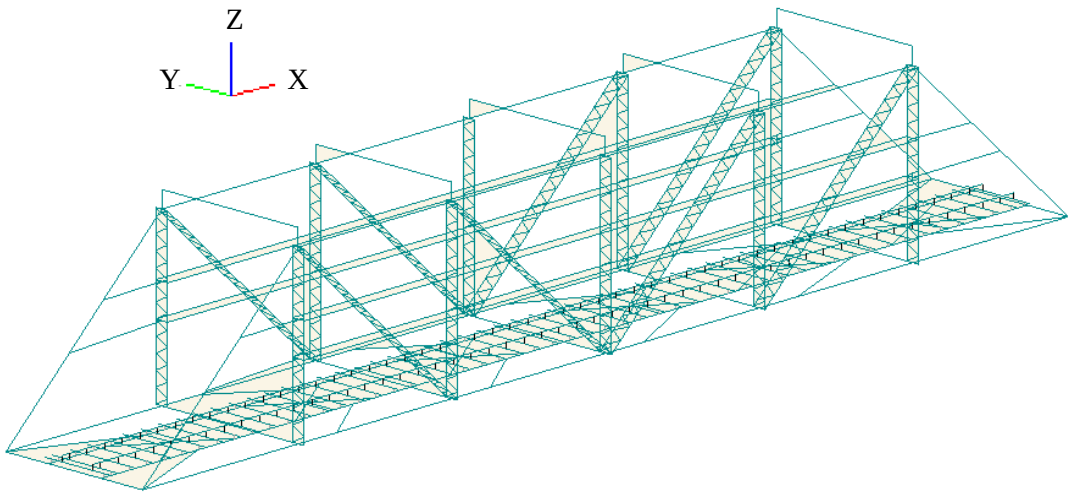

Figure 4.1: Bridge FEM using beam elements

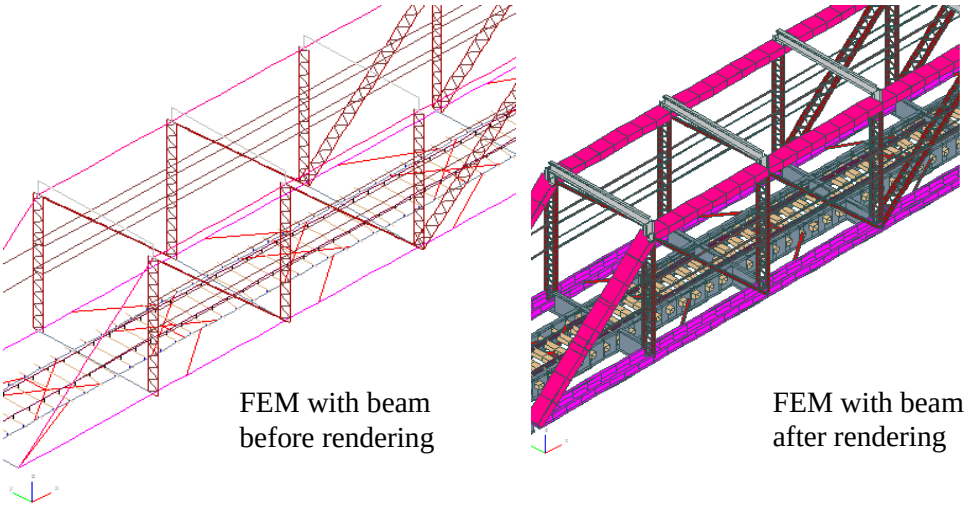

Figure 4.2: FEM using beam elements; before and after rendering

4.3.2 Bridge FEM using Shell Elements

When utilising this type of model, all the members in the FEM were made of shell elements, except for the web members, rail and sleeper, as shown in Figure 4.3. The shell elements were made of QUAD4 elements consisting of four sides and four nodes. Modelling the structure using the shell element model was a time-consuming exercise. However, it was found advantageous as it shows the static responses more clearly such as stress.

Figure 4.3 is a better representation of the bridge as specified in Chapter 3. It was made of mainly shell elements with all members of the bridges, including the main beam, cross beam, web members, top bracing, rail, sleeper, bracing and stiffener on both the bottom chord and cross beam being included. The rivet connections such as on the vertical web members were represented as a simple node to node connection in the FEM. Refer Figure 4.5. The standard universal beam dimension of size UB152x89x16 was taken for top bracing which is an assumed dimension as measurement was difficult to conduct safety wise as it is about 5600mm high above the top of bottom chord as shown in Figure 4.3. The complete FEM in both cases were analysed. In all models the walkway was ignored, assuming its existence has no significant effect on all of the measured responses.

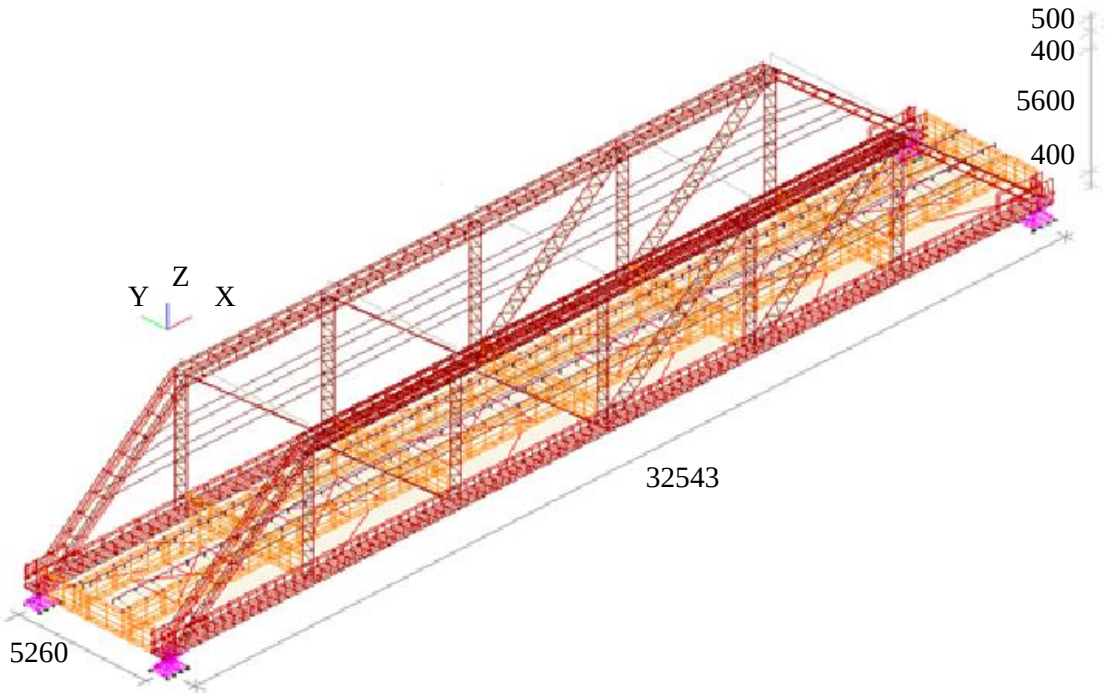

Figure 4.3: Bridge FEM using shell elements

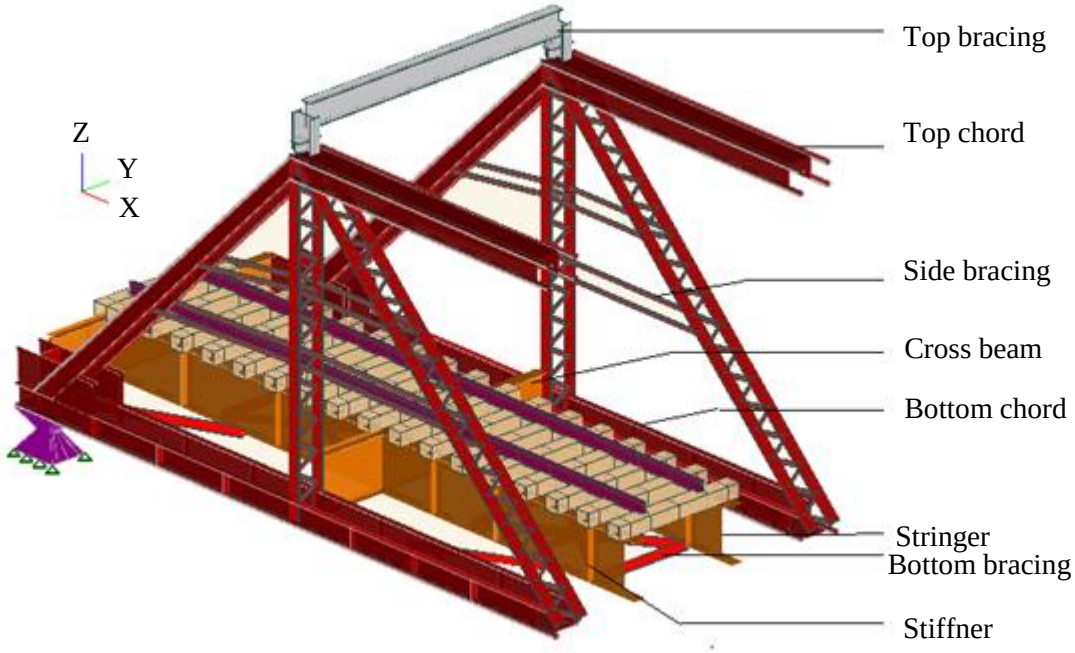

Figure 4.4: Section view of FEM using shell elements

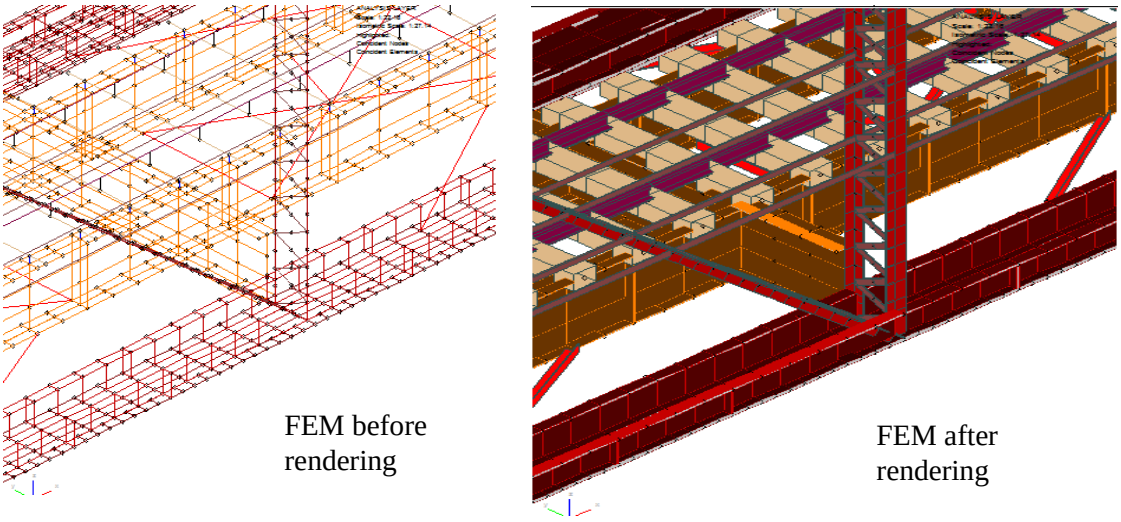

Figure 4.5: FEM using shell elements; bottom chord and cross beam

4.4 MATERIAL PROPERTY

Some of the common properties of the material used in the structure that should be considered during an elastic analysis are: Young's modulus, Poisson's ratio, density and the coefficient of thermal expansion.

All elements in the bridge FEM were made of steel with elastic isotropic model. Standard properties of steel were used such as: Young's modulus of 205MPa, Poisson's ratio of 0.3, density of 7850kg/m^3 and a coefficient of thermal expansion of 11.7×10^{-6} /°C (National Committee SABS SC59I, 2010). A unit mass of 57kg/m was taken for the rail.

Wooden sleepers and rail were the only exceptions in all FEM, where user-defined properties were required. The sleeper was assumed to be made of wood having an orthotropic model. For the purpose of simplification, all the properties in x, y and z direction were assumed to be equal. The properties are: Young's modulus of 9.6GPa, Poisson's ratio of 0.3, a density of 600kg/m^3 and a coefficient of thermal expansion of 5×10^{-6} /°C.

4.5 LOADINGS

Self-weight of the structure was used during modal analysis of FEM and computation of static deflection. The EI value is calculated from this deflection. The later one is further

discussed in Section 5.3 and Section 7.4.10. The self-weight of the structure in addition to load due to train were used to check the stress in the structure as discussed at the end of this section.

Here, the maximum arrangements of axle loads that the bridge can carry at once were considered. Please refer to the actual train configuration in Chapter 3 and compare this with the span of the bridge shown in Figure 4.3. The 12 vertical arrows in the Figure 4.6 represent the train axle loads resting on the full shell element model of the bridge. The self - weight is represented by GSA as a uniformly distributed loading all over the structure directed to gravity.

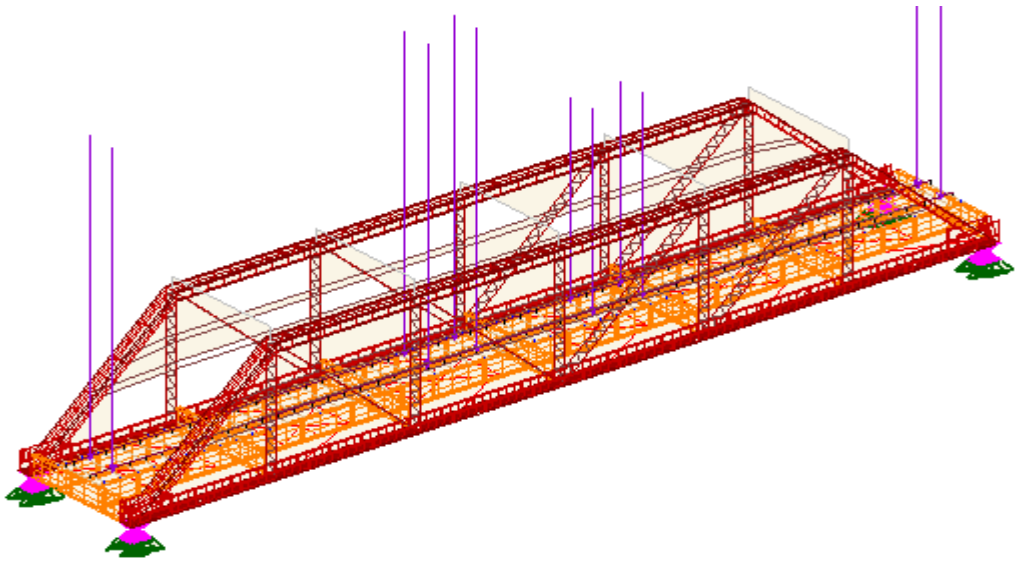

Figure 4.6: Representation of static loading due to train

As explained in Chapter 2, the steel that is used for Irene bridge has an ultimate tensile strength between 386MPa to 455MPa. Detail static analysis of the bridge was not the concern of the research. However the author has checked the maximum tensile stress obtained at the mid span of the bottom chord of the bridge and compares it to the specified ultimate strength of the steel. Please refer as shown in Appendix F.7 & Appendix F.8. This will not be discussed further in this study.

4.6 BOUNDARY CONDITIONS

Based on the visual observation of the bridge support as shown in Figure 4.7 which are visually similar at four corner, the author decide to use pin supports through out to simplify

the realistic condition. All supports were modelled therefore as pin supports where translation in the x, y and z direction is restricted and rotation about y axis is allowed. These models with all pin suppors are used for comparision in Chapter 7.

The author however believes the boundary conditions will have an influence on the results. The reader must therefore refer the results for models with different supports in Appendix F. For comparison purpose the two supports located adjacent to each other are modelled as roller supports where movement are allowed in the longitudinal direction and the natural frequency of the bridge is checked. The natural frequency result for the vertical vibration mode when two rollers and two pin supports are modelled gives 9.26Hz where as the result shown in the Table 4-1 gives 10.03Hz when all supports are modelled as pin with shell elements. Refer the outputs in the Appendix F. The model with two pin and two roller supports gives a closer results to both mathematical approaches and field measurement result. Please refer Table 7-1

Figure 4.7: Support condition of the actual bridge

In FEM using beam element, the top chord and bottom cord were connected at one node which makes a total of four boundary conditions assigned to four corners of the bridge. All supports were modelled as pin supports.

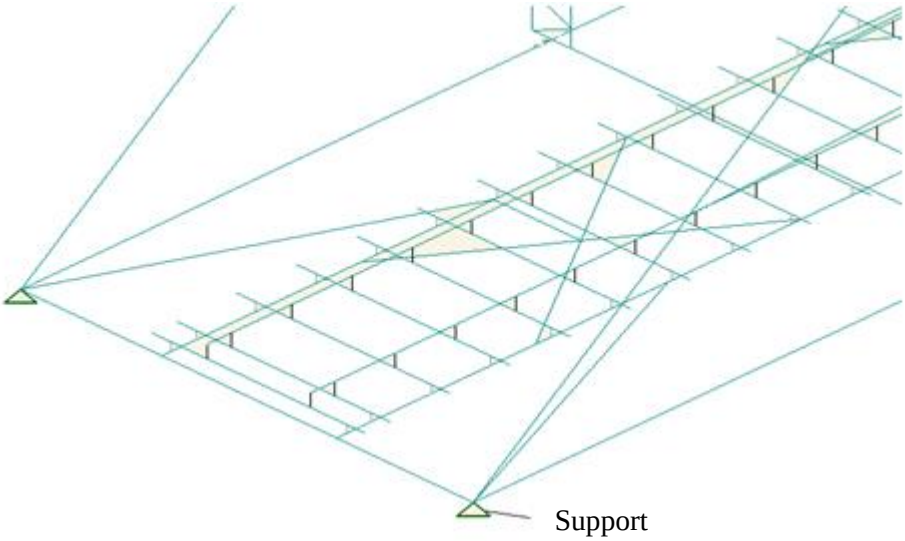

Figure 4.8: Support condition for FEM with beam elements

In the FEM using shell element, an assumed closer approximation to the support was modelled similar to the actual support is shown in Figure 4.9.

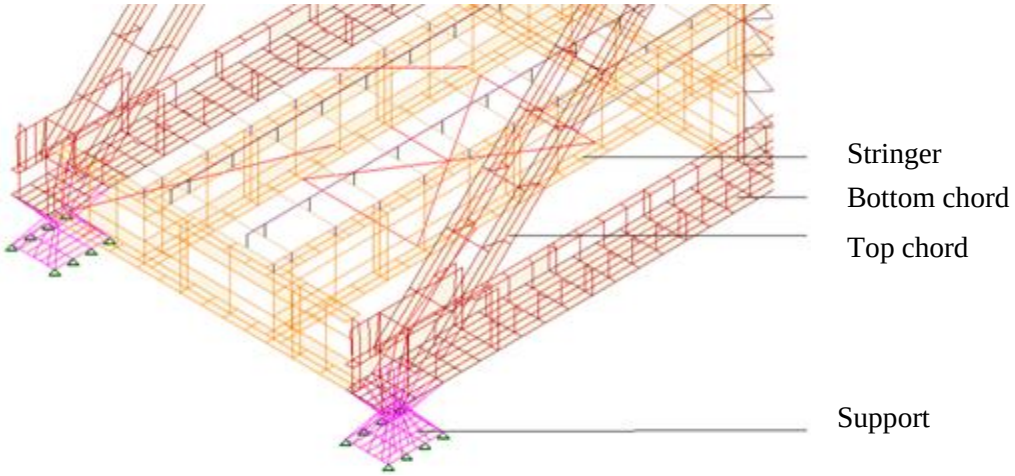

Figure 4.9: Support condition for FEM with shell elements

4.7 DESCRIPTION OF MODAL ANALYSIS INPUTS

In this section, results from all types of models analysed using OaSYS GSA are presented. Prior to each modal analysis, few parameters needed to be set. These included selecting the required number of modes, defining the way the mass effect is considered and defining the load cases. 50 modes selected randomly for modal analysis which was found to be sufficient to observe the first vertical vibration modes in the global z-direction.

There are three methods proposed by GSA for considering the mass effect on the modal response. One of these methods is a lumped mass approach, where the mass is lumped at nodes, where half of the mass of the element is distributed to each node and inertia is ignored. The second option is to calculate the mass from the shape function. In the second method, the mass and inertia of elements are accounted for. The difference in the result obtained from using the two options is found to be less than 0.2% and can be ignored. In addition, according to the GSA, calculating the mass from the shape function may lead to modes which involve the vibration of individual elements rather than the structure as a whole. Therefore, the lumped mass approach was selected for the simplicity of analysis. The third option is to ignore masses of all elements except mass elements. Therefore, this option was also ignored. An externally applied load from the train was also added during the analysis. Here, the train loads were defined as a live load .The loaded and unloaded bridge responses were observed from FEM.

4.8 MODAL ANALYSIS RESULTS

The modal analysis result from FEM for different kind of loadings explained in Section 4.5 is summarized in Table 4-1. During the modal analysis, the number of modes was set to run for the first 50 modes for each kind of loading and FEM types. Only the vertical mode of vibration is discussed in this dissertation as it is the major response resulted from the type of load under consideration which is train load. The other mode of vibration such as lateral and twist was ignored; assuming relatively minimum lateral or twisting force is present may be resulted due to the vertical load. The first natural frequencies of the bridge when subjected to the vertical vibration modes as obtained from the two types of models are presented in Table 4-1. The first vertical mode shape is presented in Figure 4.10.

Table 4-1: Natural frequencies of the bridge for vertical vibration

Description	**1st mode natural frequency [Hz]**
Bridge FEM using beam elements	10.06
Bridge FEM using shell elements	10.03

For unloaded bridge, the magnitude of natural frequency in the first vertical vibration modes show a higher frequency for FEM using beam elements by 0.08-1.2% as compared

to those that uses shell elements. Similar results were found by Kaliyaperumal *et al* (2008). A second important result that needs to be observed is the mode shapes as it is easier to visualize how the structure respond to specific type of loading. Figure 4.10 shows the mode shape for the first vertical bending mode.

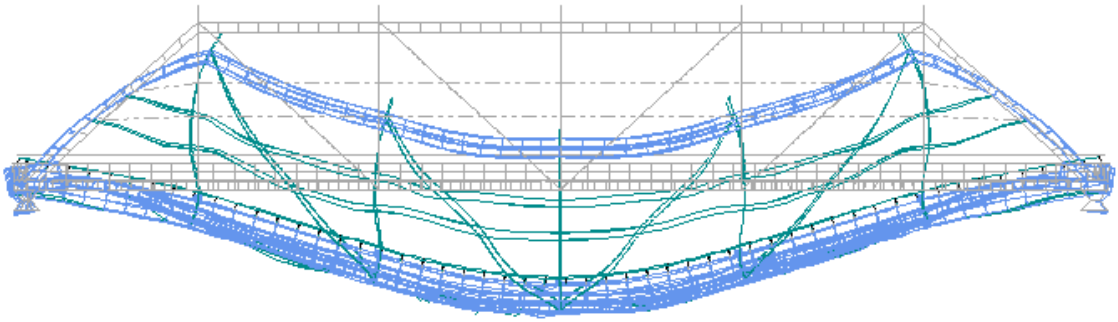

Figure 4.10: Mode shape for the first vertical bending mode

4.9 SUMMARY

In this Chapter, FEM which is one of the three methodologies to perform dynamic analysis as described in Chapter 1 is discussed. The three-dimensional FEM of the bridge similar to the field measured bridge discussed in Chapter 3 is modelled using the OaSYS GSA software. Then the modal analysis is performed from which the modal frequency and mode shapes of the bridge is obtained. During modal analysis only the self-weight of the structure is used. The flexural rigidity is calculated from the static deflection of the FEM due to the self-weight of the bridge.

The modelling types used in this research report are named as: Bridge FEM using beam elements and Bridge FEM using shell elements. The members modelled are the web members, the bottom and top chord, stringer, bottom top and side bracings, rail, sleeper and stiffener. These are discussed in Section 4.3. The different parameters used during FEM such as material types, loadings and boundary conditions are discussed in Section 4.4 to Section 4.6.

The results show that for unloaded bridge, the magnitude of natural frequency in the first vertical vibration modes show a higher frequency for FEM using beam elements by 0.08-1.2% as compared to those that uses shell elements.

5 MATHEMATICAL APPROACH

5.1 INTRODUCTION

In this chapter, a dynamic analysis of a single span simply supported steel truss railway bridge when subjected to metro rail is presented using the one dimensional mathematical approach. Mathematical way of analysing the dynamic property and responses of structure subjected to rapid train is one of the main motives for the inclusion of this chapter.

There are a few basic dynamic principles that were used to model the situation as proposed by Chopra (2007), Yang *et al* (2004), Kargarnovin *et al* (2005) and Michaltsos *et al* (2009). The principle of virtual displacement is applied as a basis for the derivation of the equation of motion, which assisted in performing a time history analysis of the train passing along the bridge. Parameters that may alter the bridge response are span length of the bridge, mass of the bridge, weight of the train or magnitude of axle load, stiffness of the bridge and speed of the train. The effect of variation of bridge parameters on bridge dynamic response is compared by selecting realistic parameters from different articles as presented in Chapter 6. Two kinds of loadings were used for comparison; a single load moving and a successive load representing the wheel axle loads on the bridge. The applied force from wheel loads which is called ‘loading’ in the remainder of this chapter is expressed as forcing function using Dirac delta function. The wheel loading creates a forced vibration on the system. The equation of motion developed is utilized to extract some of the dynamic responses of the bridge such as displacement and acceleration. The procedure for determining these responses based on the equation developed is discussed in Chapter 6. Dynamic property of structure such as natural frequency is also obtained from the generalized mass, length and stiffness. The calculations and comparison with field measured and FE model result from Chapter 3 and Chapter 4 is included in Chapter 6.

Assumptions and generalization were made on the mass, length and stiffness of the bridge as proposed by Chopra (2007), which forms a core foundation for discussion in this chapter. In addition, the stiffness of the bridge is approximated using backward calculation from the maximum deflection obtained from FEM static analysis result. The equation of motion developed is based on the assumption that the bridge is a simply supported uniform cross section with generalized properties. This is discussed further in this chapter. The following chapter also explains the shape function which is used in generalization of the properties of structure. The assumption of the shape function is based on the shape of deflection of the

entire bridge globally when subjected to train loading as prescribed by Chopra (2007). The maximum static response of the structure, mainly deflection, is calculated separately. All the mathematical approaches in this report do not consider damping. However, the effect of damping is compared based on the result previous literature as discussed in Chapter 2.

5.2 SIMPLIFIED MODEL OF BRIDGE UNDER MOVING LOAD

A single span simply supported steel truss railway bridge subjected to single axle load, P_0, moving at a constant speed (V) can be simplified as shown in Figure 5.1, under the assumption of linear elastic model where axial force can be neglected. The bridge is assumed to have a uniform cross section with constant $m(x)$ and $EI(x)$ with some assumptions and approximations made as stated in the next section.

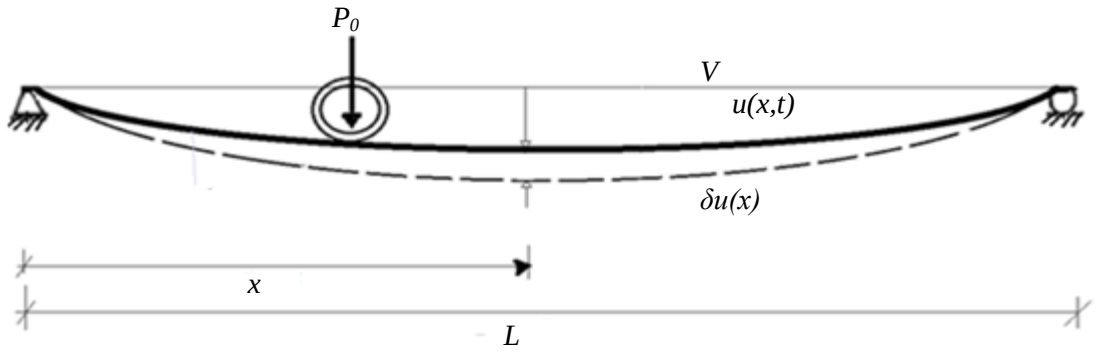

Figure 5.1: Simplified model of a simply supported bridge subjected to moving load

In Figure 5.1:

x = Distance from one edge of bridge where the response is required

L = Span of the bridge

$u(x,t)$ = Displacement at distance *'x'* and time *'t'*

$\delta u(x)$ = Virtual displacement or fictitious displacement

P_0 = Axle load moving

$m(x)$ = Mass of the bridge per unit length

$EI(x)$ = Flexural rigidity of bridge per unit length

5.3 APPROXIMATING THE BRIDGE WITH MDOF TO A GENERALIZED SDOF

A steel truss railway bridge is considered to be a complex system with an infinite number of DOF. The system can deflect in an infinite variety of shapes and one should consider it as a MDOF for exact analysis of the system. This may also mean dealing with infinite number of natural frequencies and modes of vibration matching the infinite deflected shapes. However, in this research work, the system is simplified to a generalised system proposed by Chopra (2007) from which an approximate result for dynamic responses is obtained. This is performed by restricting the deflections of the system in vertical downward direction to a single shape function which is discussed below.

This approximation of the MDOF system is performed by treating the system as a generalized SDOF. The method gives more accurate results for an assemblage of rigid bodies supported, such that it can deflect in one shape, while a system with distributed mass and flexibility will give approximate results. Therefore, in order to approximate the system to a generalized SDOF, the following assumptions were made:

a. Bridge properties such as EI and m were approximated. The flexural rigidity (EI) is back ward calculated from maximum deflection obtained using FEM static analysis when the bridge is subjected to self-weight only. A standard beam table deflection formula for a simply supported beam under uniformly distributed load is applied for backward calculation of EI. Similarly, from the same static analysis, the mass is calculated by summing up all the reaction obtained under self-weight of the bridge. The total mass is also checked by adding the volume of each element and multiplies it with steel unit weight of 7850kg/m^3. The sleepers volume were also added and multiplied with the wood unit weight of 600kg/m^3 as described in Section 4.4. The deflection formula used is $\Delta = 5\omega_b L^4 / 384EI$ where Δ equals deflection of the bridge taken as 3.5mm from FEM result when the bridge is subjected to self-weight. ω_b stands for distributed load which in this case is taken as the self-weight of the bridge calculated as 1879 kg/m, L is a span of the bridge equal to 32.5 m and E equals 205GPa as referred in Section 4.4. The value calculated for I is equal to 0.38m^4. Section 7.3.10 can be referred for different values of I calculated from different values of deflections.

b. The bridge is assumed to deflect significantly in the vertical direction as compared to deflections in other direction as a result of the axle load which is vertically downward. The shape of this vertical deflection is summarized into one shape

function which is discussed at the end of this section. In this way, deflection can be related to single generalized displacement coordinate *z(t)* through shape function which gives:

$$u(x,t) = \psi(x) * z(t) \qquad \text{Equation 5-1}$$

If we can define displacement at any location in the system in terms of generalized displacement coordinate *z(t)* through shape function $\psi(x)$, then we call the system a generalized SDOF system.

c. The rail is assumed to have no roughness, irregularity or discontinuity. The relevance of these parameters on the response of the bridge is further explained in Section 2.7.3 and Section 7.3.3 to Section 7.3.4.

Chopra (2007) explained the shape function for a simply supported beam with a uniform cross section as a half sine curve written as $\psi(x) = \sin(\pi x / L)$. This shape function is the approximate shape of fundamental natural vibration mode of simply supported beam. It is dependent on the boundary condition which indirectly reflects the deflected shape of beam when subjected to vertically downward loads like the axle load of the train on the bridge. For instance, a deflection of cantilever beam cannot have a shape of half sine curve. Here, a simply supported beam indicates a beam in which all translation in x, y and z directions of one support is restrained and in the other support only translation in the y and z direction is restrained.

It is important to check the mass ratio of the vehicle to bridge to check if it is large. As explained in Section 2.3 of Chapter 2, a large mass ratio indicates that the bridge sub-system or vehicle's response is influenced easily by the vehicle-bridge interaction. However this research is limited to simulation of the movement in a generalized system of bridge as referred to in Chapter 5. The mass ratio is calculated as follows: mass of vehicle is calculated by adding the total mass of axle loads that can rest on the bridge. The maximum number of axle loads that can rest on the bridge at once is six, meaning three axle loads from one coach and three axle loads from the second coach as shown in Figure 5.2. The worst case scenario is three axles from a fully loaded motor coach and three axles from a fully loaded trailer, giving a mass ratio of the train to bridge equal to 1.58 to 1. Please refer to Chapter 6 Section 6.2 for the calculated axle loads.

The mass, length and stiffness of the structure are properties of the structure that have a direct influence on the dynamic behaviour of structure. From these properties, a natural frequency of the structure can also be calculated, which is the first step needed in any dynamic analysis. The terminology for these properties of the structure need to be changed to generalised mass, length and stiffness. These formula for generalized properties are derived from the equations presented in Section 5.6 where each property relates to the shape function of the structure selected for a specific restricted deflection shape assumed (i.e. vertically down in this case) and integrating it to the entire length of the beam or structure. The calculation is presented as follows (Chopra, 2007):

Generalised Mass

$$\tilde{m} = \int_0^L m(x)[\psi(x)]^2 dx$$

$$\tilde{m} = \int_0^L m(x)\sin^2(\pi x/L)dx = mL/2 \qquad \text{Equation 5-2}$$

Where:

$\tilde{m}$ = Generalised mass of bridge

$\psi(x)$ = Shape function of the bridge

Generalised Stiffness

Here stiffness is calculated based on the approximated EI as follows.

$$\tilde{k} = \int_0^L EI(x)\left[\psi''(x)\right]^2 dx$$

$$\tilde{k} = \int_0^L EI(\pi^2/L^2)^2 \sin^2(\pi x/L)dx = \pi^4 EI/2L^3 \qquad \text{Equation 5-3}$$

Where:

$\tilde{k}$ = Generalised stiffness of bridge

EI = Flexural rigidity of the structure

L =Span length of bridge

Natural (Fundamental) Frequency

Natural frequency of a structure with uniform and homogenous cross section is determined from the following formula (Chopra, 2007).

$$\omega_n = \sqrt{\frac{\tilde{k}}{\tilde{m}}} = \frac{\pi}{L^2}^2 \sqrt{\frac{EI}{m}}$$ Equation 5-4

Numerical example is attached in Appendix A.1.

5.4 LOADINGS

In this section, force functions are presented to generalize the two types of loading that were considered in the equation of motion developed in the next section. This is later used for a time history analysis of the system presented in the next chapter. These functions were developed based on the Dirac delta function (Chopra, 2007 and Yang *et al*, 2004).

The two type of loading considered were:

a. Single moving load
b. Successive moving load representing the actual train configuration

Single moving load

A single moving load crossing a bridge can be expressed as follows (Chopra (2007) and Yang *et al* (2004)). Please refer Figure 5.1 above.

$$P(x,t) = \begin{cases} P_0\delta(x-vt) & 0 \le t \le t_d \\ 0 & t \ge t_d \end{cases}$$ Equation 5-5

Where:

$t_d = L/V$ = Time to cross the bridge

$\delta(x-Vt)$ = Dirac delta function centred at x= vt

This force can be changed to a generalized force for the entire span of the bridge, in the same way that the mass and stiffness were generalized previously. Therefore, the generalized force becomes:

$$\widetilde{P}(t) = \int_0^L P(x,t)\psi(x) \qquad \text{Equation 5-6}$$

$$\widetilde{P}(t) = \begin{cases} \int_0^L P_0 \delta(x - vt)\sin(\pi x/L) & 0 \le t \le t_d \\ 0 & t \ge t_d \end{cases}$$

$$\widetilde{P}(t) = \begin{cases} P_0 \sin(\pi V t/L) = P_0 \sin(\pi t/t_d) & 0 \le t \le t_d \\ 0 & t \ge t_d \end{cases}$$

As stated in Equation 2-5, the term π/t_d gives an excitation (forcing) frequency ω which is a function of span length of the bridge and the velocity of the travelling train (Chopra, 2007 and Yang *et al*, 2004).

Therefore the load can be rewritten as:

$$\widetilde{P}(t) = \begin{cases} P_0 \sin(\omega t) & 0 \le t \le t_d \\ 0 & t \ge t_d \end{cases}$$

This force, $\widetilde{P}(t)$, is discussed in Chopra (2007) in terms of pulse duration t_d where $\omega = \pi/t_d$ and P_0 is the amplitude or maximum value of the force which in this case is the axle load.

Successive moving load representing the actual train configuration

The general arrangement of the train set is briefly explained in Chapter 3. The train is modelled as the composition of two subsystems of wheel loads of constant intervals, $d = L_c + L_d$, with one subsystem consisting of all the front wheel assemblies and the other the rear assemblies. The representation of L_c and L_d are shown in Figure 5.2.

Where:

L_c =denote the distance between the two wheel assemblies of a coach, and

L_d =the distance between the rear wheel assembly of a coach and the front wheel assembly of the following coach.

.

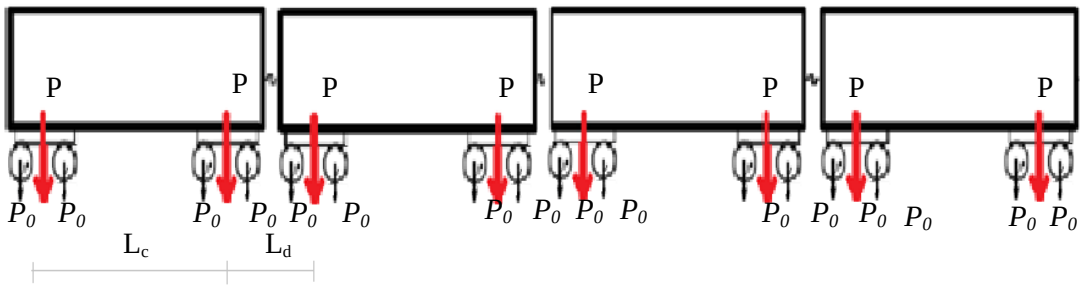

Figure 5.2: Loading system replacing the actual wheel set system

The equation given by Yang *et al* (2004) is valid for identical axle loads spaced at equal intervals car length d, whereas the simple addition from Chopra (2007) can be applied to different axle loads and spacing. The axle loads utilized by the two types of equations: equation by Yang *et al* (2004) and simple addition are termed as 'P' which are a series of lumped loads which combines the two axle loads on both front and rear bogies and 'P_0' which takes each axle load as it is respectively as shown in Figure 5.2. The magnitude of P_0 however may vary depending on the train set arrangement as explained at the end of Section 5.3.

One of the criteria to use to the equation from Yang *et al* (2004) presented at the end of Section 5.5 is to make sure that $L \leq 2d$. In this research, the train configuration presented in Chapter 3 indicates L_c =13563.5 mm and L_d =5863 mm which gives d=19426.5. Since the span of the bridge is L=32.5. $L \leq 2d$

5.5 EQUATION OF MOTION

The system needs to be represented in an equation of motion to determine the dynamic responses of structure such as: displacement, velocity or acceleration. The equation of motion is derived from dynamic equilibrium of the system at instant of time based on D'Alembert's principle. Following the principle, the system is in dynamic equilibrium at any instant of time under the action of the internal resisting bending moments and the fictitious inertia forces.

5.6 DYNAMIC DISPLACEMENT

In this section, an equation of motion is derived based on the principle stated in Yang *et al* (2004) and Chopra (2007). The author added the loading function which is discussed in Section 5.3 in to the equation of motion and further simplified the quation. This equation of motion is used to determine the dynamic displacement of the bridge for the two type loads under consideration. The equation can be derived by using the virtual displacement principle. The principle states that if the system in equilibrium is subjected to virtual displacement $\delta u(x)$, the external virtual work δW_E is equal to internal virtual work δW_I.

The external work is resulted from the applied force, $P(x, t)$, and the fictitious inertia force, $f_I(x, t)$, which results in actual deflection, $u(x,t)$, and virtual displacement, $\delta u(x)$ respectively. The internal work, W_I, at any *'t'* and *'x'* is the work done due to internal bending moment, $M(x,t)$, which causes the curvature of the bridge defined with $\delta \kappa(x)$. In this case, the internal work done due to shear deflection is neglected. The generalized form of external and internal work of system is described as δW_E and δW_I respectively. Following the principle of virtual displacement (Chopra, 2007):

External virtual work, δW_E = Internal virtual work, δW_I Equation 5-7

The principle of virtual displacement is expressed in Equation 5-7. The total external virtual work which is symbolically represented as δW_E, is calculated by summing up the external works at each instant *'t'* and *'x'* along the length of the bridge. This is shown in Equation 5-8.

$$\delta W_E = \int_0^L f_I(x, t)\, \delta u(x) dx \qquad \text{Equation 5-8}$$

Similarily the total internal virtual work done by the bridge is shown in Equation 5-9..

$$\delta W_I = \int_0^L M(x, t)\, \delta \kappa(x) dx \qquad \text{Equation 5-9}$$

The fictious inertia force presented in Equation 5-10 is the taken as the algebraic sum of the external force excitation and the inertia force resulted due to acceleration of the bridge.

$$f_I(x,t) = -m(x)\ddot{u}(x,t) + P(x, t) \qquad \text{Equation 5-10}$$

Whereas the internal bending moment is expressed in Equation 5-11.

$M(x, t) = EI(x)u''(x,t)$ Equation 5-11

The virtual displacement and virtual curvature are presented in Equation 5-12 and Equation 5-13 respectively.

$\delta u(x) = \psi(x)\, \delta z$ = virtual displacement Equation 5-12

$\delta \kappa(x) = \psi''(x)\, \delta z$ = virtual curvature Equation 5-13

$P(x, t)$ represents the external force excitation (axle loads expressed as a function 'x' and 't'). Refer Equation 5-5 and Equation 5-13.

$u''(x,t) = \psi''(x)\, z(t)$ = curvature expressed as second derivative of displacement with respect to distance

Equation 5-14

$\ddot{u}(x,t) = \psi(x)\, \ddot{z}(t)$ = acceleration expressed as second derivative of displacement with respect to time

Equation 5-15

Equation 5-17 is further simplified as follows:

$\delta W_E = \delta W_I$

$$\int_0^L f_I(x, t)\, \delta u(x) dx = \int_0^L M(x, t)\, \delta\kappa(x) dx$$

$$-\int_0^L m(x)\ddot{u}(x, t)\, \delta u(x) dx + \int_0^L P(x, t)\, \delta u(x) dx = \int_0^L EI(x)u''(x, t)\, \delta\kappa(x) dx$$

$$-\int_0^L m(x)\psi(x)\ddot{z}(t)\psi(x)\, \delta z dx + \int_0^L P(x, t)\, \psi(x)\delta z dx = \int_0^L EI(x)[\psi''(x)]^2\, z(t)\delta z$$

Taking out all δz from both sides of the above equation and rewriting the rest of the equation in terms of generalized mass, stiffness and load as defined in Section 5.5 gives:

$$-\tilde{m}\ddot{z}(t) + \tilde{P}(t) = \tilde{k}z(t)$$

Therefore equation of motion for undamped system of the bridge can be written as:

$$\tilde{m}\ddot{z}(t) + \tilde{k}z(t) = \tilde{P}(t) \qquad \text{Equation 5-16}$$

The mathematical solution is given in Chopra (2007) for a similar equation written in terms of 'u' instead of 'z' as $m\ddot{u}(t) + ku(t) = P(t)$ developed for a SDOF system subjected to half-cycle of sinusoidal force, $P(t) = P_0 * \sin(\omega t)$. This expression is the same as the mathematical function described for moving load in Equation 5-6. The initial condition is considered at rest. We can apply the same solution by changing the notation 'u' to 'z' as follows for different type of loading considered:

Single moving load

Substituting the generalized loading in the above equation from Section 5.4, we get the following equation which is divided in two phases. The two phases considered were a forced vibration phase ($0 \le t \le t_d$) and free vibration phase ($t \ge t_d$).

$$\tilde{m}\ddot{z}(t) + \tilde{k}z(t) = P_0 * \sin(\omega t) \qquad \text{for } 0 \le t \le t_d$$

$$\tilde{m}\ddot{z}(t) + \tilde{k}z(t) = 0 \qquad \text{for } t \ge t_d$$

Each equation is further classified according to two cases where:

Case I. $\omega \equiv \frac{\pi}{t_d} \neq \omega_n$ or $\frac{t_d}{T_n} \neq 1/2$ i.e. when excitation frequency is different from natural frequency and

Case II. $\omega = \omega_n$ or $\frac{t_d}{T_n} = 1/2$

Therefore:

Case I: $\omega \equiv \frac{\pi}{t_d} \neq \omega_n$ or $\frac{t_d}{T_n} \neq 1/2$

$$\frac{z(t)}{(Z_{st})_0} = \frac{1}{1 - \left(T_n / 2t_d\right)^2}\left[\sin\left(\pi \frac{t}{t_d}\right) - \frac{T_n}{2t_d}\sin\left(2\pi \frac{t}{T_n}\right)\right], \qquad \text{for } t \le t_d$$

$$\frac{z(t)}{(Z_{st})_0} = \frac{\left(T_n/t_d\right)\cos\left(\pi t_d/T_n\right)}{\left(T_n/2t_d\right)^2 - 1}\sin\left[2\pi\left(\frac{t}{T_n} - \frac{1}{2}\frac{t_d}{T_n}\right)\right] \qquad \text{for } t \geq t_d$$

Case II: $\omega = \omega_n$ or $\frac{t_d}{T_n} = 1/2$

$$\frac{z(t)}{(Z_{st})_0} = \frac{1}{2}\left(\sin\frac{2\pi t}{T_n} - \frac{2\pi t}{T_n}\cos\frac{2\pi t}{T_n}\right) \qquad \text{for } t \leq t_d$$

$$\frac{z(t)}{(Z_{st})_0} = \frac{\pi}{2} \qquad \text{for } t \geq t_d$$

The displacement and velocity at t=t_d is obtained by substituting the above equation in the forced vibration equation. Some mathematical manipulation gives the free vibration equation included with the two cases above.

In the above equations (Chopra, 2007):

T_n = Natural period calculated from the natural frequency $= 2\pi/\omega_n$

$(Z_{st})_0$ = Static deflection due to $P_0 = P_0/\tilde{K} = P_0 2L^3/\pi^4 EI$

After making the above substitutions, the generalized displacement *z (t)* for both cases is rewritten as:

Case I: $\omega \equiv \frac{\pi}{t_d} \neq \omega_n$ or $\frac{t_d}{T_n} \neq 1/2$

$$z(t) = \frac{2P_0 L^3 \omega_n^2}{\pi^4 EI} * \frac{1}{\omega_n^2 - \left(\frac{\pi V}{L}\right)^2} * \left[\sin\left(\frac{\pi V t}{L}\right) - \left(\frac{\pi V}{L\omega_n}\right)\sin(\omega_n t)\right] \qquad \text{for } t \leq t_d$$

Equation 5-17

$$z(t) = -\frac{2P_0 L^3 \omega_n}{\pi^4 EI} * \frac{\left(\frac{2\pi V}{L}\right) * \cos\left(\frac{\omega_n L}{2V}\right)}{\omega_n^2 - \left(\frac{\pi V}{L}\right)^2} * \sin\left(\omega_n\left(t - \frac{L}{2V}\right)\right) \qquad \text{for } t \geq t_d$$

Equation 5-18

Case II: $\omega = \omega_n$ or $\frac{t_d}{T_n} = 1/2$

$$z(t) = \frac{P_0 L^3 \omega_n}{\pi^4 EI} * \left(\sin(\omega_n t) - \omega_n t \cos(\omega_n t)\right) \quad \text{for } t \le t_d$$

Equation 5-19

$$z(t) = \frac{P_0 L^3 \omega_n}{\pi^3 EI} * \cos(2\pi(\frac{\omega_n t}{2\pi} - \frac{1}{2})) \quad \text{for } t \ge t_d$$

Equation 5-20

The deflection $u(x,t)$ at any point along the span of the bridge can therefore be obtained from the generalized displacement coordinate *z(t)* through the shape function as follows:

$$u(x,t) = \psi(x) z(t)$$

Equation 5-21

Successive moving loads representing the actual train configuration

The effect of the train load is taken in to consideration by summing up the effect of each axle load entering and leaving the bridge. Two procedures can be followed alternatively: (1) simple addition of all wheel loads effect by using the equation derived for single load by Chopra (2007), and (2) using the equation developed by Yang *et al* (2004) as discussed below. Similarly, the velocity and acceleration response can be obtained by differentiating the equation used to determine displacement response.

The equation of motion written by Yang *et al* (2004) is similar to the one developed for a single moving load by Chopra (2007). However, the first one utilized this concept further for successive moving loads such as axle load of train. This is also applied by Michaltsos *et al* (2009).

Following the work of Yang *et al* (2004), the generalized displacement of bridge when subjected to the train load neglecting the effect of damping and considering first mode of vibration can be written as:

$$z(t) = \frac{2PL^3 \omega_n^{\,2}}{\pi^4 EI} * \frac{1}{\omega_n^{\,2} - \left(\frac{\pi V}{L}\right)^2} * \left(\tilde{P}(V,t) + \tilde{P}(V, t - t_c)\right)$$

Equation 5-22

Where:

$\widetilde{P}(V,t)$ = Contribution of the front wheel sets

$$= \sum_{K=1}^{N} \{([\sin(\frac{\pi V}{L} * (t - t_j)) - (\frac{\pi V}{L\omega_n}) * \sin\omega_n (t - t_j)] * H(t - t_j)$$

$$+ [(\sin(\frac{\pi V}{L} * (t - t_j - \frac{L}{V})) - (\frac{\pi V}{L\omega_n}) * \sin\omega_n (t - t_j - \frac{L}{V})] * H(t - t_j - \frac{L}{V})\}$$

$\widetilde{P}(V, t - t_c)$ = rear wheel load expression expressed by substituting $t - t_c$ in place of t in $\widetilde{P}(V,t))$

P = series of lumped loads as explained in Section 5.3,

x = the coordinate of the beam,

H (•) = a unit step function,

t_j = $(j-1) * \frac{d}{V}$ =the arriving time of the j[th] load at the beam or bridge

N = the total number of moving loads considered.

t_c = $\frac{L_c}{V}$ = a time lag between the front and rear wheel two sets of moving loads

$H(t - t_j)$ =j[th] moving load action entering the beam

$H(t - t_j - \frac{L}{V})$ =j[th] moving load action leaving the beam

As explained in Section 5.4, the term P is used here in place of the term P_0, which is used as a single load model. However, the two terms are different in magnitude. The first one represents the lumped load from the first two pair of the front bogie and the later one represents one full axle load. Please refer Appendix A.4 to refer the mathematical simplification made by the author to compare the equations derived by Yang *et al* (2004) vs. Chopra (2007)

Similarly, the deflection $u(x,t)$ at any point along the span of the bridge can therefore be obtained from the generalized displacement coordinate *z (t)* through the shape function as follows:

$u(x,t) = \psi(x) z(t)$

5.7 ACCELERATION

The author performed a double differentiation of Equation 5-17 and Equation 5-18 from which the acceleration required for both type of loading is determined. These equations are

Equation 5-23 and Equation 5-24. Here only the first case is presented for the reasons explained in Chapter 6.

Single moving load

Case I: $\omega \equiv \frac{\pi}{t_d} \neq \omega_n$ or $\frac{t_d}{T_n} \neq 1/2$

$$\ddot{z}(t) = \frac{2P_0 L^3 \omega_n^2}{\pi^4 EI} * \frac{1}{\omega_n^2 - \left(\frac{\pi V}{L}\right)^2} * \left[-\left(\frac{\pi V}{L}\right)^2 * \sin\left(\frac{\pi V t}{L}\right) + \frac{\pi V}{L} * \omega_n * \sin(\omega_n t) \right]$$

for $t \leq t_d$

Equation 5-23

$$\ddot{z}(t) = \frac{2P_0 L^3 {\omega_n}^3}{\pi^4 EI} * \frac{\left(\frac{2\pi V}{L}\right) * \cos\left(\frac{\omega_n L}{2V}\right)}{\omega_n^2 - \left(\frac{\pi V}{L}\right)^2} * \sin\left(\omega_n \left(t - \frac{L}{2V}\right)\right)$$

for $t \geq t_d$

Equation 5-24

The acceleration $\ddot{u}(x,t)$ at any point along the span of the bridge can therefore be obtained from the generalized displacement coordinate z (t) through the shape function as follows:

$$\ddot{u}(x,t) = \psi(x)\ddot{z}(t)$$ Equation 5-25

Successive moving load representing the actual train configuration

$$\ddot{z}(t) = \frac{2PL^3 {\omega_n}^2}{\pi^4 EI} * \frac{1}{{\omega_n}^2 - \left(\frac{\pi V}{L}\right)^2} * \left(\tilde{\tilde{P}}(V,t) + \tilde{\tilde{P}}(V, t - t_c)\right)$$ Equation 5-26

Where:

$$\tilde{\tilde{P}}(V,t)) = \sum_{K=1}^{N} \{ [-\left(\frac{\pi V}{L}\right)^2 \sin(\frac{\pi V}{L} * (t - t_j)) + (\frac{\pi V \omega_n}{L}) * \sin \omega_n (t - t_j)] * H(t - t_j)$$

$$+ [-\left(\frac{\pi V}{L}\right)^2 \sin(\frac{\pi V}{L} * (t - t_j - \frac{L}{V})) + (\frac{\pi V \omega_n}{L}) * \sin \omega_n (t - t_j - \frac{L}{V})] * H(t - t_j - \frac{L}{V}) \}$$

Similarly, the acceleration $\ddot{u}(x,t)$ at any point along the span of the bridge can therefore be obtained from the generalized displacement coordinate z (t) through the shape function as follows:

$$\ddot{u}(x,t) = \psi(x)\ddot{z}(t)$$

5.8 SUMMARY

This Chapter discusses the principles applied to develop the mathematical approach used to analyse the dynamic properties and responses of structure subjected to train loads. As discussed in Section 5.2 and Section 5.3, the first step taken during this approach is to simplify the bridge and train system to a single span simply supported generalized beam. In order to proceed with this step, the bridge is assumed to have a uniform cross section with constant mass and flexural rigidity. The bridge is assumed then to deflect to a single shape which is assumed to be similar to a half sine curve. This assumption of a generalized system is expressed using the generalized properties of the bridge as expressed in Equation 5-2, Equation 5-3 and Equation 5-4. These three equations are used in Chapter 6.

The train axle loads on the bridge are assumed as successive moving loads on the beam. For comparison, a single load moving on a beam at different speeds is also analysed as discussed in Section 5.4. The function for the load is developed using a Dirac delta function by defining the function of a unit load while it is on the beam and after it leaves the beam as presented in Equation 5-5. An equation of motion which is shown in Equation 5-16 is developed to determine the dynamic responses of structure such as: displacement or acceleration using the concept of dynamic equilibrium of the system based on D'Alembert's principle. The main concept used while developing equation of motion is the principle of virtual displacement which is summarized in Equation 5-7. Then using the formulas from Equation 5-8 to Equation 5-15, the equations of motion presented in the Equation 5-16 are derived. However this is a general formula and one cannot put easily the parameters to get out put immediately. Therefore these are further simplified to explicit formulas as shown from Equation 5-17 to Equation 5-26 which is used together with Equation 5-1 to get the required response discussed in later chapter.

The displacement of the bridge is calculated by two different methods: simple addition and using equation from Yang *et al* (2004). The simple addition method consists of calculating the displacement of the bridge due to the train axle loads using the Equation 5-21 from the generalized displacement coordinate (Z(t) of bridge calculated using Equation 5-17 and

Equation 5-18. This is further discussed in the Appendix B.1. The displacement results obtained from Yang *et al* (2004) is calculated using the equation (Equation 5-22). This is also further discussed in the Appendix B.1. Similarity the acceleration results are obtained using Equation 5-22 & 5-23.

The formulas that are selected to be used in Chapter 6 are mainly; Equation 5-4 to compare the effect of parameters on natural and excitation frequency of the bridge, Equation 5-1 to determine the displacement of the bridge, Equation 5-17 & Equation 5-18 to determine the generalized displacement coordinate of the bridge which will be used as an input to the Equation 5-4 this will form part of the simple addition method discussed, Equation 5-23 and Equation 5-24 are used to calculate the corresponding generalized acceleration coordinate which will be used as an input for Equation 5-25.

6 APPLICATION OF MATHEMATICAL APPROACH FOR DIFFERENT PARAMETERS

6.1 INTRODUCTION

The following chapter explains how a time history analysis of a single span simply supported steel truss railway bridge when subjected to a single load and train load is performed. The equations developed in the preceding chapter are utilized to determine dynamic responses of the structure namely displacement and acceleration using the time history analysis. All parameters that were considered are also presented. The dynamic property of the structure such as a natural frequency is also calculated and will be discussed in the following chapter. A few example calculations are attached in Appendix A.

6.2 PARAMETERS

The different parameters that affect the dynamic responses were compared and discussed for mid-span of the bridge. In all cases, the flexural rigidity of the bridge is assumed as constant; however the bridge response is also sensitive to change in moment of inertia of the bridge as highlighted in Section 7.3.10 in Chapter 7. Please note that the parameters selected in this Chapter are taken randomly and yet not meant to be compared with field measurement results including moment of inertia. The comparision of result from the three methodologies discussed in Section 1.5 can be referred from Chapter 7. The parameters that were considered are:

a. Speed of the train ,V
b. Span length of the bridge, L
c. Axle load of the train, P_0
d. Mass of the bridge per meter length, m

Speed of train

The train speed at the time of field measurement is calculated by dividing the total length of the train sets (from the front wheel of the first coach to the last wheel of the twelfth coach) with the average time obtained from the video motion recorded. For instance, the speed 85km/h is calculated as 229.4/9.7=23.7m/s ≈85.1km/h.

The maximum allowed speed of a train crossing the bridge under consideration is 90km/h. The different speeds chosen for comparison purpose using the mathematical approach were

5 km/h, 60 km/h, 85.1 km/h, 100 km/h, 160 km/h, 200 km/h and 288km/h. Table 6-1 to Table 6-2 is used as a reference to select these ranges of speeds. The critical speeds that were calculated based on formula extracted from existing literatures are also analysed here. These critical speeds, which are closer to the maximum allowed speed on the bridge, were considered. These speeds are 39.5 km/h, 42.3 km/h, 45.5 km/h, 53.8 km/h, 74 km/h, 65.8 km/h, 84.5 km/h, 98.6 km/h and 118km/h.

Higher speed is also the main interest of this research. One of the initiatives for this interest is the results obtained by Yang *et al* (2004) and Kargarnovin *et al* (2005), showing responses above the allowable range set by different references when a structure, mainly track, is subjected to much higher speed such as 225km/h.

Span length of the bridge and mass of the bridge per meter length

The span lengths of the bridge, mass of the bridge per meter length and axle loads of the train were selected to match the measured bridge discussed in Chapter 3. Table 6-1 to Table 6-3 were presented to give a general feeling of the above mentioned parameters of existing bridges presented by different research works.

Table 6-1: Reference bridges

Bridge No.	Name of bridge	Location	Reference article	No. of Spans	Train type	Bridge type
1	N/A	Istanbul	Caglayan *et al* (2011)	4	Suburban commuter train	Composite with riveted steel plate girder bridges
2	N/A	N/A	Yang *et al* (2004)	1	N/A	Mathematical approach; Bridge as a beam (with defined E =28.7GPa and I=6.635m^4)
3	Sesia viaduct	Italy	Liu *et al* (2009)	7	TR500Y High speed	Composite with steel double box section, girder and concrete deck
4	Sacavem	Lisbon	Rodrigues (2002)	1	High speed: active tilting, locomotive hauled, electric tripled train	Steel Truss Railway Bridge

N/A: the information is either missing from the reference or not considered originally

Note: Please refer Section 2.7.1 for detail description of bridge and analysis approach. Stiffness values are not quoted by some of the references.

Table 6-2: Parameters used for comparison of responses using time history analysis

Bridge No.	L [m]	M [kg/m]	Axle load [kN] Locomotive	Passenger	Speeds tested for [km/h]
1	13.5	N/A	N/A	N/A	5
2	30	3240	218	218	60,100
3	46	3000	176	113	288
4	31.4	1800	N/A	N/A	160,200

N/A: the information is either missing from the reference or not considered originally

Table 6-3: Comparison of dynamic responses from various research works

Bridge No.	Natural frequency[Hz]	Mid span deflection[mm]	Mid span acceleration[m/s^2]
1	19	N/A	-0.3 to 0.3
2	N/A	1.22 (60km/h)	-0.03 to 0.03 (60km/h)
		1.56(100km/h)	-0.12 to 0.12(100km/h)
3	4.14	1.9	-
4	6.95-7.04	N/A	5.9 for high speed: active tilting train
			14.7 for locomotive hauled train
			15.7 for electric tripled train

N/A –the information is either missing from the reference or not considered originally

The lengths of the span taken for comparison were 13.5m, 32.5 m and 46 m. Similarly, the bridge mass of 3000kg/m and 1879 kg/m were taken. The mass of the measured bridge is calculated approximately by summing up all vertical reactions, Fz, as obtained from the FEM static deflection result under self-weight. The extracted reaction is equal to 150kN ($\approx$15290kg) and gives a total mass of the bridge per meter length, which is approximately equal to 1879 kg/m.

Axle load

The axle load of the train, P_0, is calculated based on a typical train set arrangement which consists of a total of twelve coaches, three motor coaches (MC) and nine trailer coaches (TC) which are the locomotive and passenger part of the train respectively.

A train set arrangement is configured as: 1MC+3TC+1MC+6TC+1MC or 1MC+6TC+1MC+3TC+1MC. The axle load calculated from the fully loaded train and a semi-loaded train are included in Table 6-4.

An average mass of 80kg per person is assumed when considering the capacity. By assuming each wheel shares the total mass equally, the axle load is calculated by simply dividing the total mass by four. The total mass includes gross mass of the coach and the mass of the passengers. The context of fully loaded and semi-loaded in this study represent the way the axle load is calculated, i.e. assuming the train is travelling at its full and half capacity respectively. For instance, the 163kN is calculated as follows from Table 6-4: Half the capacity of the motor coach consists of 55 standing and 28 seated people weighing 6649kg and the gross mass of the coach itself is 60000kg. This gives a total mass of 66649kg or weight of 653.8kN. Dividing this total weight by four gives a result of 163kN.

Table 6-4: Metrorail gross mass, capacity and axle load

Type of coach	**Full Capacity**	**Gross Mass**	**Axle load[kN]**	
		[kg]	Fully loaded	Semi loaded
Motor	110 standing, 56 seated	60,000	180	163
Trailer	149 standing, 52 seated	30,500	114	95

From Table 6-4, we can observe that the MC is almost double the TC weight as it contains additional components such as the traction motor, power supply system, compressor and exhaust which give power to the entire train set. However, the capacity of TC is comparatively higher than the MC.

This study considered the axle load when the train is semi-loaded. Therefore, the axle loads of 163kN and 95kN are considered for the MC and TC respectively.

6.3 PROCEDURES

The following procedures were followed in this chapter to determine displacement and acceleration values at mid span of the bridge:

a. The natural and excitation frequencies were calculated
b. The appropriate equation is then chosen from the previous chapters depending on the frequency calculated
c. The responses were obtained and plotted using the equation chosen above based on the parameter discussed on previous section and
d. Results were finally discussed

6.4 NATURAL AND EXCITATION FREQUENCY

Natural frequency

Using the natural frequency formula obtained in the previous chapter in Equation 5-4 which is re-rewritten as follows:

$$\omega_n = \sqrt{\frac{\tilde{k}}{\tilde{m}}} = \frac{\pi^2}{L^2}\sqrt{\frac{EI}{m}}$$

Table 6-5 and Table 6-6 give values of natural frequency for different masses and span lengths of the bridge.

Where:

E ≈ 205GPa (i.e. 29500ksi)

I =0.33m^4 (Obtained from the rounded up maximum deflection under self-weight of the bridge obtained from FEM i.e from 3.5 to 4mm. Refer Table 7-2)

Excitation frequency

The excitation frequency (ω) is a function of span length of the bridge and the velocity of the travelling train as stated in Equation 2-5. That is calculated as:

$$\omega = \frac{\pi}{t_d}$$ (Chopra, 2007) and (Yang *et al*, 2004)

Table 6-7 consists of the different excitation frequency for different speed and span length. This is a frequency experienced by the bridge besides the inherent frequency created from repetitive nature of the wheel loading as discussed in Section 6.6. Numerical example is attached in Appendix A2.

6.5 SELECTION OF EQUATION OF MOTION

The displacement and acceleration equations were selected on the bases of the cases defined in the previous chapter. Referring to the results obtained in Table 6-5 and Table 6-7, all natural and excitation frequency are not equal, i.e. case I applies. Therefore, only the first case is used for the purpose of this research report. The effect of the train load is approximated by adding the effect of each single load entering the bridge at a different time.

The displacement and acceleration equation is presented in Chapter 5 from Equation 5-17 to Equation 5-26. For instance, the generalized displacement coordinate presented in the Equation 5-17 and Equation 5-18 is simplified to the equation below by considering a 32500mm span bridge weighing 1879 kg/m when subjected to a single load travelling at a speed of 85.1km/h.

$$z(t) = 1.05 * 10^{-8} P_0 (\sin 2.28t - 0.041 \sin 55.9t) \qquad t < L/V$$

$$z(t) = -8.55 * 10^{-10} P_0 (\cos 38.49x \sin[55.9(t - 0.69)]) \qquad t \geq L/V$$

6.6 EFFECT OF PARAMETERS ON NATURAL AND EXCITATION FREQUENCY

The different parameters considered for comparisons of the natural frequency of the bridge were: bridge span length, bridge mass and train speeds. Stiffness comparision is left out for this section as the result is obvious and is taken as constant parameters as referred from Table 6.5. Please refer Equation 5-4. It is unrealistic that bridges of different lengths will have the same stiffnesses.. However the comparison exercises in this Chapter are done mainly for mathematical observation of the effect of altering parameters. Therefore one must not directly compare the results with the field measurement results or FEM results directly. Some of the parameters selected in Section 6.6 to Section 6.10 are intended to be used for comparison purpose only and may not match the bridge parameters and therefore should not be referred to other chapters.

A shorter bridge will have a higher natural frequency as compared to longer span bridges. This is also applies to excitation frequency. This shows the frequency of the bridge is inversely proportional to the span length. In this case, it is assumed that the mass of the

bridge, moment of inertia of the bridge and speed of the train is constant in both cases. This can be observed from Table 6-5 and Table 6-7.

Table 6-5: Natural frequencies for different span length

L [m]	ω_n [rad/s]
13.5	324.9
32.5	56.1
46	28

$E \approx 205GPa$, $I=0.33m^4$ and bridge mass of 1879 kg/m all cases

The effect of mass of the bridge on the natural frequency of the bridge can be observed from Table 6-6. This shows the lighter the bridge, the higher the natural frequency is. However, the excitation frequency is not influenced by the mass of the bridge. Here it is assumed that the span length, moment of inertia and speed of the train is constant.

Table 6-6: Natural frequencies for different mass of bridge

M [kg/m]	ω_n [rad/s]
1879	55.9
3000	14

$E \approx 205GPa$, $I=0.33m^4$ and span length of 32.5 m all cases

The natural frequency of the bridge is not influenced by the train speed however the speed can easily influence the excitation frequency. Speed is one of the important parameters one should carefully consider while studying the dynamic behaviour of structure. Table 6-7 shows that the excitation frequency increases when train speed increases. It is furthermore important to consider the critical speeds as discussed in Section 7.3.7. The natural frequency of the bridge is also not influenced by the axle load of the train.

Table 6-7: Excitation frequencies for different span length and train speeds

Train Speed [km/h]		**32.5**	**56.8**	**65**	**85.1**	**100**	**113.6**	**160**	**194.9**	**200**	**288.0**
	13.5	2.1	3.7	4.2	5.5	6.5	7.3	10.3	12.6	12.9	18.6
	32.5	0.9	1.5	1.7	2.3	2.7	3.0	4.3	5.2	5.4	7.7
Span length [m]	**46.0**	0.6	1.1	1.2	1.6	1.9	2.2	3.0	3.7	3.8	5.5

6.7 MID SPAN DISPLACEMENT OF THE BRIDGE

The response of the bridge to train loads is calculated using two methods: simple addition and the equation proposed by Yang *et al* (2004). These methodologies are briefly discussed in Chapter 5. In addition, the difference between the results obtained when the bridge is subjected to two types of train axle load arrangement is considered. One arrangement considered is when the entire axle loads meaning assuming all axle loads from each coach in the train set are the same in terms of capacity and gross mass resulting in equal axle load. For instance, Figure 6.1 shows two adjacent semi-loaded trailer coaches resulting in 48 axle loads from 12 similar trailer coaches. The second arrangement occurs when the train arrangement is 1MC+6TC+1MC+3TC+1MC as discussed in Section 6.2 in which there is a change for the MC and TC to be adjacent to each other, resulting in an unequal axle loads of which 36 axle loads are from 9 trailer coaches and 12 axle loads are from 3 motor coaches. Both Figure 6.1 and Figure 6.2 are presented to show equal and unequal axle loads that may occur on the bridge at instant of time while the train crosses the bridge. It does not imply there are only two coaches or 8 axles crossing the bridge. The magnitude of axle load when the train is travelling with its different capacity is referred from Table 6-4. The displacement obtained using simple addition and equation from Yang *et al* (2004) for the same axle load is shown in Figure 6.4.

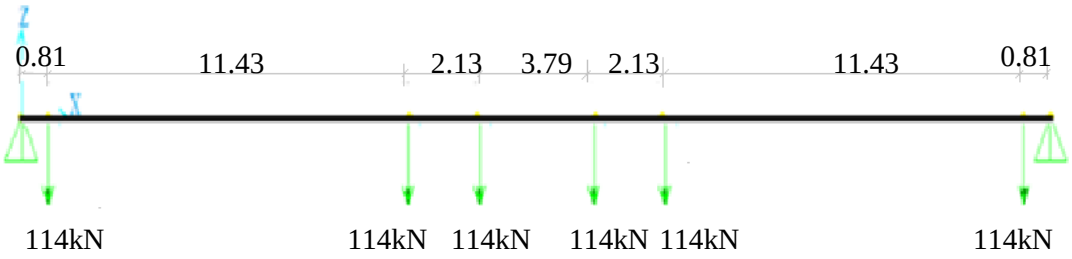

Figure 6.1: Equal axle loads from two adjacent TC

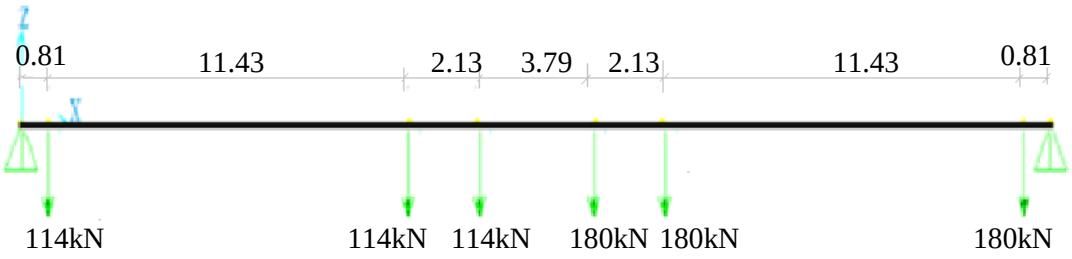

Figure 6.2: Unequal axle loads from two adjacent MC and TC

The comparison of displacement obtained when a bridge is subjected to these types of loadings and single loading is presented in Figure 6.3 using simple addition methodology discussed in Chapter 5 and also discussed in Appendix B.1 and Appendix B.2. A fully loaded train is considered to be the worst case scenario. Similarly, the acceleration response is compared in Figure 6.7. The comparison shown in Figure 6.3 is plotted by taking one fully loaded axle load of TC for single load moving, fully loaded axle loads of TC for equal train axle load moving similar to Figure 6.1 and fully loaded axle loads of MC and TC used together as shown in Figure 6.2 for actual train axle load moving. All other parameters are kept constant i.e. span length of 32.5 m, train speed of 85.1km/h, bridge unit mass of 1879 kg/m and moment of inertia of 0.33m^4. Refer Appendix B.1 to understand how the parameters are taken for Figure 6.3.

.

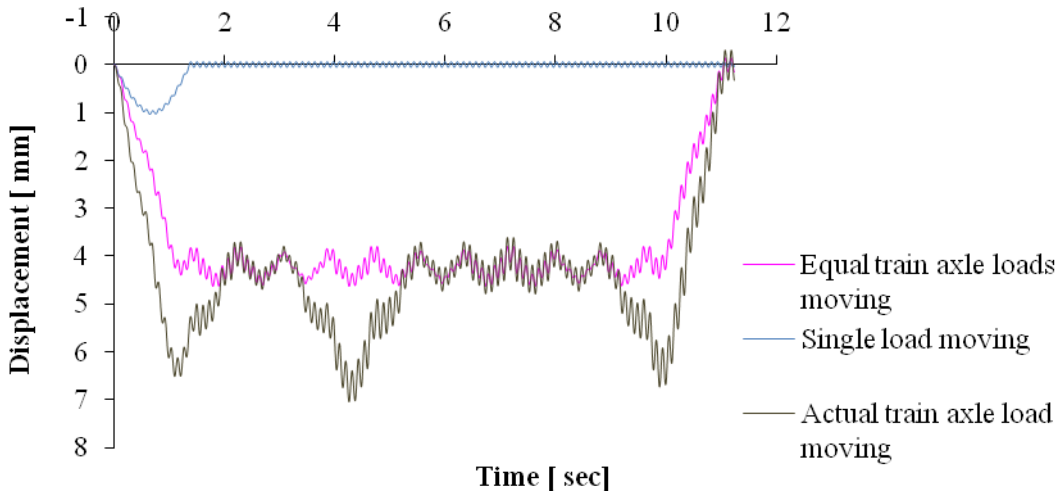

Figure 6.3: Displacement vs. time at mid span when bridge subjected to different loadings

The term single load is used to express a concentrated load or one axle load crossing the bridge. Even though a single load moving on a bridge does not often occur in the life time of the bridge, the results obtained would visualize the difference in the magnitude of the results created when considering a single load and train load on the bridge. The maximum bridge mid-span displacement due to a single load is 20% and 24% of displacement when train moving with an equal axle load and actual axle loads respectively.

The results calculated are based on the simple addition and equation presented by Yang *et al* (2004) as described in Figure 6.4. In both cases, identical axle load of 163kN for semi loaded motor were taken mainly for comparison of the two methods only. However in the later approach since the two axle loads are combined, an identical load of 163kN x 2= 326kN were used. The comparison shown in Figure 6.3 are done by taking all other parameters constant i.e. span length of 32.5 m, train speed of 85.1km/h, bridge unit mass of 1879 kg/m and moment of inertia of 0.33m^4. From this comparison, one can observe the following: the maximum displacement value obtained from simple addition and equation from Yang *et al* (2004) taking identical axle loads indicates 8.79mm and 8.99mm respectively, which simple addition is lower by 2.12%. This is negligible difference.

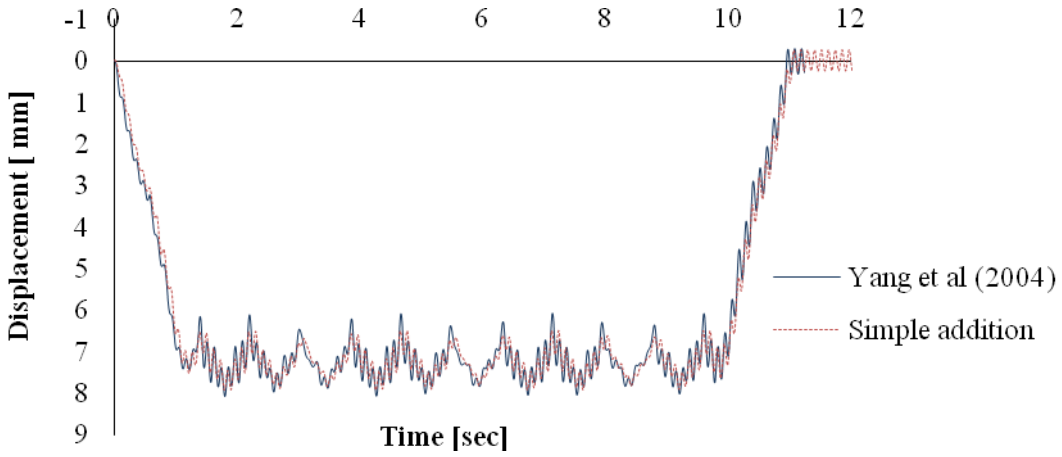

Figure 6.4: Mid span displacement using simple addition (Equation 5-17 and Equation 5-18) and Yang *et al* (2004) equation (Equation 5-22)

6.8 DISPLACEMENT AT DIFFERENT LOCATIONS ON THE BRIDGE

The comparison of responses at different locations on the bridge were performed using displacement as shown in Figure 6.5 for single load, and Figure 6.6 for train loads using the simple addition methodology as discussed. The locations randomly chosen were at x=1/20L, 1/4L, 1/2L and 3/4L. Both Figure 6.5 and Figure 6.6 were plotted using a simple addition methodology discussed in Chapter 5.

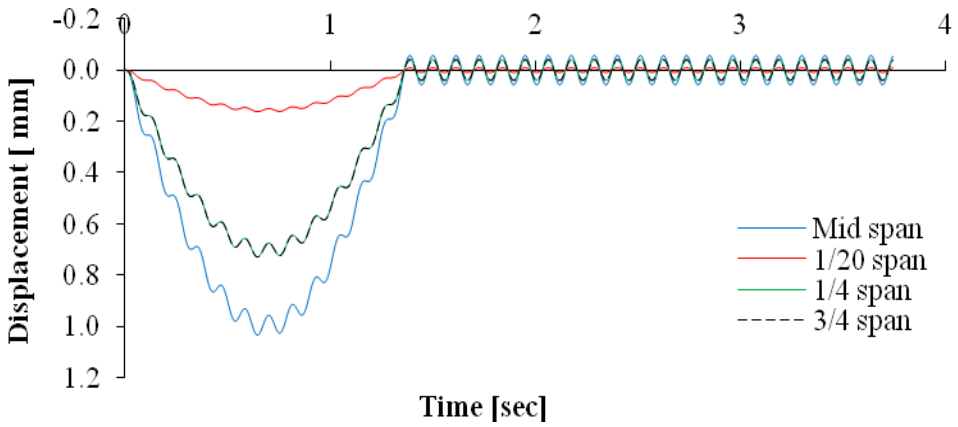

Figure 6.5: Displacement at different location when bridge subjected to single load

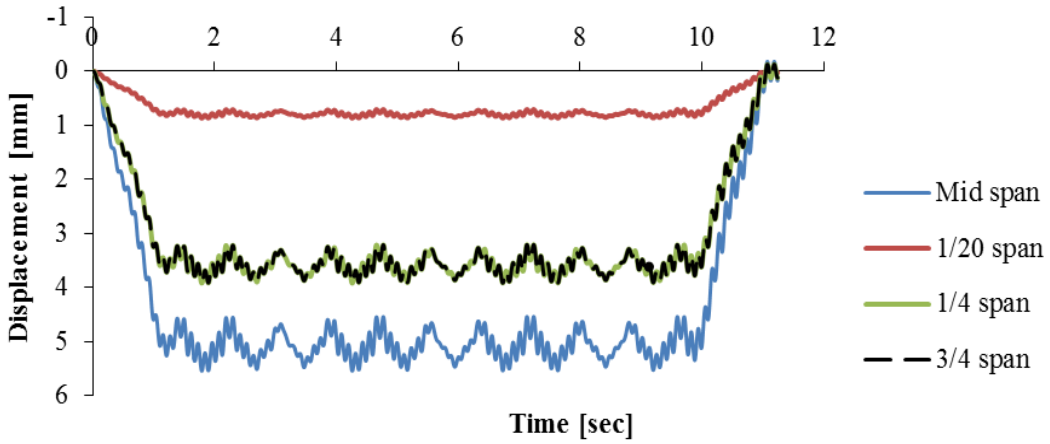

Figure 6.6: Displacement at different location when bridge subjected to train loads

Both displacement curves shown in Figure 6.5 and Figure 6.6 indicate that the bridge behaves in a more or less similar way at all locations with the maximum magnitude at mid-span.

6.9 MID SPAN ACCELERATION OF BRIDGE

In this section a typical acceleration results obtained from Equation 5-23 to Equation 5-25 are shown in Figure 6.7. Similar to displacement comparison, the following parameters were taken constant i.e. axle load of 163kN which is equal to axle load of semi loaded MC,

span length of 32.5 m, train speed of 85.1km/h, bridge unit mass of 1879 kg/m and moment of inertia of 0.33m^4.

Unlike the displacement results, the difference calculated in acceleration is more exaggerated when calculated based on the simple addition and equation from Yang *et al* (2004). This can be noted in Figure 6.7 which shows a maximum acceleration response of 1.2m/s^2 and 1.51m/s^2 respectively, giving a difference of 20.77%. The difference in acceleration is almost 10 times that of displacement which implies how sensitive the acceleration response is.

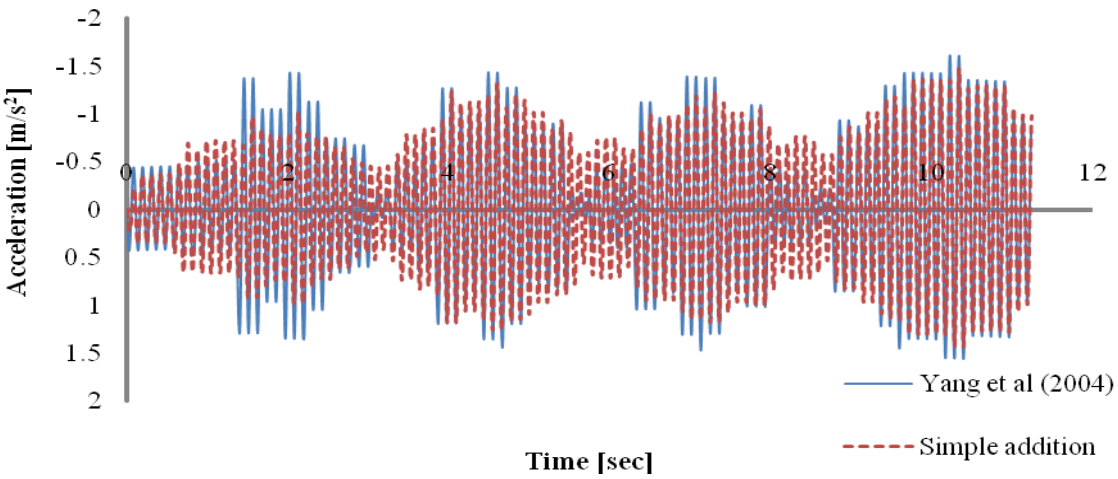

Figure 6.7: Mid span acceleration using simple addition and Yang *et al* (2004) equation

6.10 EFFECTS OF DIFFERENT PARAMETERS ON DISPLACEMENT AND ACCELERATION

Mathematically, it is possible to conduct comparisons of the maximum bridge response for different parameters. The parameters that were analysed were the bridge span length, bridge mass and train speed. Displacement and acceleration for different stiffness is discussed in Chapter 7.

Speeds of the train

Upgrading of existing bridges or new trains mostly involves increasing the train speeds: this changes the maximum response of the bridge as shown in Figure 6.8 and Figure 6.9. The

ranges of speeds were selected based on train critical speed that is assumed to create resonance, based on the different articles discussed below.

As explained by Goicolea and Gabaldon (2008) which is also explained in Chapter 2, we may not see the resonance effect as several axle load enters the bridge at different axle spacing, which results in phase difference or cancellation of the resonance effects. The magnitude of axle load in a train set vary from coach to coach, as explained in Section 6.2, which also prevents the resonance from occurring.

Using the two formulas included in Section 2.3, we calculated the possible critical or resonance speeds that cause magnitude of acceleration and displacement to increase. These speeds are used to plot Figure 6.8 and Figure 6.9. The calculation is based on the available repetitive axle spacing present in the train set. The critical speeds are selected by visual inspection of the acceleration pattern and also the magnitude of the response. The first formula from Yang *et al* (2004) is valid for equal axle spacing between the loads, which unfortunately is not the case in the actual situation. These inherent frequencies coming from wheel loads are experienced with the excitation frequency discussed in Section 6.4. To check the validity of the formula, all possible available axles spacing that may repetitively occur when the train passes on the bridge were considered. These were 2.13m, 3.73m and 11.43m occurring at a frequency of 0.47V, 0.27V and 0.09V respectively, where V is speed in m/s .The other possible axle spacing can be centre to centre distance between coaches or between front and rear wheels, which gives 13.56m and 19.49m. These occur at a frequency of 0.07V and 0.05V respectively. For instance, at a speed of 65km/h or 18.06 m/s the mathematical approach shows a continuously increasing magnitude of acceleration, giving a maximum value of 0.81m/s^2. From visual inspection of the calculated acceleration pattern and the fact that the frequency of occurrence of axle spacing of 2.13 is 0.47V, one may expect resonance to occur. This is because 0.47x18.06=8.49Hz is very close to the natural frequency of the bridge if we make a backward calculation check: please refer to Section 7.2 for the magnitude of frequency of the bridge. However, this magnitude of acceleration is not so high that the condition may not be considered as resonance.

The second formula from Michaltsos *et al* (2010) utilises the length of coach at constant spacing. However, this is also different from actual condition as it ignores the spacing between axles and coaches. To check all possible critical speeds that may cause resonance as per these two formulas, the following cases were taken: $\omega_1 e/2\pi$ where e is 2.13m, 3.73m, 11.43m, 13.56m or 19.49m and $\omega_1 d/2i\pi$ where d=19.43 and i=1, 2, 3…

Figure 6.8 and Figure 6.9 utilize a range of speeds considered as critical speeds that may cause resonance or maximum responses in bridges, calculated based on the formula discussed above. However, according to the calculated maximum results, almost all the speeds calculated did not show a clear resonance due to cancellation. It is only a speed of 74km/h that causes resonance with the maximum acceleration.

The maximum responses shown in Figure 6.8 and Figure 6.9 are calculated considering the axle load of the actual train configuration by using the simple addition method discussed in Chapter 5 and Chapter 7. It is also found that acceleration response is a better indication of possible resonance. The relationship between response and speed can be observed differently from Figure 3.27 and Figure 3.33 in Chapter 3 that is obtained from conducting measurements. This is especially obvious for the acceleration response. The magnitude of the displacement of the bridge is less affected by the speed of the train. Please note that the parameters used to plot Figure 6.8 and Figure 6.9; more specically moment of inertia; is different than the rest of the figures in this Chapter to make reading easier for Chapter 7. The following parameters were constant i.e. axle load of fully loaded MC and TC, span length of 32.5 m, train speed of 85.1km/h, bridge unit mass of 1879 kg/m and moment of inertia of 0.38m^4. The train speeds considered were 39.5 km/h, 42.3 km/h, 45.5 km/h, 53.8 km/h, 74 km/h, 65.8 km/h, 84.5 km/h, 98.6 km/h and 118km/h.

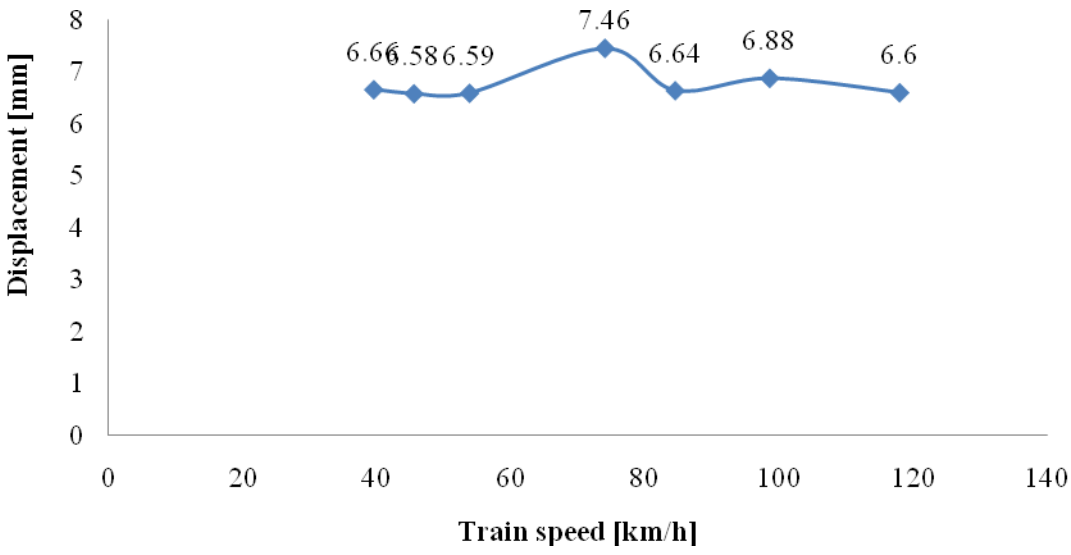

Figure 6.8: Maximum displacement of bridge for different range of train speeds

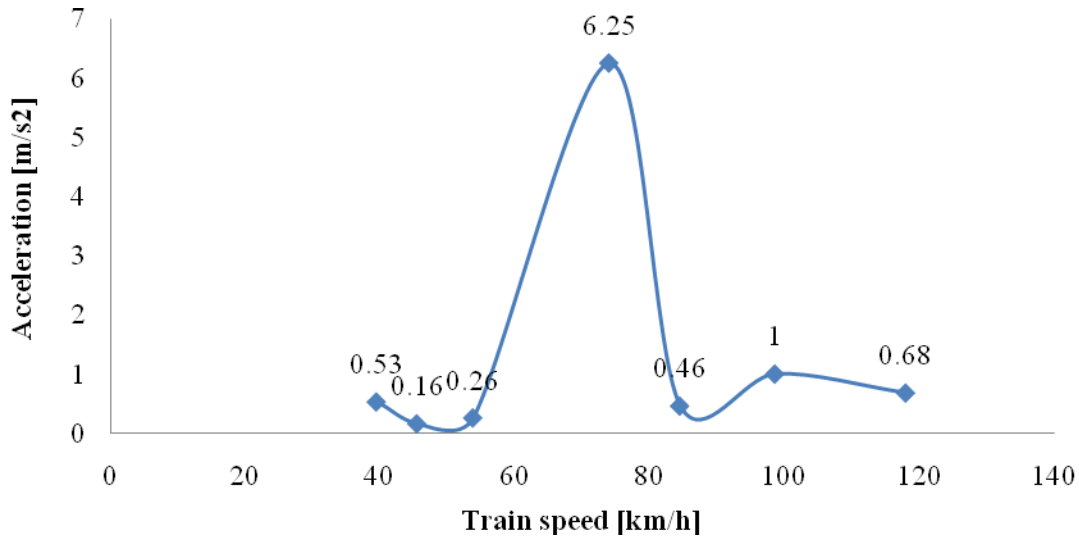

Figure 6.9: Maximum acceleration of bridge for different range of train speeds

Span length

All parameters were made constant except for span length. Similar to axle loads comparisons, the parameters that were made constant are: equal axle load of 163kN for semi-loaded passenger train defined in Section 6.2, a speed of equal to 85.1km/h and bridge unit mass of 1879 kg/m. The lengths of the span taken as mentioned in Section 6.2 were 13.5m, 32.5 m and 46m. Therefore it is advised to perform further analysis if one is investigating a much longer span. The bridge responses are tabulated in Table 6-8 and Table 6-9.

Table 6-8: Maximum displacement of the bridge when bridge span length varies

Span length [m]	**Maximum displacement [mm] Equal axle load**
13.5	0.41
32.54	8.79
46	31.25

Table 6-9: Maximum acceleration of the bridge when bridge span length varies

Span length [m]	**Maximum acceleration [m/s^2] Equal axle load**
13.5	1.12
32.54	1.2
46	0.64

Based on the equation of motion developed in 7.5 and from Table 6-8 and Table 6-9, it is obvious that the maximum displacement of the bridge increases with span length, i.e. bridges with longer span, deflects more than a shorter span. This analysis is mainly useful for new bridges design stage.

Axle load

The axle loads considered were 164 and 180kN for semi-loaded and fully loaded passenger train as discussed in Section 6.2 and assumed axle load of heavy haul which is 30t (294kN) is considered. This comparison is done by taking all other parameters constant .i.e. span length of 32.5 m, train speed of 85.1km/h and bridge unit mass of 1879 kg/m. The result is tabulated in Table 6-10 and Table 6-11. Here the bridge response is compared assuming all the axle loads in the train set has equal magnitude.

Table 6-10: Maximum displacement of the bridge when axle load varies

Axle load [kN]	Maximum displacement [mm]	Type
163	8.79	Semi-loaded passenger
180	9.71	Fully loaded passenger
294	15.86	Heavy Haul

Table 6-11: Maximum acceleration of the bridge when axle load varies

Axle load [kN]	Maximum acceleration [m/s^2]	Type
163	1.2	Semi-loaded passenger
180	1.32	Fully loaded passenger
294	2.16	Heavy Haul

Based on the results tabulated in Table 6-10 and Table 6-11, the displacement result is more sensitive to the change in the magnitude of axle load as compared to the acceleration response. This is opposite to the results obtained by changing the train speed. This analysis is mainly useful for the upgrading of existing bridges when a need arises to run a new type of train.

Different bridge mass

The comparison of 1879 kg/m and 3000kg/m weighing bridges is made to observe how lighter and heavier bridges behave. Here, the span length of 32.5 m, train speed of 85.1km/h

and equal axle load of 163kN were taken as the constant for both cases. The results are presented in Table 6-12 and Table 6-13.

Table 6-12: Maximum displacement of the bridge when bridge mass varies

Bridge mass [kg/m]	Maximum Displacement [mm]
1879	8.79
3000	9.5

Table 6-13: Maximum acceleration of the bridge when bridge mass varies

Bridge mass [kg/m]	Maximum acceleration [m/s^2]
1879	1.2
3000	0.28

From Table 6-12 and Table 6-13, one can observe that the lighter bridge displaces less and accelerates more. Even though this gives an indication for new bridges design stages, further analysis is always required for specific cases.

6.11 SUMMARY

In this chapter all equations derived in Chapter 5 are analysed using examples. A sample of calculation is also attached in Appendix A. The parameters discussed and believed to have an impact on the response of the bridge are: speed of the train, span length of the bridge, axle load of the train, mass of the bridge per meter length and flexural rigidity of the bridge.

By alternating the constant parameter from the parameters mentioned above, the natural frequency and excitation frequency, displacement and acceleration values of the bridge were calculated from the equations of motions discussed. The different results are summarized as below:

- The natural frequency of the bridge is mainly dependent on its inherent properties such as the mass, the flexural rigidity and the span length of the bridge. The magnitude of the natural frequency of the bridge is independent of the force applied on the bridge or the speed of the train. A shorter bridge will have a higher natural frequency as compared to longer span bridges. The lighter the bridge, the higher the natural frequency is. The excitation frequency however is dependent on the span length of the bridge or axle spacing and the speed of the train.

- The displacement and acceleration is dependent on the flexural rigidity, natural frequency, axle load, span length, axle spacing, and speed of the train and boundary condition of the beam which will define the shape function. The displacement and acceleration values are obtained from two methods: simple addition and the equation proposed by Yang *et al* (2004). The first method takes any combination of axle loads and axles spacing of different coaches where as the later can only use axle loads of equal magnitude and uniform axles spacing of different coaches. The moment of inertia of $0.33m^4$ is kept constant during all comparisons except Figure 6.8 and Figure 6.9.

Generally this Chapter is presented to analyse the effect of different parameters on the response of the bridge. In the next Chapter the same exercise is applied using the parameters that match the field measured data.

7 COMPARISON OF RESULTS AND DISCUSSIONS

7.1 INTRODUCTION

Following the initial objective of the research, the dynamic responses of a single span simply supported steel railway bridge when subjected to train are discussed in Chapters 3 to 6, using three methodologies: FEM, Mathematical Approach and Field Measurement. The dynamic responses that were specifically discussed are displacement, acceleration and natural frequency of the bridge.

In this chapter of this research, all important parts of the results from each approach are compared and discussed. The first comparison is made on the magnitude of frequency as extracted from field measurements, calculation and FEM. The second comparison is on dynamic responses such as displacement and acceleration as obtained from the mathematical approach and field measurement only. This involved the comparison of dynamic responses that is obtained from time history analysis using the mathematical approach elaborated in Chapters 5 to 6 and from unprocessed and processed field-measured acceleration data as discussed in Chapter 3.

The second point that is taken into consideration during the mathematical approach is the response of a bridge when subjected to a single load and train load travelling at a constant speed. This comparison is presented in more detail in Chapter 6 using the derived mathematical equations. During the train load consideration, two different axle loads arrangements were compared, i.e. considering an equal magnitude for all axle loads and using the actual train coach arrangement as discussed in Chapter 5 and Chapter 6.

The effect of different parameters such as the bridge span length, bridge mass and train speeds on the dynamic response using the mathematical approach is also evaluated in Chapter 6. Subsequently the effect of different modelling techniques in FEM on the modal analysis result, instrument fixing techniques and at last comparison of maximum acceleration, displacement, frequency and impact factor obtained using the three approaches with the code limit and formula as presented in Chapter 2 from different research works are discussed.

An impact factor is then calculated from the static and dynamic response, mainly deflection, and is then compared with the factor given in literatures and references as proposed by Ahmad *et al* (2010).

7.2 NATURAL FREQUENCY

The natural frequency of the bridge can be extracted from FEM using modal analysis as discussed in Chapter 5, or by converting the forced and free vibration time domain data obtained using field measurement and the mathematical approach as discussed in Chapter 3 to Chapter 6.

The results obtained from free vibration data give a clear answer when determining the natural frequency of the structure which is equal to 9.1Hz. This can be observed from the comparisons made in Figure 3.32 in Chapter 3. A magnitude of frequency close to 9.1Hz is obtained from these plots with the field measurement results which are lower by 0.93Hz and 0.96Hz from FEM using shell and beam elements respectively. Please refer to Table 7-1.

It is possible to obtain the first natural frequency of the bridge in the vertical direction by using the three approaches discussed in this research report; however it is not as obvious to ascertain the second and third mode frequency from conducting field measurements. If one wants to observe the higher modes, it is better to observe the FEM modal analysis results or to compute it by using the mathematical approach. A comparison of the results obtained from different methodologies is shown in Table 7-1. In this research, all measurements or calculations of frequency were performed on the unloaded bridge only. The frequency obtained from mathematical approach is calculated based on the Equation 5-4 from the Section 5.3 by keeping the span length of 32.5 m, the mass of the bridge per meter length at 1879 kg/m and the moment of inertia as 0.38m^4 constant.

Table 7-1: Frequency results from field measurement, mathematical and FEM

Description	**1st mode natural frequency [Hz]**
Bridge FEM using beam elements	10.06
Bridge FEM using shell elements	10.03
Mathematical approach	9.58
Field measurement result	9.10

7.3 DYNAMIC RESPONSES

In this section, a comparison of the field measured data with time history analysis from mathematical approach is performed. Specific train speeds, span length, mass and the frequency of the bridge which are believed to match the actual field measurement conditions were selected. The speeds are 38.3km/h, 63.5km/h and 91.8km/h, by keeping the span length of 32.5 m, the mass of the bridge per meter length at 1879 kg/m and the moment of inertia as 0.38 constant. The axle load is calculated based on the number of people that were estimated to be present in the train during the field measurement. The train is almost empty carrying about 8 people per coach which results in axle loads of 148.8kN and 76.4kN for MC and TC respectively.

Due to the vast nature of the subject matter, the scope of this research is limited to studying the vertical response of the bridge, which therefore did not include other responses such as lateral displacement, torsion or the dynamic stress of the bridge.

The field acceleration data is taken from accelerometer readings and that of displacement is taken from displacement transducer reading as described in Chapter 3. Mid span acceleration measured and obtained from mathematical approach are presented in Figure 7.1, Figure 7.2 and Figure 7.3. Data processing is performed on the field measured acceleration data as explained in Chapter 3. This data is then compared with Figure 7.4 and Figure 7.6 obtained from mathematical approach.

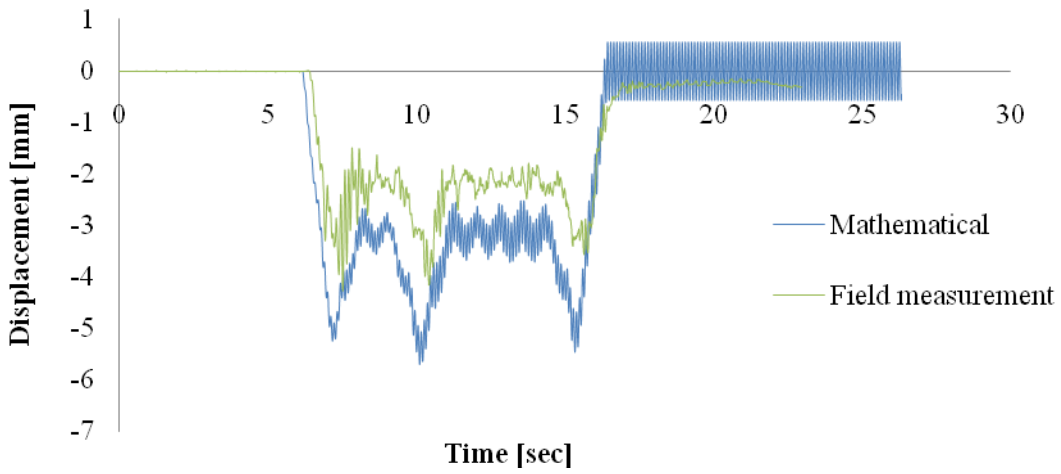

Figure 7.1: Mid span displacement data at point 'c' measured at train speed of 91.8km/h

Four points may be observed in Figure 7.1: 1) The displacement pattern obtained from both measured and calculated data is similar. 2) The displacement from the motor coach is higher than the displacement from the trailer coach by nearly 57.7%. This is almost equal to the ratio of mass of the trailer coach to the motor coach, indicating that a linear relationship exists between the mass of the coach and resulting displacement. 3) The appearance of the resulting pattern suggests that there is an indication of continuously increasing response or resonance.Therefore, it is better to refer the acceleration result to confirm if this condition actually occurs. 4) The maximum displacement obtained using the mathematical approach seems to be overestimated, giving a magnitude 32.6% higher than the 4.31mm obtained from the field measurement. One of the possible reasons for obtaining a lower displacement value from the field measurement is that the measured value is relative to the adjacant bridge, which therefore means that the actual displacement of the bridge may be equal to the measured value plus the displacement of the adjacent bridge.

The displacement measured at 38.3km/h and 63.5km/h which are taken at Point ‘b’ and Point ‘c’ are also compared with mathematical result in Figure 7.2 and Figure 7.3 respectively. There is a slight difference to wheel displacement pattern observed especially at a train speed of 38.3km/h. This may be resulted from imperfections in the mathematical approach in assimilating the effect of axle loads from motor and trailer coaches.

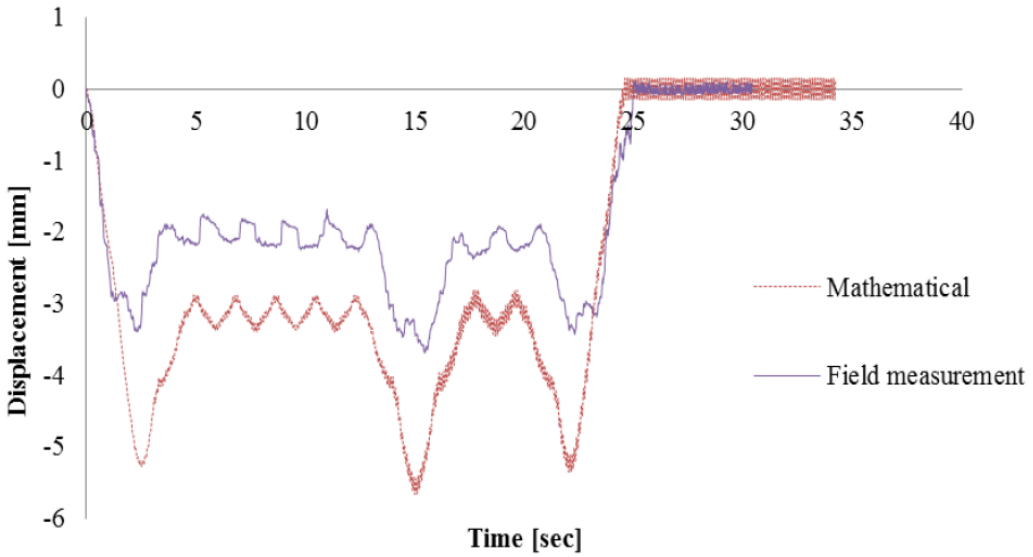

Figure 7.2: Mid span displacement data at point ‘b’ measured at train speed of 38.3km/h

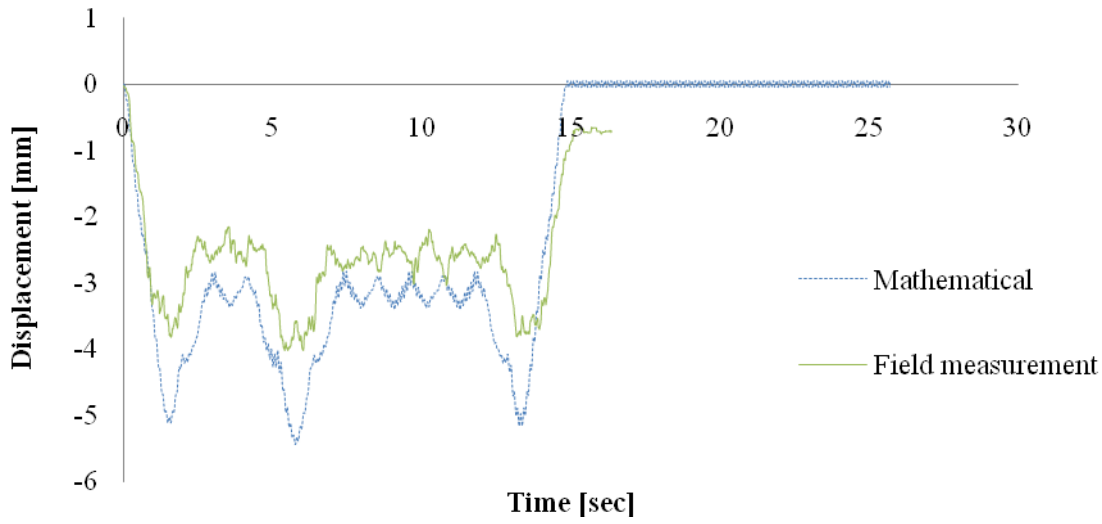

Figure 7.3: Mid span displacement data at point 'c' measured at train speed of 63.5km/h

Comparison of maximum value of displacement and acceleration obtained from measurement and mathematical approach is presented in Figure 7.5 and Figure 7.6. The acceleration data plotted on Figure 7.4 is taken from the accelerometer fixed at point '5' onn Figure 3.17 while the train is travelling at 91.8km/h.

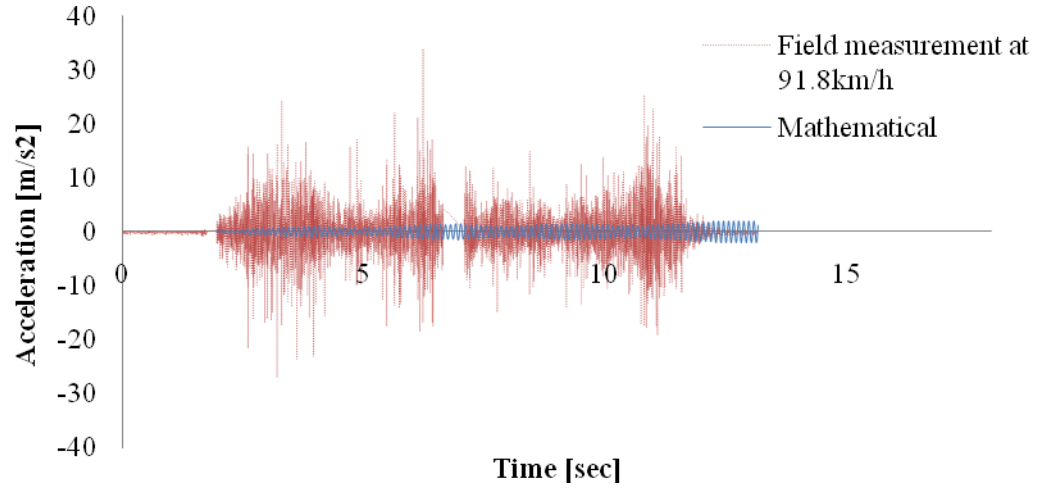

Figure 7.4: Mid span acceleration data at point '5' measured at train speed of 91.8km/h

The measured acceleration data is unreliable as compared to the acceleration data obtained mathematically which is found to underestimate the measured data by giving roughly 16 to 54 times lower results depending on the speed. A comparison of the maximum displacement and acceleration for different speeds are presented in Figure 7.5 and Figure 7.6.

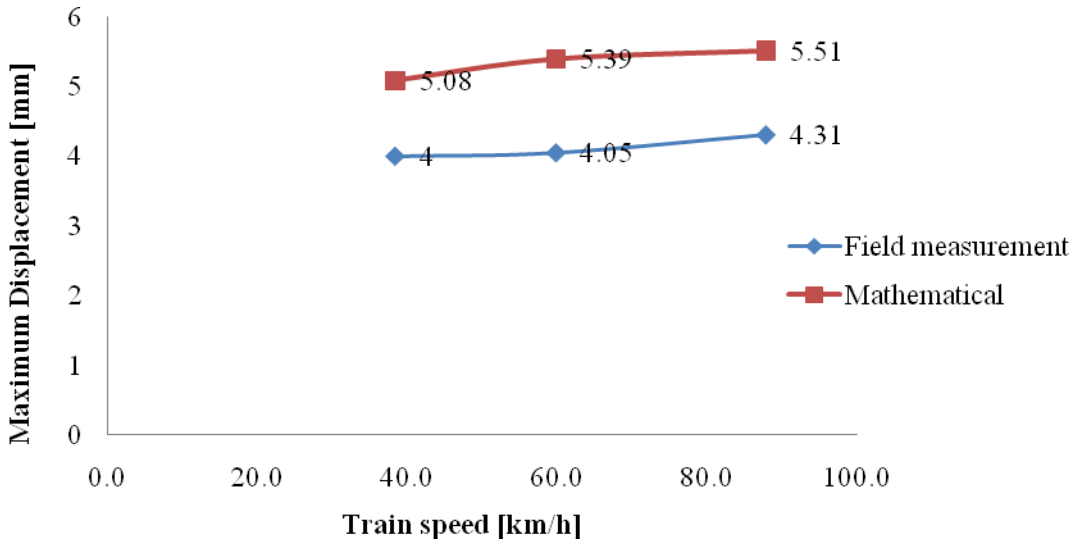

Figure 7.5: Comparison of maximum displacement of bridge for different train speeds

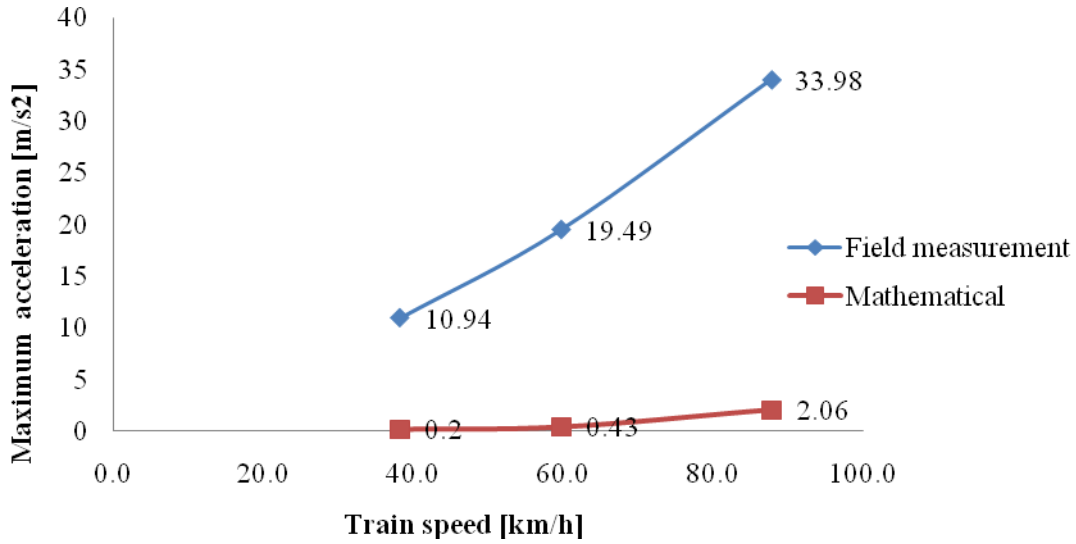

Figure 7.6: Comparison of maximum acceleration of bridge for different train speeds

Both Figure 7.5 and Figure 7.6 show approximately linear relationship between the responses and speed. However, this is plotted from the three points measured and calculated. The effect of speed on maximum displacement is insignificant as shown in Figure 7.5. The measured displacement is taken relative to the adjacent bridge. The actual displacement of the bridge might be different from the measured relative displacement value. Quantifying the displacement of adjacent bridge is beyond the scope of this study. The measured acceleration is between 16 to 54 times higher than that of the mathematical results, and the relative displacement measured is about 1.27 to 1.38 times lower than the absolute displacement calculated. This shows that the gap between the field measurement and the mathematical result is much lower for displacement than acceleration. The possible source of these gaps on magnitude of response is discussed below.

7.4 DIFFERENCES BETWEEN MEASURED AND CALCULATED RESPONSES

In this section, the possible reason for the difference between the measured and the calculated responses, more specifically acceleration is discussed. In this study the following factors that were not considered in the calculation might be assumed to create a major difference in the magnitude of the response of the bridge as explained later in this section;

a) Wheel defects or irregularity
b) Rail discontinuity
c) Simplification of the bridge-train interaction to a generalized simplified system
d) Measurement discrepancy
e) Shape function
f) Speed determination matching the actual train speed during the measurement
g) Possible train braking
h) Train speed
i) Damping in the structure
j) Miscalculation of moment of inertia of the structure
k) How the effect of train axle loads are incorporated in the equation of motion

7.4.1 Wheel and rail defects or irregularity

Wheel defects or irregularity may include imperfection of the roundness of wheel, deformation of the wheel, suspension defect and etc. This may result in a variation of the wheel load which can alter the magnitude of the dynamic responses. The work of Rodrigues

(2002) proposes to amplify the dynamic responses using a dynamic factor calculated from Eurocode1 which is quoted from Rodrigues (2002) to take into account wheel and rail defects or irregularity. It is also shown that the irregularity of the track has a major influence on the train response and a negligible impact on the vertical displacement of the mid-span of the bridge, as is explained by Yang *et al* (2004). Therefore it is advisable to consider the track irregularity whenever one studies a sensitive dynamic analysis such as the ride comfort of the train.

7.4.2 Rail discontinuity

This portion is not covered in this the scope of this research as the measured bridge has no discontinuity on the rail. From the work of Michaltsos *et al* (2010), we can observe that the presence of a discontinuity in the rail may increase the displacement by about 20% to 150%, assuming that the discontinuity occurs at the same location on both rails. Generally it is advised to avoid creating discontinuity of the rail at the mid-span of the bridge as it is the point at which the bridge experiences all higher responses.

7.4.3 Simplification of the bridge-train interaction to a generalized simplified system

The ratio of mass of the train to that of the bridge is relatively high: the ratio is up to 1.47. The response of the bridge is therefore influenced by the interaction between the bridge and the train. The effect of train suspension system or engine on the bridge is not taken into consideration while developing the mathematical model. It is advised to investigate further to what extent the dynamic response is underestimated when simplifying a single span simply supported bridge as one dimensional generalized simplified system, as has been discussed in Chapter 5. This illustrates that the subject of this research might require a three dimensional, non-linear and time dependent analysis to extract an accurate result. One can refer to the work of Yang *et al* (2004) to understand the detailed analysis of interaction between train and bridge.

7.4.4 Measurement discrepancy

The measurement discrepancy can be resulted from: 1) The type of material used for fixing the instrument on the field, 2) The accuracy of the instrument setup in the field as compared to the laboratory setup.

Laboratory testing is performed to find a suitable fixing material to install the accelerometer in the field. The accuracy of the measurements taken when using the specific fixing material is compared to a standard instrument screwed to a rotary machine as is shown in Figure 3.10. The results from this testing showed a reasonable result. However, this may not be achieved in the field due to parameters such as the temperature or how tightly the accelerometer is fixed, or how the doubled-sided tape performed on a rough surface, which is different from the smooth rotary machine top used in the lab. This may result a relatively loose connection between the accelerometer and the bridge which may alter the results significantly.

7.4.5 Difference between the assumed shape function and shape of actual deflection

The shape function is selected based on an approximation of the ideal shape of the deflected bridge, which is assumed as half sine curve as discussed in Chapter 5. The acceleration is calculated by the double differentiation of displacement equation which involves the double differentiation of the assumed shape function, which may magnify the discrepancy in assumption. A closer representation of the actual deflected shape is assumed to be represented using FEM deflection when subjected to the bridge self-weight. The assumed shape function and FEM deflection is compared in Figure 7.7.

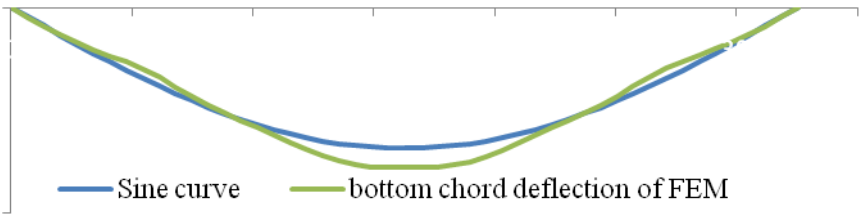

Figure 7.7: Representation of shape function: assumed vs. deflected shape from FEM

Based on Figure 7.7, even though the difference between the assumed function and FEM deflection cannot be quantified exactly, one should bear in mind that these discrepancies can contribute to the difference that exists between the mathematical approach and the field measurement results. This difference may be more pronounced in acceleration response as there is double differentiation involved as explained above.

7.4.6 Possible train braking

This portion is similarly not also covered in the scope of this research. The following observation is made based on existing literature. If the train brakes accidentally or intentionally while crossing the bridge, the response of the bridge may not be influenced, unless a noticeable change in speed occurred while the train is on the bridge. However, due to short span of the bridge there will not be enough time for a noticeable change of train speed to occur. Yang *et al* (2004) has shown that a bridge subjected with a vehicle in deceleration may not experience a change in response, and its response is solely dependent on the initial speed of the train before the brake is applied. However, it is recommended in this study to investigate the matter specific to any project.

7.4.7 Train speed

Whether the speed is higher or lower, when the train is travelling at a speed closer to the critical speed the structure either starts resonating or experience high magnitude response. These effects often occur if the axle spacing is constant or no cancellation occurs. This effect is explained in Chapter 6 from a mathematical point of view.

7.4.8 Damping

This research does not include a thorough analysis of damping, but a generalization is made based on previous research works. The damping can be generated either from vehicle suspension system or structure itself due to loose rivet connections or other reasons. The effect of damping may only influence slightly the magnitude of displacement response of the bridge. Yang *et al* (2004) explained this in terms of the difference in the magnitude of impact factor. Increasing the magnitude of train's suspension damping by 3 times decreases the impact factor by 5.26% and acceleration by 52%

7.4.9 Inaccurate speed determination

In this study, in order to calculate the train speed, a time is recorded both manually and from video recorded motion. This time is equal to the time it takes the train to cross the bridge. In this process it is difficult to get the time recorded in milliseconds, which might create a minor discrepancy on the calculated train speed. For instance, if one refers to Section 6.2, the speed of 85.1km/h calculated can easily be mistaken to be 81km/h by

assuming the time taken to cross the bridge is 10.2 sec instead of 9.7 sec. The difference between the two time measurements is 0.5 sec, which is a possible discrepancy. However, this difference will increase the acceleration from 0.89m/s^2 to 1.44 m/s^2 and the displacement from 8.51mm to 8.89mm. This shows that the discrepancy is exaggerated in acceleration response as compared to the displacement response by giving a difference of 61.8% and 4.27% respectively. Since this discrepancy is unpredictable we cannot quantify the percentage difference it creates in the response. Therefore, the only recommendation is to understand that the raw calculated response cannot be automatically assumed to be true without further consideration.

7.4.10 Miscalculation of moment of inertia of the structure

Similar to the other factors, the miscalculation of the moment of inertia of the structure is believed to affect the magnitude of the dynamic responses. In this study, the moment of inertia of the structure is calculated from the maximum deflection of the bridge obtained from FEM when subjected to its self-weight only. The calculated moment of inertia may vary with the static deflection of the bridge obtained from FEM which is dependent on the type of support or element used for FEM. Refer Appendix F.11 to Appendix F.14. One can observe that the static displacement is affected by the type of support and model. A standard beam table deflection formula for a simply supported beam under uniformly distributed load is applied. Table 7-2 is presented to show how maximum acceleration and displacement are sensitive to change in stiffness expressed in terms of flexural rigidity. These tabulated responses were extracted for constant span length of the bridge, train speed and mass of the bridge which are 32.5 m, 85.1km/h and 1879 kg/m respectively. The axle load arrangement is considered similar to actual train as shown in Figure 7.2.

Table 7-2: Maximum responses for different moment of inertia of the bridge

		Maximum Dynamic Response	
Static Deflection[mm]	**Moment of inertia [m^4]**	**Displacement [mm]**	**Acceleration [m/s^2]**
3	0.44	5.23	1.92
3.5	0.38	5.88	0.39
4	0.33	7.05	1.37
4.5	0.29	7.99	0.75

Following Equation 5.22-5.24, one expects the stiffness to be inversely proportional to both displacement and acceleration. However the mathematical result presented in Table 7-2

indicates that the acceleration and displacement is mainly dependent on the time dependent function that contains the sine and cos terms to cancel out each other.

7.4.11 How the train axle loads are incorporated in the equation of motion

The calculated maximum magnitudes of displacement and acceleration are dependent on the way the equation of motion is written. Based on Yang *et al* (2004), this is valid for identical axle loads spaced at equal intervals (d), whereas the simple addition from Chopra (2007) can be applied to different axle loads and spacing. The simple addition method is found more accurate in the representation of the displacement pattern and magnitude of maximum displacement when the axle load of the coaches in the train set varies.

7.5 LIMITS SET BY EXISTING REFERENCES

In this section the maximum acceleration and displacement obtained are compared with limits set by existing references. The maximum acceleration of the bridge obtained from mathematical approach is within the limit set by the Safety and Serviceability Standards of Bridges which is 3.5m/s^2 (Xia *et al*, 2005). However, the measured acceleration is beyond this limit as discussed in Chapter 7. As mentioned above, the measured acceleration is not a representation of the acceleration of the bridge. The displacement values are within the allowable maximum deflection limit for live load set by AASHTO which is L/800, where L is span length in mm. This limit is quoted by Adams (2014). All displacement results are less than 40mm, which is the maximum allowable for the bridge under consideration. However these cannot give us proof that this limits quoted by Adams, 2014 is applicable to railway bridges which therefore requires further investigation.

7.6 IMPACT FACTOR

The impact factor is obtained using formula presented in Table 2-1 from different research works. The static deflection is calculated for a 32.5 m span bridge subjected to six axle loads, of which three loads come from the trailer and the three other loads are derived from motor coaches which are adjacent to each other. The magnitude of the loads is taken as 180kN and 114kN assuming a fully loaded train. The loadings considered were positioned as shown in Figure 7.8 and Figure 7.9. The figure is repeated below from Chapter 6 for ease of reference. The axle load is calculated assuming both the motor and trailer coaches as fully loaded as described in Table 6-4.

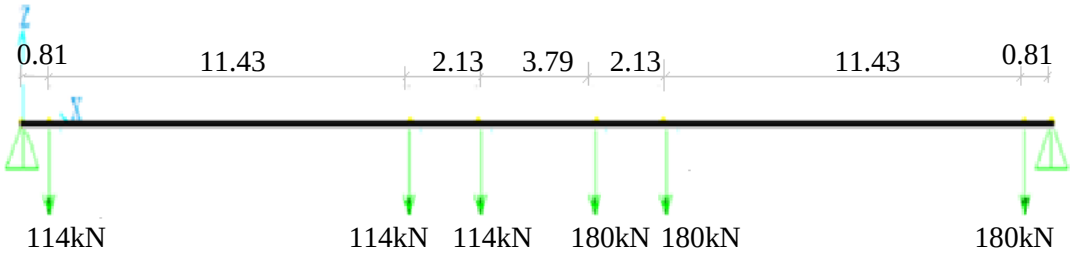

Figure 7.8: Position of axle loads on the bridge for maximum static deflection

The dynamic deflection of a bridge is dependent on the train speed and it also changes the magnitude of the impact factor as shown in Figure 7.9. Therefore, the impact factor for various speeds is calculated using the Equation 2.1 in Chapter 2. The impact factors calculated based on the AASHTO manual, AREMA and OHBD as referred in Table 2-1 give 0.216, 0.238 and 0.25 respectively. These references are quoted by Hamidi and Danshjoo (2010) and Yang *et al* (2004). The calculated results shown in Figure 7.9 are higher than the values given by different references. The upper limits of the impact factors calculated by the Iranian and French code are less than some of the results obtained in this research, as shown in Figure 7.9. These references are also quoted by Hamidi and Danshjoo (2010) and Yang *et al* (2004). We can observe a low coefficient of correlation between the speed and the impact factor. This is mainly due to the fact that some speeds such as 60 km/h, 85.1 km/h, 64.98km/h, 200km/h and those mentioned in Section 7.3.7 are very close to critical speed causing a larger magnitude of dynamic deflection as discussed in Section 7.3.7. Due to this fact, the linearity of the relationship between the speed and impact factor is compromised.

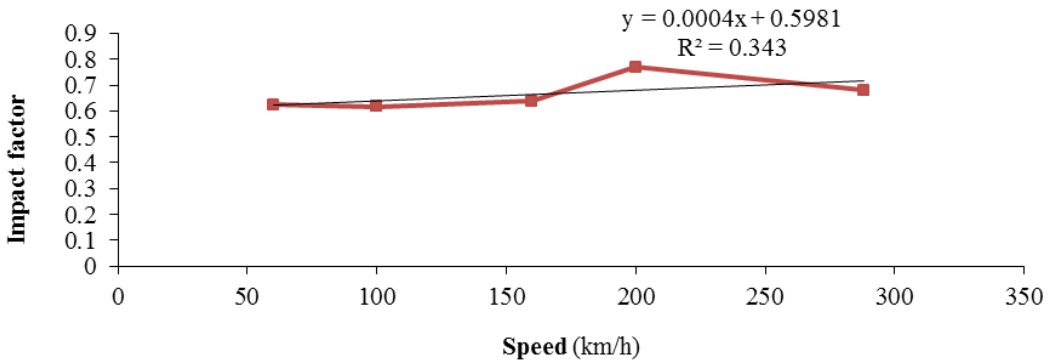

Figure 7.9: Calculated impact factors as a function of speed

However, it is advised to check with the allowable maximum deflection limit for railway bridges due to live load as set by AASHTO which is L/800. Following this, the maximum allowed limit for the bridge under consideration is 40mm and all the results obtained are below this limit.

7.7 EMPIRICAL FORMULA FOR FIRST NATURAL PERIOD

The empirical formulas collected by Kaliyaperumal *et al* (2008) are utilized in this section to calculate the first natural frequency of the bridge as included in Table 7-3. The description for each formula is found in Table 2.5. The results obtained from FEM range from 10.03Hz to 10.06Hz and that of field measurement is about 9.1Hz as shown in Table 7-1. The empirical formula did not give a closer result to both FEM and field measurement as shown in Table 7-3. Therefore, it is important to avoid calculating the natural frequency from empirical formula only.

Table 7-3: Calculation of first natural frequency (in Hz) using an empirical formulas (all quoted by Kaliyaperumal *et al*, 2008)

	Fryba		UIC & BS EN 1991-2	
	lower limit $133*l^{-0.9}$	upper limit $208*l^{-1}$	lower limit $23.58*l^{-0.592}$	upper limit $94.76*l^{-0.748}$
Empirical Formula				
First natural frequency	5.79	6.39	3.00	7.00

7.8 SUMMARY

This chapter is mainly included to compare the results obtained using the three methodologies for the dynamic analysis of steel bridges as discussed in Chapter 1. The frequency, displacement and acceleration of the bridge are the main dynamic responses considered. These responses are determined from the data collected from field measurement, FEM and mathematical approach.

The frequency results extracted from field measurements, calculation, FEM using beam elements and shell element show a 9.1Hz, 9.54Hz, 10.03Hz and 10.06Hz respectively. The

difference between the result ranges from 4.6 to 10.6%. This is fairly similar value considering the number of assumptions taken during the analytical approaches.

The second comparison is on dynamic responses such as acceleration and displacement as obtained from the mathematical approach and field measurement only. This involved the comparison of dynamic responses that is obtained from the time history analysis using the mathematical approach elaborated in Chapters 5 to 6 and from unprocessed and processed field-measured acceleration data as discussed in Chapter 3.

The displacement results from this comparision show an average difference of 27% between the field measurement and the mathematical approach as shown in Figure 7.5. This is also a relatively fair result. However there is a common observation made in all displacement results. These are: 1) The displacement pattern obtained from both measured and calculated data is similar. 2) The displacement from the motor coach is higher than the displacement from the trailer coach by nearly 57.7%. This is almost equal to the ratio of mass of the trailer coach to the motor coach, indicating that a linear relationship exists between the mass of the coach and resulting displacement. 3) An approximately linear relationship between the responses and speed is observed. The measured acceleration is between 16 to 54 times higher than that of the mathematical results, which basically means 1550% to 5370% higher. This shows that the acceleration result is unreliable. Several possible reasons for the difference between measured and calculated response are discussed in Section 7.4.

The results are compared with available references in Section 7.5. Impact factors at different train speeds are calculated using the formulae obtained from Hamidi and Danshjoo (2010) and Yang *et al* (2004). Similarly the frequency of the bridge is calculated using the empirical formula obtained from Kaliyaperumal *et al* (2008).

8 GENERAL CONCLUSIONS AND RECOMMENDATIONS

8.1 GENERAL CONCLUSIONS

This chapter includes a brief conclusion and recommendation on what has been analysed and discussed in previous chapters. Following the main objectives of this research report namely the dynamic response of a single span simply supported steel bridge when subjected to train loads, the study is analysed using three methodologies: FEM, Mathematical Approach and Field Measurement. In this study it is found that there is no easy methodology for dynamic analysis of such a bridge, but instead a suggestion will be made to use all three methodologies to have a clear view of the situation. One may also not try to calculate based solely on existing references and empirical formulas as these may not be valid in some cases. The effects of higher speed on the dynamic behaviour of a steel truss railway were studied using mathematical approach only. The maximum permitted train speed is 90km/h and therefore results for higher speed above this is not supported with field measurement in this study.

8.1.1 Methodologies

The dynamic response of a single span simply supported steel bridge when subjected to train loads is analysed using three methodologies: FEM, Mathematical Approach and Field Measurement. These are explained briefly below. The dynamic analysis involves determining the dynamic responses such as natural frequency, acceleration and displacement. A representative steel railway bridge is selected mainly based on its availability, ease of access, visibility of the structural frame work and from which the form and size of structural elements can be measured.

The mathematical approach involved developing equation of motion as shown in Equatiom 5-16. From this equation a time history analysis is performed to obtain dynamic responses such as displacement and acceleration using Equation 5-17 to Equation 5-18 and Equation 5-23 to Equation 5-24 respectively. The equation of motion in Equation 5-16 derived based on an assumption of the entire steel truss bridge as a generalized system. Two types of loading were considered: a single moving load and successive loads representing train axle loads.

The FEM is developed to perform modal analysis. The FEM package is selected based on the access to the software, the ease of analysis speed, versatility of modelling and the

accuracy of the results where an initial check on static and dynamic response has been done using a simple beam model. Two types of models were exercised: FEM using shell and beam elements as shown in Figure 4.3 and Figure 4.1 resp. The modal analysis is performed on the bridge without considering external applied loads meaning only self-weight is considered during analysis.

The field measurement is conducted to support the mathematical approach and FEM. Accessibility of the bridge for measurement, type of bridge and the intensity of the traffic on the bridge were considered during the selection of such bridge. This is done to make sure there is sufficient traffic flow with in the field measurement schedule. Displacement transducers and USB accelerometers were utilized to measure acceleration and displacement respectively. Displacement transducers were mounted on self-designed mounting sections and USB accelerometers were fixed with double sided tape and the. Displacements were directly measured. The acceleration is measured as a time domain data. As explained in Section 2.2.5, this data is converted to frequency domain data using a Matlab software from which frequency of the bridge is extracted.

8.1.2 Results

Conclusions were made for vertical displacement of the bridge, vertical acceleration and the natural frequency of the bridge which are presented in Figure 6.3 to Figure 7.6 and Table 7-1. By observing Figure 7.1 to Figure 7.3 and Figure 7.5, it can be concluded that the simple mathematical approach provided a good estimation to the actual displacement value. The FEM also gave a good estimation of the frequency as compared to the frequency extracted from acceleration data using FFT as presented in Table 7-1 . However the magnitude of measured acceleration shown in Figure 7.4 and Figure 7.6 is not reliable. That may have resulted from the difference in the laboratory and actual conditions set up or due to other factors discussed below.

The vertical displacement and acceleration of the bridge are dependent on many factors such as the span length of the bridge, mass per length of the bridge, stiffness of the bridge and speed of the train. In addition to this the magnitude of the dynamic responses calculated may vary from the actual conditions due to some assumptions and contributing factors that were not considered in the calculation. These factors are: wheel and rail defects or irregularity, rail discontinuity, simplification of the bridge-train interaction to a generalized simplified system, measurement discrepancy, shape function, possible train braking, train

critical speed, damping in the structure, resonance, miscalculation of train speed or moment of inertia of the structure. These are briefly discussed in more detail in Chapter 7.

The other observation made from different equations of motion is that the equation written based on research done by Yang *et al* (2004) in Equation **5-26** is valid for identical axle loads spaced at equal intervals (d) whereas the simple addition of Equation 5-17 & Equation 5-18 used in Chapter 5 and 6 from Chopra (2007) can be applied to different axle load and spacing. This is discussed in Appendix B.1. The simple addition method is found to be more accurate in representation of the displacement pattern and magnitude of maximum displacement when the axle load of the coaches in the train set varies. Please refer to Figure 6.3.

Displacements were measured relative to the adjacent bridge as shown in Figure 3.21. This means the actual displacement of the bridge may be different to the measured value. Measurements were conducted by allowing the train to travel at a speed of 38.3km/h, 63.5km/h and 91.8km/h. For instance, the measured displacements taken at Point 'c' for these speeds as shown in Figure 3.27 are 4, 4.1 and 4.3mm respectively. Similarly, the calculated result at mid span shows 5.1mm, 5.4mm and 5.5mm respectively as shown Figure 7.5. The magnitude of displacement increases with speed except for critical speeds as discussed in Section 7.3.7. Measurement among different locations along mid span give similar results within a difference of less than 5% as discussed in Chapter 3 where Point 'c' gave higher magnitude as compared to the one measured at Point 'b' and Point 'a'. A similar pattern of deflection is observed in all the measurements. The bridge experiences a maximum static deflection of 3.5mm when subjected to its self-weight only for the flexural rigidity of 0.38m^4 as presented in Table 7-2. Please also refer Appendix F. Impact factors calculated for different speeds can be referred from Section 7.5 in Figure 7.9.

The magnitude of the maximum acceleration response obtained from mathematical approach is more sensitive to change in any of the parameters than that of displacement. For instance compare Figure 7.5 and Figure 7.6. The magnitude of acceleration is read directly from signal absolute maximum value. The only processing performed in order to read the magnitude of acceleration is removing gravity by deducting value equal to gravity or 9.81m/s^2 and synchronization with time. This measured acceleration of the bridges as shown in Figure 7.6 reaches up to 16 times the calculated acceleration. This suggests discrepancies in acceleration measurements.

The natural frequency of the bridge is mainly dependent on its inherent properties such as mass, stiffness or flexural rigidity and span length of the bridge. The magnitude of the natural frequency of the bridge is independent of the force applied on the bridge or the speed of the train. In this study acceleration is used to extract the frequency of the bridge as shown for instance in Figure 3.28 and Figure 3.29. In order to identify this dominant frequency, a frequency domain method is applied that uses Fourier transformation, which converts time domain data to frequency domain data using a Matlab script as explained in Appendix C.1. Field measurement data needs to be separated in terms of free and forced vibration data. The data may need to be pre-processed before the relevant information is extracted. Pre-processing that were included are separating the free and forced vibration data, synchronisation and de-trending. The relevant information required from data is fundamental frequency extracted from free vibration. This does not mean that the data cannot be extracted from unprocessed data. However results are more clearly observed in pre-processed data. This is significantly manifested in frequency domain plot discussed in Chapter 3.

The differences in magnitude of frequency of the bridge obtained using the three methodologies are insignificant as presented in Table 7-1. The frequency obtained from field measurement is about 9.54% lower than the one obtained using FEM which is 10.06Hz. This may be a result of the effect of damping or leakage in measurement as explained by Rodrigues, 2002. The boundary conditions assigned to FEM also change the magnitude slightly. Please refer Chapter 4. Data measured at mid-span gives more accurate magnitudes than at other locations in the structure.

8.1.3 Comparison with the limits set by existing references and empirical formulas

In this study, the measured maximum responses of the bridge were compared in Figure 7.5 and Figure 7.6 with the safety and serviceability standards of bridges as discussed in Chapter 2. The maximum response of the train itself is not measured in this study, but the limits set by different references were presented in Table 2-3. The author couldnot find the relevant reference interms of maximum deflection limit which is specifically applicable for railway bridges. The displacement values are within the allowable maximum deflection limit for bridges subjected to live load set by AASHTO, which is L/800 where L is span length in mm. This is quoted by Adams, 2014. However these cannot give us proof that this limits quoted by Adams, 2014 is applicable to railway bridges which therefore requires

further investigation. All displacement results are less than 40mm which is the maximum allowable for the bridge under consideration. The calculated maximum acceleration of the bridge presented in Figure 7.6 is within the limit set by the safety and serviceability standards of bridges which is 3.5m/s^2. However, the measured acceleration is beyond this limit as discussed in Chapter 3 and Chapter 7.

Dynamic factors such as the impact factor are one way of adding the effects of dynamic load during analysis. This can be easily extracted from different references and compared to the formula proposed by different literatures which is discussed in the above sections. However, dynamic analysis of a structure must not be ignored as there are some cases where the structure responds beyond the values set by the references as explained from the results obtained by different research works. The impact factor from different references such as AASHTO and AREMA were presented for comparison. The impact factors calculated based on AASHTO manual, AREMA and OHBD gives a value of 0.216, 0.238 and 0.25 respectively. These references are quoted by Hamidi and Danshjoo (2010) and Yang *et al* (2004). The calculated results shown in Figure 7.9 are higher than the values given by different references. Therefore, it is advised to consider each bridge on its own as the values given by references may sometimes underestimate the situation. Some empirical formulas presented to calculate natural frequency may not be valid as discussed in Chapter 7.

8.1.4 Effect of train speed

The effect of higher speed on the dynamic behaviour of steel truss railway is studied mainly using mathematical approach. This is also supported to certain extent by taking measurement at 38.3km/h, 63.5km/h and 91.8km/h as shown in Figure 7.1 to Figure 7.6. It is impossible to take much higher speeds such as 200km/h as the maximum speed limit of the train passing on actual bridge is 90km/h. The result shows that there is a linear relationship between displacement and train speed except when the train is passing the bridge at its critical speed. This is also true for acceleration response. Therefore this is not valid for critical speeds where resonance conditions or maximum magnitude of displacement or acceleration occur.

8.2 POSSIBLE ADVANCEMENT FOR PHD RESEARCH STUDIES

a) A dynamic analysis of a continuous span bridge using three-dimensional vehicle bridge interaction system.

b) A more detailed finite element modelling to observe the interaction between a vehicle and bridge or between each element of the structure.

9 REFERENCES

Ashebo, D.B. Tommy, H.T. and Chan, L.Y. 2007. Evaluation of dynamic loads on a skew box girder continuous bridge. Part I: Field test and modal analysis. *Engineering Structures*, Vol 29, September, pp 1052–1063.

Adams, R.J. 2014. *Comparison of deflection and vibration limits for high performance steel bridges*. Greenman-Pedersen,Inc., Proceedings of the 9th International Conference on Structural Dynamics. New Jersey, United States of America.

Bates, W. 1991. *Historical Structural Steelwork Handbook*. 4th impression. The British Constructional Steelwork Association Limited. London, England.

Caglayan, O. Ozakgul, O. Tezer, O. and Uzgider, E. 2011. Evaluation of a steel railway bridge for dynamic and seismic loads. *Journal of Constructional Steel Research*, Vol 67, pp 1198-1211.

Chopra, A.K. 2007. *Dynamics of Structures*. 3rd ed. Pearson Education. Inc, New Jersey, United States of America.

GCDC. 2012. *GCDC_X16-1C_User_Manual*. Gulf coast Data concepts. Operating manual, www.gcdataconcepts.com.

Goicolea, J.M. and Gabaldon, F. 2008. *Research related to vibrations from high speed railway traffic*. Unpublished article.

Hamidi, S.A. and Danshjoo, F. 2010. Determination of impact factor for steel railway bridges considering simultaneous effects of vehicle speed and axle distance to span length ratio. *Engineering structures*, Vol 32, pp 1369-1376.

HBM. 1997. *Inductive displacement transducer*. Hottinger Baldwin Messtechnik GmbH. Operating manual. Darmstadt, Germany.

PCP Piezotronics. 2000. *Model 626A02 Industrial ICP Accelerometer*. PCP Piezotronics. Installation and Operating Manual. New York, United States of America.

Kaliyaperumal, G. Imam, B. Righiniotis, T. and Chryssanthopoulos, M. 2008. *Dynamic FE analysis of a continuous steel railway bridge and comparisons with field measurements.* Unpublished article.

Kargarnovin, M.H. Younesian, D. Thompson, D. and Jones, C. 2005. Ride comfort of high-speed trains travelling over railway bridges. *Vehicle dynamics: International journal of vehicle mechanics and mobility*, Vol 43, No 3, March, pp 173-199.

Kassimali, A. 2012. *Structural Analysis*. 4th ed. Cengage Learning, Stamford, United States of America.

Liu, K. Lombaert, G. Roeck, G.D. Leuven, K.U. Chellini, G. Nardini, L. Salvatore, W. Peeters, B. 2009. The structural Behaviour of a composite bridge during the passage of High-speed Trains. *Structural Engineering International*, Vol 19, No 4, pp 427-431.

Madshus, C. and Kaynia, A.M. 2000. High-speed railway lines on soft ground: Dynamic behaviour at critical speed. *Journal of Sound and Vibration*, Vol 231, No.3, pp 689-701.

Michaltsos, G.T. and Raftoyiannis, I.G. 2010. The influence of a train's critical speed and rail discontinuity on the dynamic behaviour of single-span steel bridges. *Engineering structures*, Vol 32, pp 570-579.

National Committee SABS SC59I, 2010. Bases of structural design and actions for buildings and industrial structures. *SANS 10160-7:2010.* 1st ed. SABS Standards Division, Pretoria, pp 17.

OaSYS GSA. 2012. *Version 8.6.1*.23. OaSYS copyright©Oasys 1985-2012. GSA manual. London, England.

Penny & Giles. 2009. Penny + Giles Controls Ltd. *Lvdt Displacement Transducers.* Technical notes. Christchurch, Dorset.

Policy Briefing 54. August 2012. ©SAIIA 2012 *Implementing development Corridors: Lessons from the Maputo Corridor*. Braamfontein, South Africa.

Rodrigues, J. 2002. *Dynamic performance of steel truss bridge under railway traffic*.Unpublished article.

Transnet. 2014. *Africa Transport Infrastructure 06*. Long Term Planning Framework. Johannesburg, South Africa.

Xia, H. Zhang, N. Gao, R. 2005. Experimental analysis of railway bridge under high-speed trains. *Journal of Sound and Vibration*, Vol 282, pp 517–528.

Yang, Y.B. Yao, Z. and Wu, Y.S. 2004. *Vehicle-Bridge Interaction Dynamics: with applications to high-speed railways*. World Scientific Publishing Co. Plc. Ltd, London, England.

APPENDIX A

LIST OF CALCULATION AND DERIVATIONS (BY AUTHOR)

APPENDIX A LIST OF CALCULATION AND DERIVATIONS (BY AUTHOR)

A.1 Calculation of Natural Frequency

Using the natural frequency formula obtained from
Equation 5-4 that is re-rewritten as follows:

$$\omega_n = \sqrt{\frac{\tilde{k}}{\tilde{m}}} = \frac{\pi}{L^2}^2 \sqrt{\frac{EI}{m}}$$

Let us take an example of the measured bridge described in Chapter 3. The parameters that match the bridge are:

E≈205GPa (i.e. 29500ksi)

I =0.38m^4 (calculated from maximum deflection under self-weight of the bridge obtained from FEM)

m =1879.5 kg/m (calculated from support reaction under self-weight of the bridge obtained from FEM)

L=32.5m

$$\omega_n == \frac{\pi}{32.5^2}^2 \sqrt{\frac{(205*10\text{^}11*0.38)}{1879.5}} = 60.2 rad/s$$

$$f = \frac{\omega_n}{2\pi} = \frac{60.2}{2\pi} = 9.58 Hz$$

The frequency value calculated above is the same as value in Table 7-1 of Chapter 7.

A.2 Calculation of Excitation frequency

The excitation frequency (ω) is a function of span length of the bridge and the velocity of the travelling train. That is calculated as:

$$\omega = \frac{\pi}{t_d}$$ (Chopra, 2007) and (Yang *et al*, 2004)

For instance for a train travelling at 85.1km/h (23.6);

$$t_d = \frac{L}{V} = 1.38 \sec$$

Therefore,

$$\omega = \frac{\pi}{1.38} = 2.28 \approx 2.3 rad/s$$

Please refer Table 6-7 for comparison. The uniform axle spacing can also be taken to calculate the excitation frequency.

A.3 Calculation of Moment of Inertia

The moment of inertia of the bridge denoted as 'I' is back ward calculated from maximum deflection obtained using FEM static analysis when the bridge is subjected to self-weight only as follows:

The deflection formula used is:

$$\Delta = 5\omega_b L^4 / 384EI$$

Where:

Δ = Deflection of the bridge taken as 3.5mm from FEM result

ω_b = Distributed load which in this case is taken as the self-weight of the bridge calculated as 18.79 kN/m,

L = Span of the bridge equal to 32.5 m and

E= 205GPa

Therefore I is equal tis calculated as:

$$I = 5*18.95*1000*32.5^4/(384*205*10^9*3.5*10^{-3})$$

$$I = 0.38m^4$$

A.4 Comparison of equations derived by Yang *et al* (2004) vs. Chopra (2007)

The author used trigonometric identities to simplify and check the similarity between the equations derived by Yang *et al* (2004) and Chopra (2007). In order to do the comparison the displacement equation derived by Yang *et al* (2004) for train loads is simplified to single load equation. This simplified equation is then compared with equation Chopra (2007) since the equation from Chopra (2007) is only applicable to single load moving.

1) Simplifying Yang *et al* (2004) displacement equation derived for train loads to single load equation.

$$z(t) = \frac{2PL^3{\omega_n}^2}{\pi^4 EI} * \frac{1}{{\omega_n}^2 - \left(\frac{\pi V}{L}\right)^2} * \left(\tilde{P}(V,t) + \tilde{P}(V,t-t_c)\right)$$

Equation 5-22

Where:

$\tilde{P}(V,t))$ = Contribution of the front wheel sets

$$= \sum_{K=1}^{N} \{([\sin(\frac{\pi V}{L} * (t-t_j)) - (\frac{\pi V}{L\omega_n}) * \sin\omega_n(t-t_j)] * H(t-t_j)$$

$$+ [(\sin(\frac{\pi V}{L} * (t-t_j - \frac{L}{V})) - (\frac{\pi V}{L\omega_n}) * \sin\omega_n(t-t_j - \frac{L}{V})] * H(t-t_j - \frac{L}{V})\}$$

$\tilde{P}(V,t-t_c)$ = rear wheel load expression expressed by substituting $t-t_c$ in t in $\tilde{P}(V,t))$

P = series of lumped loads as explained in Section 5.3,

x = the coordinate of the beam,

H (•) = a unit step function,

t_j $= (j-1) * \frac{d}{V}$ =the arriving time of the j[th] load at the beam or bridge

N = the total number of moving loads considered.

t_c $= \frac{L_c}{V}$ = a time lag between the front and rear wheel two sets of moving loads

$H(t-t_j)$ =j[th] moving load action entering the beam

$H(t-t_j - \frac{L}{V})$ =j[th] moving load action leaving the beam

For single load; by setting N=1, tj=0 and $\tilde{P}(V,t-t_c)$ =0

$\tilde{P}(V,t)$ term becomes

$$= \{[\sin(\frac{\pi V}{L} * t) - (\frac{\pi V}{L\omega_n}) * \sin\omega_n t] * H(t)$$

$$+ [(\sin(\frac{\pi V}{L} * (t - \frac{L}{V})) - (\frac{\pi V}{L\omega_n}) * \sin\omega_n(t - \frac{L}{V})] * H(t - \frac{L}{V})\}$$

Forced Vibration:

$H(t-\frac{L}{V})$ terms disappears as $(t-\frac{L}{V})$gives negative value all the times resulting in zero of, $H(t-\frac{L}{V})$

therefore,

$$=\{\sin(\frac{\pi V}{L}*t)-(\frac{\pi V}{L\omega_n})*\sin\omega_n t]*H(t)$$

$$=\sin(\frac{\pi V}{L}*t)-(\frac{\pi V}{L\omega_n})*\sin\omega_n t$$

This is exactly equal to the forced vibration part of Equation 5-17 described in Chopra(2007) as shown below. Similarily the free vibration part of the equation can be simplified from Yang (2004) equation to Equation 5-18 eventhough their equation is not clearly divided in to forced and free vibration part.

Free Vibration:

$$=\sin(\frac{\pi V}{L}*t)-(\frac{\pi V}{L\omega_n})*\sin\omega_n t+[(\sin(\frac{\pi V}{L}*(t-\frac{L}{V}))-(\frac{\pi V}{L\omega_n})*\sin\omega_n(t-\frac{L}{V})]$$

Using the following trigonometric identities;

$\sin(x-y)=\sin x\cos y-\cos x\sin y$

$$=\sin(\frac{\pi V}{L}*t)-(\frac{\pi V}{L\omega_n})*\sin\omega_n t+[(\sin\frac{\pi Vt}{L}\cos\pi-\sin\pi\sin\frac{\pi Vt}{L})-(\frac{\pi V}{L\omega_n})*\sin\omega_n(t-\frac{L}{V})]$$

$$=\sin(\frac{\pi V}{L}*t)-(\frac{\pi V}{L\omega_n})*\sin\omega_n t-\sin\frac{\pi Vt}{L}-(\frac{\pi V}{L\omega_n})*\sin\omega_n(t-\frac{L}{V})$$

$$=-(\frac{\pi V}{L\omega_n})*[\sin\omega_n t+\sin\omega_n(t-\frac{L}{V})]$$

Therefore;

$$z(t)=-\frac{2P_0L^3\omega_n}{\pi^4EI}*\frac{\left(\frac{\pi V}{L}\right)}{\omega_n^2-\left(\frac{\pi V}{L}\right)^2}*[\sin\omega_n t+\sin\omega_n(t-\frac{L}{V})]$$

Further simplifying;

$$z(t) = -\frac{2P_0L^3\omega_n}{\pi^4 EI} * \frac{\left(\frac{\pi V}{L}\right)}{\omega_n^2 - \left(\frac{\pi V}{L}\right)^2} * [\sin\omega_n t + \sin\omega_n t \cos\frac{\omega_n L}{V} - \cos\omega_n t \sin\frac{\omega_n L}{V}]$$

$$= -\frac{2P_0L^3\omega_n}{\pi^4 EI} * \frac{\left(\frac{\pi V}{L}\right)}{\omega_n^2 - \left(\frac{\pi V}{L}\right)^2} * [\sin\omega_n t(1 + \cos\frac{\omega_n L}{V}) - \cos\omega_n t \sin\frac{\omega_n L}{V}]$$

Substituting the following trigonometric identities:

$$\cos^2\theta = \frac{1+\cos 2\theta}{2} \text{ and } \sin(2x) = 2\sin x \cos x$$

$$= -\frac{2P_0L^3\omega_n}{\pi^4 EI} * \frac{\left(\frac{\pi V}{L}\right)}{\omega_n^2 - \left(\frac{\pi V}{L}\right)^2} * [\sin\omega_n t(2\cos^2\frac{\omega_n L}{2V}) - \cos\omega_n t \sin\frac{\omega_n L}{V}]$$

$$= -\frac{2P_0L^3\omega_n}{\pi^4 EI} * \frac{\left(\frac{\pi V}{L}\right)}{\omega_n^2 - \left(\frac{\pi V}{L}\right)^2} * [\sin\omega_n t(2\cos^2\frac{\omega_n L}{2V}) - \cos\omega_n t(2\sin\frac{\omega_n L}{2V}\cos\frac{\omega_n L}{2V}]$$

$$= -\frac{2P_0L^3\omega_n}{\pi^4 EI} * \frac{\left(\frac{2\pi V}{L}\right) * \cos\frac{\omega_n L}{2V}}{\omega_n^2 - \left(\frac{\pi V}{L}\right)^2} * [\sin\omega_n t(\cos\frac{\omega_n L}{2V}) - \cos\omega_n t(\sin\frac{\omega_n L}{2V})]$$

Therefore,

$$z(t) = -\frac{2P_0L^3\omega_n}{\pi^4 EI} * \frac{\left(\frac{2\pi V}{L}\right) * \cos\frac{\omega_n L}{2V}}{\omega_n^2 - \left(\frac{\pi V}{L}\right)^2} * [\sin\omega_n(t - \frac{\omega_n L}{2V})]$$

This is exactly equal to the free vibration part described in Chopra (2007) in Equation 5-18.

APPENDIX B

DEMONSTRATION OF APPLICATION OF EQUATIONS

APPENDIX B DEMONSTRATION OF APPLICATION OF EQUATIONS

B.1 Displacement result using the simple addition method

The displacement results using mathematical approach are shown in Figure 6.3 to Figure 6.5. Figure 6.3 is discussed in this section to have better explanation for the Simple addition method. Table B-1 below shows the similarities and differences of graphs shown in Figure 6.3.

Table B-1: Similarities and differences of parameters in Figure 6.3

Similarities	**Difference**
1) The following parameters are taken. ✓ The span length of 32.5 m, ✓ The train speed of 85.1km/h, ✓ The bridge unit mass of 1879 kg/m and ✓ The moment of inertia of 0.33m^4 2) Simple addition of equations is applied to determine the generalized displacement coordinate from Equation 5-17 and Equation 5-18. The displacement is then calculated using Equation 5-21. The example for simple addition is explained 10-1 in in Table C9 3) The frequency of data calculated is 400Hz meaning every 0.0025sec as shown in Table C10-2. 4) All graph is plotted at mid-span of the bridge	• For the equal train axle load moving, the twelve coaches with a total of 48 axles considered. Equal magnitude of a 95kN axle load is considered. Refer Table 6.2. • For the actual train axle load moving, the twelve coaches with a total of 48 axles considered. Out of which the three axle loads are MC and the remaining nine axle loads are of TC of magnitude 163kN and 95kN respectively. Refer Table 6.2. • For Singe load moving, only one axle load considered. The magnitude of this axle loads 95kN which is TC axle load. Refer Table 6.2.

The simple addition method consists of calculating the displacement of the bridge due to the train axle loads using Equation 5-21 from the generalized displacement coordinate (Z(t)) of bridge calculated using Equation 5-17 and Equation 5-18. In order to show how the simple addition works, a show case of the generalized displacement coordinate s (Z(t)) due to the four axle loads from the first motor coach entering the bridge is shown in Table B-2. Once the remaining generalized displacement coordinate s (Z (t)) is obtained from the rest of the 11 coaches, each row is added to get the total generalized displacement coordinate (Z (t)). Then the displacement of the bridge due to the train axle loads is calculated using Equation 5-21. It is highlighted in Table B-2 that the generalized displacement coordinate s (Z (t)) due to each axle load will only start calculating after a certain time elapsed from the initial time axle entered the bridge. The time elapsed is the time it takes for the axle load to reach the bridge after the previous axle load. For instance, at t=0.903Sec≈ 0.9Sec, the second axle load of MC arrives on the bridge. Since the 3rd and 4th axle load is not yet arrived till 0.12Sec, generalized displacement coordinate s (Z (t)) values are shown zero.

Table B-2: The generalized displacement coordinate (Z(t)) of bridge as the first motor coach enters the bridge

Coach type		MC		
Axle spacing[m]	0.00	2.13	13.56	15.70
Time[Sec]	0.00	0.09	0.57	0.66
0.0000	0.000000000	0.000000000	0.000000000	0.000000000
0.0025	0.000000018	0.000000000	0.000000000	0.000000000
0.0050	0.000000147	0.000000000	0.000000000	0.000000000
0.0075	0.000000494	0.000000000	0.000000000	0.000000000
0.0100	0.000001163	0.000000000	0.000000000	0.000000000
0.0125	0.000002252	0.000000000	0.000000000	0.000000000
0.0150	0.000003850	0.000000000	0.000000000	0.000000000
0.0175	0.000006035	0.000000000	0.000000000	0.000000000
0.0200	0.000008878	0.000000000	0.000000000	0.000000000
0.0225	0.000012431	0.000000000	0.000000000	0.000000000
0.0250	0.000016737	0.000000000	0.000000000	0.000000000
0.0275	0.000021821	0.000000000	0.000000000	0.000000000
0.0300	0.000027696	0.000000000	0.000000000	0.000000000
0.0325	0.000034356	0.000000000	0.000000000	0.000000000
0.0350	0.000041782	0.000000000	0.000000000	0.000000000
0.0375	0.000049940	0.000000000	0.000000000	0.000000000
0.0400	0.000058781	0.000000000	0.000000000	0.000000000
0.0425	0.000068241	0.000000000	0.000000000	0.000000000

0.0450	0.000078248	0.000000000	0.000000000	0.000000000
0.0475	0.000088715	0.000000000	0.000000000	0.000000000
0.0500	0.000099549	0.000000000	0.000000000	0.000000000
0.0525	0.000110647	0.000000000	0.000000000	0.000000000
0.0550	0.000121904	0.000000000	0.000000000	0.000000000
0.0575	0.000133210	0.000000000	0.000000000	0.000000000
0.0600	0.000144453	0.000000000	0.000000000	0.000000000
0.0625	0.000155524	0.000000000	0.000000000	0.000000000
0.0650	0.000166317	0.000000000	0.000000000	0.000000000
0.0675	0.000176729	0.000000000	0.000000000	0.000000000
0.0700	0.000186669	0.000000000	0.000000000	0.000000000
0.0725	0.000196050	0.000000000	0.000000000	0.000000000
0.0750	0.000204799	0.000000000	0.000000000	0.000000000
0.0775	0.000212854	0.000000000	0.000000000	0.000000000
0.0800	0.000220168	0.000000000	0.000000000	0.000000000
0.0825	0.000226706	0.000000000	0.000000000	0.000000000
0.0850	0.000232449	0.000000000	0.000000000	0.000000000
0.0875	0.000237394	0.000000000	0.000000000	0.000000000
0.0900	0.000241553	0.000000000	0.000000000	0.000000000
0.0925	0.000244953	0.000000013	0.000000000	0.000000000
0.0950	0.000247636	0.000000126	0.000000000	0.000000000
0.0975	0.000249658	0.000000446	0.000000000	0.000000000
0.1000	0.000251087	0.000001078	0.000000000	0.000000000
0.1025	0.000252003	0.000002120	0.000000000	0.000000000
0.1050	0.000252496	0.000003662	0.000000000	0.000000000
0.1075	0.000252664	0.000005785	0.000000000	0.000000000
0.1100	0.000252611	0.000008557	0.000000000	0.000000000
0.1125	0.000252445	0.000012036	0.000000000	0.000000000
0.1150	0.000252276	0.000016264	0.000000000	0.000000000
0.1175	0.000252215	0.000021269	0.000000000	0.000000000

B.2 Application of Yang *et al* (2004) equation (Equation 5-22)

A typical example for the application of Yang *et al* (2004) equation (Equation 5-22) is Figure 6.4. The simple addition method is already explained in Section B-1. The parameters taken are:

- In both cases, identical axle load of 163kN for semi loaded motor were taken mainly for comparison of the two methods only. However in the later approach since the two axle loads are combined, an identical load of 163kN x2= 326kN were used.
- The following parameters are taken constant:
  - ✓ The span length of 32.5 m,
  - ✓ The train speed of 85.1km/h,
  - ✓ The bridge unit mass of 1879 kg/m and
  - ✓ The moment of inertia of 0.33m^4.
  - ✓ The two axle load of front or rear axle load is considered as one axle load
  - ✓ The following parameters are taken constant

The following procedures are followed:

1) First the time or arrival is calculated for each axle entering the bridge. This value is used in row 2 of Table B-3 and Table B-4.
2) Then the unit step function is calculated for each axle load. An example is shown for the first axle load in Table B-3. This will help to exclude only on the contribution of the axle load on the bridge displacement before it enters the bridge.
3) The generalized displacement coordinate is calculated using Equation 5-22 and the above mentioned information. An example is shown in Table B-4 for three axle load entering the bridge successively.
4) Then the displacement is calculated using Equation 5-21.
5) Figure 6-3 is plotted using the above stated method and simple addition method discussed in Section B-1.

Table B-3: Application of a Unit step function [part of Equation 5-22]

J					**1**
tj					**0**
tj+tc					**0.573779083**
Time	**H(t-tj)**	**H(t-tc-tj)**	**H(t-tj-L/v)**	**H(t-tc-tj-L/v)**	**Z(t)**
0	1	0	0	0	0
0.0025	1	0	0	0	6.329E-08
0.005	1	0	0	0	5.04836E-07
…….	1	0	0	0	…….
…….	1	0	0	0	…….
…….	1	0	0	0	…….
…….	1	0	0	0	…….
0.5725	1	0	0	0	0.003218823
0.575	1	1	0	0	0.003218048
0.5775	1	1	0	0	0.003228956
…….	1	1	0	0	…….
…….	1	1	0	0	…….
…….	1	1	0	0	…….
…….	1	1	0	0	…….
…….	1	1	0	0	…….
1.37	1	1	0	0	0.003234261
1.3725	1	1	0	0	0.003204261
1.375	1	1	0	0	0.003176802
1.3775	1	1	1	0	0.003038031
…….	1	1	1	0	…….
…….	1	1	1	0	…….
…….	1	1	1	0	…….
1.95	1	1	1	0	-0.000330784
1.9525	1	1	1	1	-0.000351219
1.955	1	1	1	1	-0.000364802
1.9575	1	1	1	1	-0.000371269
1.96	1	1	1	1	-0.000370492
1.9725	1	1	1	1	-0.000263355

Table B-4: The generalized displacement coordinate (Z(t)) of bridge due to the jth load [Equation 5-22]

J	**1**	**2**	**3**
Tj	**0.00**	**0.82**	**1.64**
tj+tc	**0.57**	**1.40**	**2.22**
0	0	0	0
0.0025	6.33E-08	0	0
0.005	5.05E-07	0	0
0.0075	1.7E-06	0	0
0.01	3.99E-06	0	0
…….	…….	0	0
…….	…….	0	0
…….	…….	0	0
…….	…….	0	0
…….	…….	0	0
…….	…….	0	0
…….	…….	0	0
0.8175	0.004934	0	0
0.82	0.004949	0	0
0.8225	0.004966	1.38E-09	0
0.825	0.004986	1.32E-07	0
0.8275	0.005008	7.46E-07	0
0.83	0.005032	2.21E-06	0
…….	…….	…….	0
…….	…….	…….	0
…….	…….	…….	0
…….	…….	…….	0
…….	…….	…….	0
…….	…….	…….	0
1.6425	0.002206	0.004822	0
1.645	0.002237	0.004835	1.1E-08
1.6475	0.002268	0.004853	2.39E-07
1.65	0.002297	0.004876	1.05E-06
1.6525	0.002324	0.004903	2.82E-06
1.655	0.002347	0.004935	5.88E-06
1.6575	0.002365	0.004971	1.06E-05

B.3 Demonstrating measured data pre-processing

The original measured acceleration data before pre-processing is presented in Table B-5 to make comparison of this original data with the pre-processed data presented in Table B-6 easier to comprehend.

Table B-5: Original measured acceleration data before pre-processing

;Title	http://www.gcdataconcepts.com		X16-1c			
;Version		1409	Build num	0x21E	Build date	20120404 13:16:08
;Start_time	2013-11-18		00:23:44.687			
;Temperature		45.75	deg C	Vbat	1268	mv
;Gain	Low					
;SampleRate		400	Hz			
;Deadband		0	counts			
;DeadbandTimeout		20	sec			

;Headers	Time	Ax	Ay	Az
100.264		12	2	1042
100.2666		18	-6	1022
100.2692		18	0	1024
100.2717		20	-10	1024
100.2743		8	-6	1006
100.2769		14	-18	1024
100.2795		16	-18	1022
100.2821		12	4	1020
100.2847		16	-6	980
100.2873		12	-6	1010
100.2909		12	-12	1024
100.2925		22	4	990
100.295		12	-12	998
100.2977		6	-4	1024
100.3002		6	-4	1002

The Pre-processing adopted in this research is presented in Table B-6. Synchronizing of the data involves making sure all signal starts at the same time. De-trending involves removing the mean value from the entire signal to make sure we achieve the net signal. For instance the acceleration data automatically measures the acceleration of gravity as a constant value of 9.81m/s^2 before the train arrives on the bridge. By the time the train arrive a signal

starts to read a value ±9.81m/s^2. Removing the gravity by deducting value equal to gravity or 9.81m/s^2 will give us the net acceleration signal on the bridge. The removal of a constant value of 9.81m/s^2 is called de-trending.

Table B-6: Demonstrating of pre-processing on measured acceleration data

PRE-PROCESSING

TIME		ACCELERATION			
Syncronization of time		**Applying conversion units & De-trending**			
Original	Processed	Original	Processed		
Signal start time	Adjusted to start at zero	measured data	Factored by 1024 as per with manufacturer specification	De-trending	Converted from G to m/s2
	100.263986				
100.263986	0	1042	1.017578125	0.017578125	0.172441406
100.266581	0.002595	1022	0.998046875	-0.001953125	-0.019160156
100.2692	0.005214	1024	1	0	0
100.271728	0.007742	1024	1	0	0
100.274322	0.010336	1006	0.982421875	-0.017578125	-0.172441406
100.276941	0.012955	1024	1	0	0
100.279536	0.01555	1022	0.998046875	-0.001953125	-0.019160156
100.282064	0.018078	1020	0.99609375	-0.00390625	-0.038320313
100.284749	0.020763	980	0.95703125	-0.04296875	-0.421523438
100.287277	0.023291	1010	0.986328125	-0.013671875	-0.134121094
100.290896	0.02691	1024	1	0	0
100.29249	0.028504	990	0.966796875	-0.033203125	-0.325722656
100.295018	0.031032	998	0.974609375	-0.025390625	-0.249082031
100.297704	0.033718	1024	1	0	0
100.300232	0.036246	1002	0.978515625	-0.021484375	-0.210761719

APPENDIX C

TYPICAL FIELD MEASUREMENT DATA

APPENDIX C TYPICAL MEASUREMENT DATA

C1: Typical field measured displacement (point 'b' in table 3.2)

HBM_CATMAN_DATAFILE_40

18/11/2013
15:00
CHANNELS: 5
SEPARATOR: 9
MAXLINES: 186843

MX840A_4 - default sample rate CH=1	Main Beam Middle CH=4
s	mm
18/11/2013-15:00	18/11/2013-15:00
T0 =13/11/18 14:58:05	T0 =13/11/18 14:58:05
dt =0.833333313465118 ms	dt =0.833333333333333 ms
CH 0	CH 1
Serial No. (Electronics / CP)Nicht verfbar	Serial No. (Electronics / CP)9E5003862
Nicht verfbar ID=0	MX840A ID=5036
Nicht verfbar ID=0	Nicht verfbar ID=0
Nicht verfbar ID=0	Inductive full bridge ID=356
x1=0 y1=0;x2=0 y2=0	x1=0 y1=0;x2=80 y2=50
(Electr.)	mV/V (Electr.)
(Engin.)	mm (Engin.)
0 Nominal value	75 mm Nominal value
Nicht verfbar ID=0	Nicht verfbar ID=0
Scaling = Engineering units ID=0	Scaling = Engineering units ID=0
Nicht verbar ID=0	2.5 V excitation ID=13
Filter = Nicht verfbar ID=0	Filter = Bessel lowpass ID=142
fg = Nicht verfbar ID=0	fg = 100 Hz ID=955
0 Zero	0 mm Zero
0 Tare	0 mm Tare
0 Software-Zero	0 mm Software-Zero
Gage factor = 0	Gage factor = 0
Bridge factor = 0	Bridge factor = 0
Software scaling: None	Software scaling: None
Sensor: None	Sensor: WA 50mm
Sensor T-ID: None	Sensor T-ID: HBM_WA_50mm
Cable length correction Nicht verfbar	Cable length correction Nicht verfbar

0	20.25
0.00083	20.25
0.00167	20.25
0.0025	20.25
0.00333	20.25
0.00417	20.25
0.005	20.25
0.00583	20.25
0.00667	20.25

C2: Typical field measured acceleration readings taken at mid span cross beam (point '5' in table 3.1)

Title, http://www.gcdataconcepts.com, X16-1c
;Version, 1409, Build num, 0x21E, Build date, 20120404 13:16:08,
SN:CCDC42011002298
;Start_time, 2013-03-22, 11:59:32.030
;Temperature, 30.25, deg C, Vbat, 1339, mv
;Gain, low
;SampleRate, 400,Hz
;Deadband, 0, counts
;DeadbandTimeout, 0,sec
;Headers, time,Ax,Ay,Az
135.378954,-280,242,1110
135.381573,-70,-468,1064
135.384034,292,-328,576
135.386562,572,578,2270
135.389114,-532,722,1068
135.391642,24,208,-494
135.394194,-68,-224,1084
135.396722,20,-84,1360
135.399250,410,-40,632
135.401869,-276,-50,2576
135.404330,-264,24,-248
135.406949,190,-240,982
135.409410,148,346,400
135.411938,-66,-228,1376
135.414490,116,-428,1322
135.417018,-244,204,932
135.419637,224,-90,770
135.422098,-320,366,1198
135.424626,-62,-84,1198
135.427178,108,-194,1394
135.429706,284,-150,524
135.432258,110,-72,1360
135.434786,-2,-174,1176
135.437314,-118,258,418

APPENDIX D

TYPICAL SUPPORTING DOCUMENTS

APPENDIX D SUPPORTING DOCUMENTS

D.1 Matlab script to plot frequency domain from acceleration vs time data (script originated from Matlab example modified to suit the data)

Matlab script	Description
Xd1=z1(:,1); yd1=z1(:,2); Fs=400; L= 4558; NFFT = 2^nextpow2(L);	% z1 is data containing time and acceleration at different column % time data in column 1 and all raw % acceleration data in column 2 and all raw % Sampling frequency (average is taken) % Length of signal % Next power of 2 from length of y. This is not however studied in this research. However the following definition is included as a brief introduction taken from OaSYS GSA software tutorial note. % (NFFT is a FFT length which determines the frequencies at which the PSD is estimated where NFFT stands for Nonequispace fast fourier transform and PSD stands for power spectral density. PSD is the average power in the signal over that frequency band. Identifying the different types of powe of signal is not part of the scope of this research
Yd1= fft(yd1,NFFT)/L; f = Fs/2*linspace(0,1,NFFT/2); plot(f,2*abs(Yd1(1:NFFT/2)), 'black', 'LineWidth', title(' Amplitude Spectrum of y(t)') xlabel('Frequency (Hz)') ylabel('|Y(f)|')	% fft(X) returns the discrete Fourier transform (DFT) of vector X, computed with a fast Fourier transform (FFT) algorithm. The mathematical algorithm is not part of the scope of this research % fft(X,n) returns the n-point DFT % linspace(a,b,n) generates a row vector of n points linearly spaced between and including a and b.

APPENDIX E

SNAP SHOTS

APPENDIX E SUPPORTING DOCUMENTS

E.1 Snap shot of calculation maximum bending moment

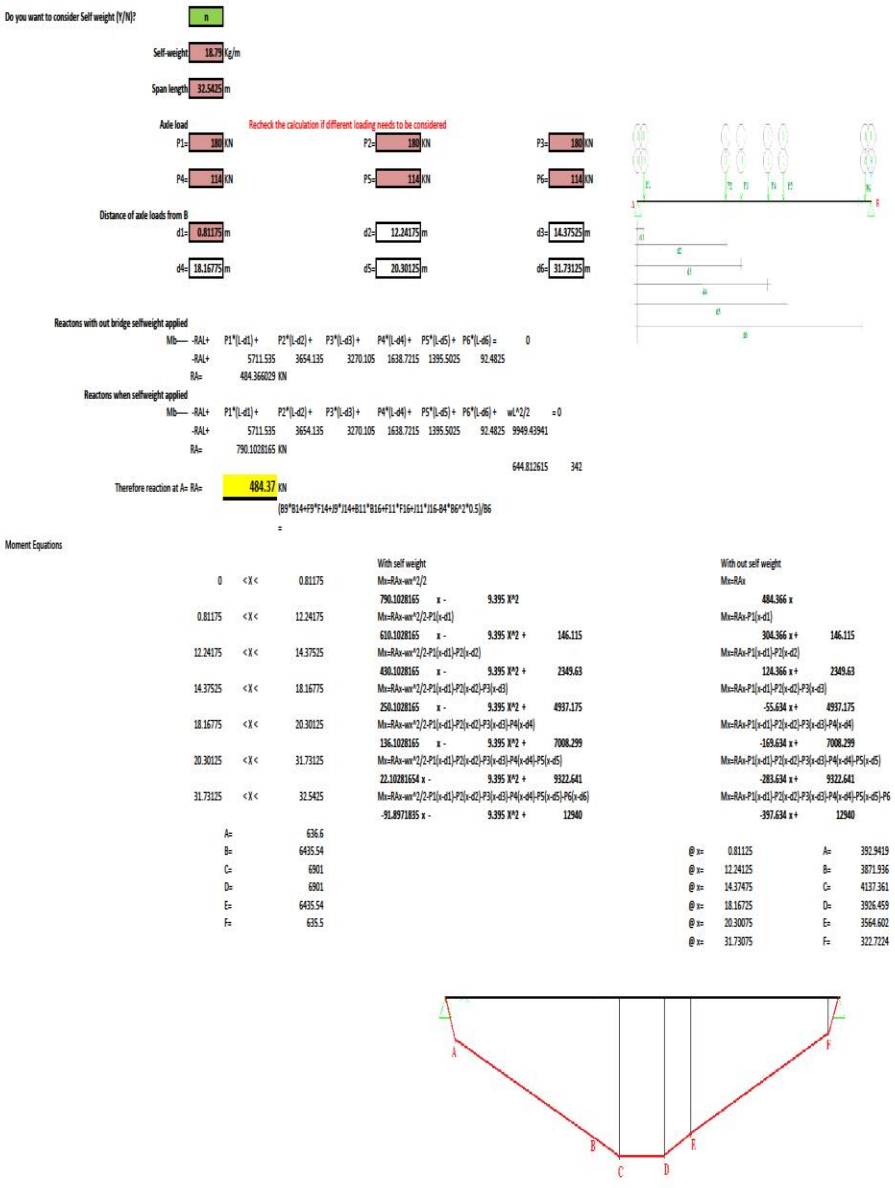

E.2 Snap shot of calculation maximum static deflection (input for Figure 7.9)

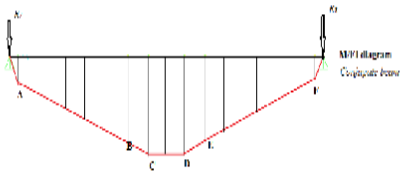

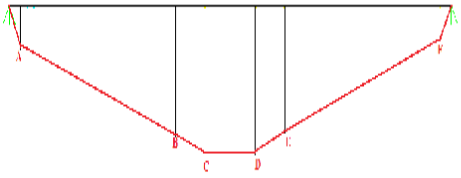

With out Self-weight of beam included

Using Congugare beam model

Shear just left of support on conjugate beam=Slope on real beam
Bending Momen on conjugate beam= Deflection on real beam

@ x=	0.81125	A=	392.9419
@ x=	12.24125	B=	3871.936
@ x=	14.37475	C=	4137.361
@ x=	18.16725	D=	3926.459
@ x=	20.30075	E=	3564.602
@ x=	31.73075	F=	322.7224

E= 205 Gpa I 0.38 m^4

c

1/2*A*(L-d6)*(d6+1/3*(L-d6)+A*(d6-d5)*(d5+1/2(d6-d5))+(B-A)*1/2*(d6-d5)*(d5+1/3*(d6-d5)+B*(d5-d4)*(d4+1/2*(d5-d4))+1/2*(C-B)*(D5-D4)*(D4+1/2*(D5-D4))+C*(D4-

Mb.... RAL- D3)*(D3+0.5*(D4-D3))+E*(D3-D2)*(D2+1/2*(D3-D2))+(D-E)*1/2*(D3-D2)*(D2+2/3*(D3-D2)+F*(D2-D1)*(D1+1/2*(D2-D1))+(E-F)*1/2*(D2-D1)*(D1+2/3*(D2-D1))+F*1/2*D1*2/3*D1

RAL- 5100.652 + 116847.4701 + 479390.7 + 158891.9 + 5345.415 + 255315.1 + -6254.56 + 101212.2

\+ 5274.486976 + 24075.33 + 156217.9 + 70.88469

Therefore reaction at A= RA= 39993.47 /EI KN

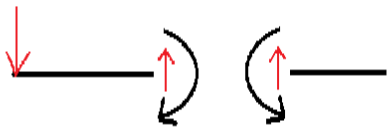

Moment @mid span on conjugate beam=Deflection @ mid span on real beam

Mc=..... M@ mid span=RA*L*1/2-1/2*A*(L/2-2/3*(L-d6)-A*(d6-d5)*(L/2-(L-d6)-0.5*(d6-d5))-1/2*(B-A)*(d6-d5)*(L/2-(L-d6)-2/3*(d6-d5))-B*(d5-d4)*(0.5(d5-d4)+0.5*(d4-d3))-1/2*(C-d4)*(1/3*(d5-d4)+0.5*(d4-d3))-C*(d4-d3)*(0.5*0.5*(d4-d3))-1/2*(D-C)*(d4-d3)*(1/3*0.5*(d4-d3))

Mc=..... RAL/2- 2507.185 - 43766.85 - 155873.4 - 24476.68 - 738.2693 - 14876.97 -

Mc=..... 408,757.13 /EI

Mc=..... 0.005247203 N-m

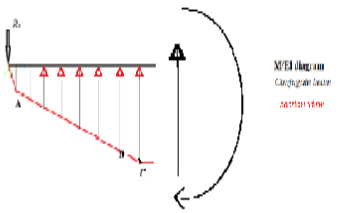

Deflection at Mid-span= 5.25 mm

E.3 Snap shot of input for displacement (using Equation 5-17 & Equation 5-18

m	L	Speed		td	E	I	ωn	T	P0	2L^3	πv/L	1.00	(πv/ωnL)X Sin (ωnt)
[kg/m]	[m]	[km/h]	[m/s]	[s]	[pa]	[m4]	[Hz]		[Hz]	Pi()^4*EI		ωn2-(π v/L)2	
1879	32.5	85.1	23.6	1.4	2.1E+11	0.33	55.9	351.3	114000	1.0E-08	2.3	3.20E-04	0.04
1879	32.5	85.1	23.6	1.4	2.1E+11	0.33	55.9	351.3	114000	1.0E-08	2.3	3.20E-04	0.04

Therefore the equation for Z(t) can be re written as,

when t ≤ L/V

Z(t) =	1.05E-08	P0 (	Sin	2.28	t	-	0.04	Sin	55.91	t
Z(t) =	1.05E-08	P0 (	Sin	2.28	t	-	0.04	Sin	55.91	t

when t ≥ L/V

Z(t) =	-8.55E-10	P0 (	Cos	38.49	X	sin [	55.91	(t-	0.69
Z(t) =	-8.55E-10	P0 (	Cos	38.49	X	sin [	55.91	(t-	0.69

E.4 Snap shot of displacement results (using Equation 5-17 & Equation 5-18)

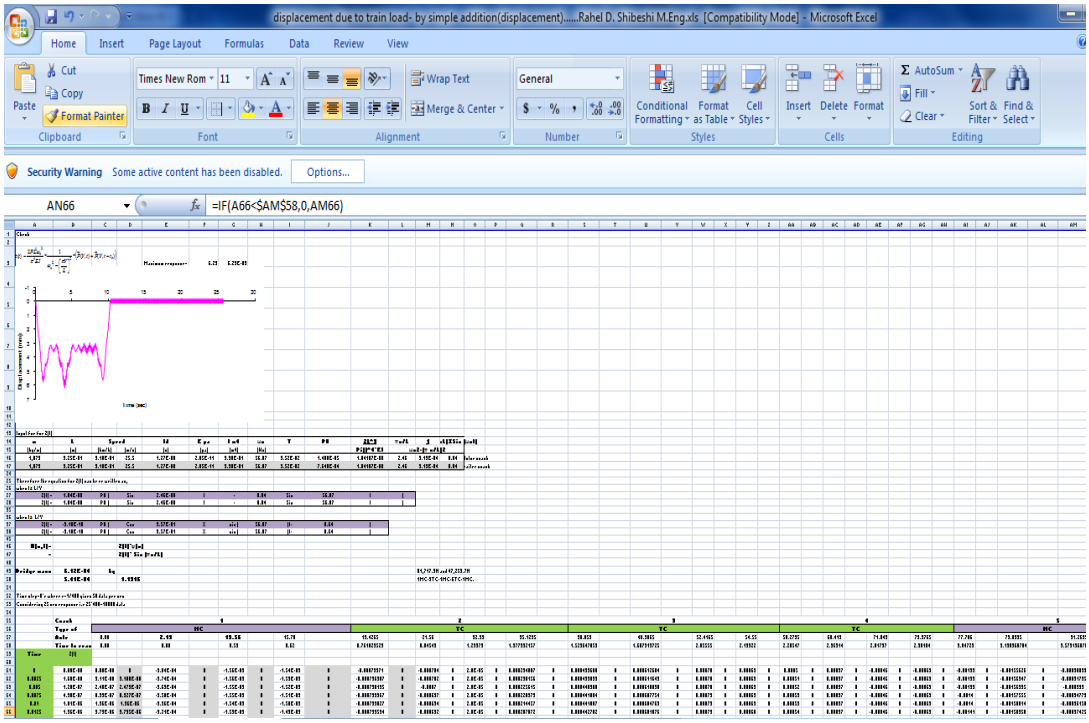

E.5 Snap shot of displacement comparision of displacement of the bridge due to single load, equal and actual train loads

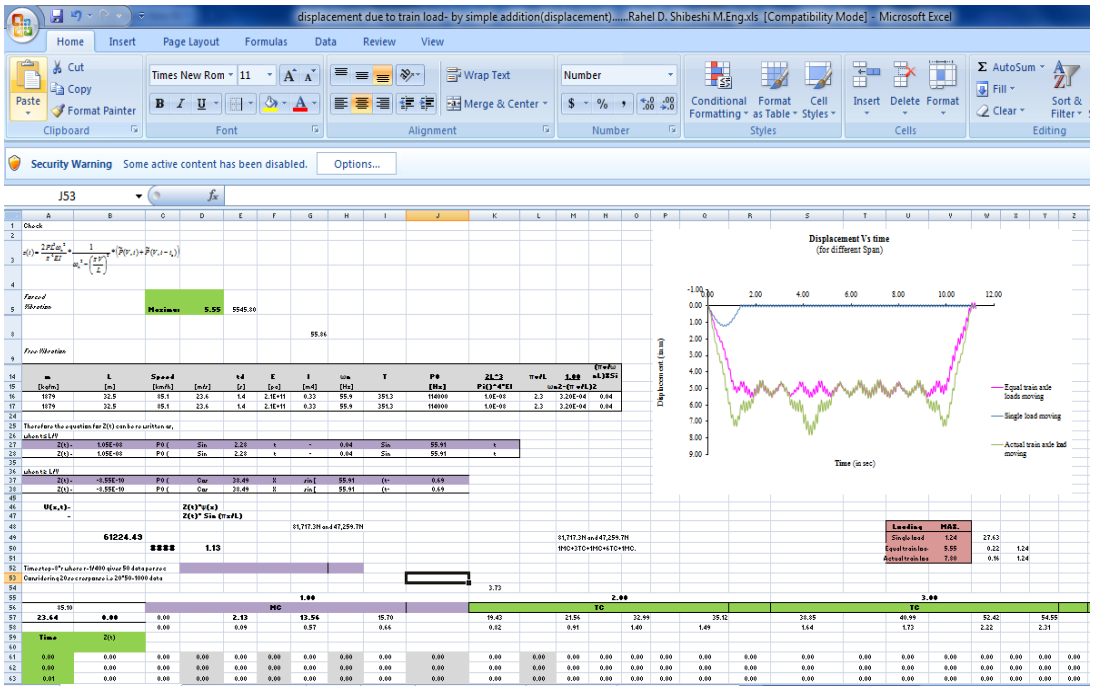

E.6 Snap shot of displacement comparision using equation from yang *et al* (2004) vs. chopra (2007)

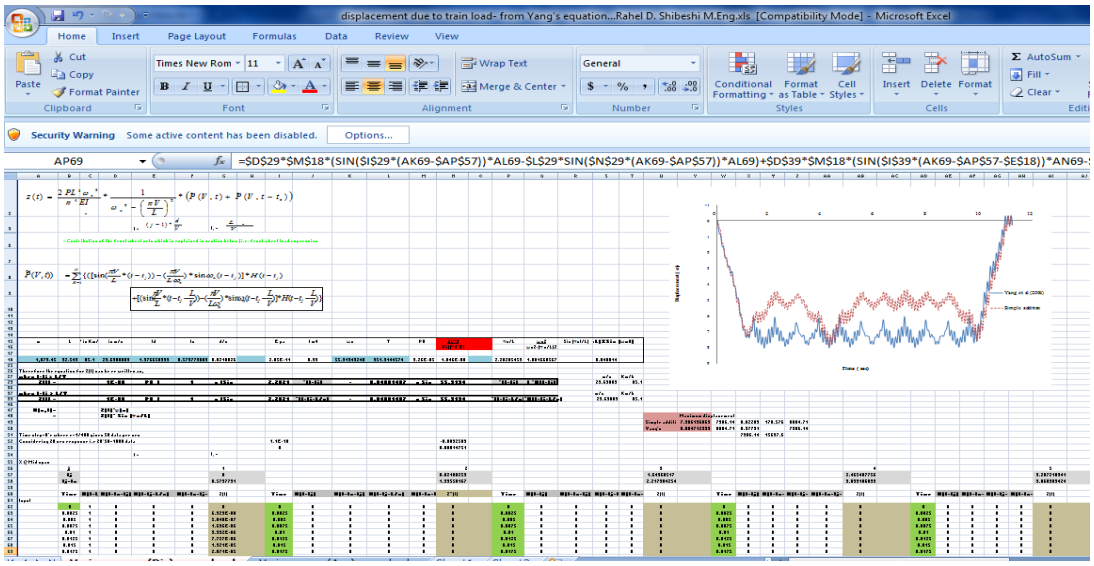

E.7 Displacement coordinate for the first two axle loads of the 1st coach

Coach number	1			
Type of coach	MC			
Axle spacing	0.00		**2.13**	
Time to reach	0.00		0.08	
Time				
0	0.00E+00	0	-3.84E-04	0
0.0025	3.11E-08	3.1083E-08	-3.74E-04	0
0.005	2.48E-07	2.4793E-07	-3.63E-04	0
0.0075	8.33E-07	8.3267E-07	-3.50E-04	0
0.01	1.96E-06	1.9602E-06	-3.36E-04	0
0.0125	3.79E-06	3.7947E-06	-3.21E-04	0
0.015	6.49E-06	6.4865E-06	-3.04E-04	0
0.0175	1.02E-05	1.0169E-05	-2.87E-04	0
0.02	1.50E-05	1.4956E-05	-2.70E-04	0
0.0225	2.09E-05	2.0941E-05	-2.51E-04	0
0.025	2.82E-05	2.8191E-05	-2.33E-04	0
0.0275	3.68E-05	3.6751E-05	-2.14E-04	0
0.03	4.66E-05	4.6639E-05	-1.95E-04	0
0.0325	5.78E-05	5.7846E-05	-1.76E-04	0
0.035	7.03E-05	7.0339E-05	-1.58E-04	0
0.0375	8.41E-05	8.4059E-05	-1.40E-04	0
0.04	9.89E-05	9.8921E-05	-1.23E-04	0
0.0425	1.15E-04	0.00011482	-1.06E-04	0
0.045	1.32E-04	0.00013163	-9.09E-05	0
0.0475	1.49E-04	0.00014921	-7.66E-05	0
0.05	1.67E-04	0.00016739	-6.35E-05	0
0.0525	1.86E-04	0.00018601	-5.17E-05	0
0.055	2.05E-04	0.00020488	-4.12E-05	0
0.0575	2.24E-04	0.00022382	-3.20E-05	0
0.06	2.43E-04	0.00024264	-2.42E-05	0
0.0625	2.61E-04	0.00026116	-1.76E-05	0
0.065	2.79E-04	0.0002792	-1.23E-05	0
0.0675	2.97E-04	0.00029659	-8.07E-06	0
0.07	3.13E-04	0.00031317	-4.94E-06	0
0.0725	3.29E-04	0.0003288	-2.72E-06	0
0.075	3.43E-04	0.00034336	-1.28E-06	0
0.0775	3.57E-04	0.00035674	-4.64E-07	0
0.08	3.69E-04	0.00036887	-9.80E-08	0
0.0825	3.80E-04	0.00037968	-3.16E-09	0
0.085	3.89E-04	0.00038916	4.72E-09	4.7188E-09

E.8 Displacement coordinate of the 12th coach and total sum of all coach and resulting total displacement of the bridge (continued from section E7)

12									
MC									
213.69		215.83		227.26		229.39		TOTAL	16.25
8.38		8.46		8.91		9.00			
								Z(t)	u(t)
-0.00157	0	-0.00141	0	-4.7E-05	0	0.000348	0	0	0
-0.00157	0	-0.0014	0	-4.7E-05	0	0.000339	0	3.11E-08	3.11E-05
-0.00157	0	-0.0014	0	-4.7E-05	0	0.000329	0	2.48E-07	0.000248
-0.00157	0	-0.00139	0	-4.7E-05	0	0.000317	0	8.33E-07	0.000833
-0.00157	0	-0.00139	0	-4.7E-05	0	0.000305	0	1.96E-06	0.00196
-0.00157	0	-0.00138	0	-4.9E-05	0	0.000291	0	3.79E-06	0.003795
-0.00157	0	-0.00138	0	-5E-05	0	0.000275	0	6.49E-06	0.006486
-0.00156	0	-0.00137	0	-5.3E-05	0	0.000259	0	1.02E-05	0.010169
-0.00156	0	-0.00137	0	-5.7E-05	0	0.000242	0	1.5E-05	0.014956
-0.00155	0	-0.00137	0	-6.1E-05	0	0.000225	0	2.09E-05	0.020941
-0.00154	0	-0.00137	0	-6.7E-05	0	0.000206	0	2.82E-05	0.028191
-0.00154	0	-0.00137	0	-7.4E-05	0	0.000188	0	3.68E-05	0.036751
-0.00153	0	-0.00137	0	-8.3E-05	0	0.000169	0	4.66E-05	0.046639
-0.00152	0	-0.00138	0	-9.2E-05	0	0.00015	0	5.78E-05	0.057846
-0.00151	0	-0.00138	0	-0.0001	0	0.000131	0	7.03E-05	0.070339
-0.00151	0	-0.00139	0	-0.00012	0	0.000112	0	8.41E-05	0.084059
-0.0015	0	-0.0014	0	-0.00013	0	9.44E-05	0	9.89E-05	0.098921
-0.00149	0	-0.0014	0	-0.00014	0	7.71E-05	0	0.000115	0.11482
-0.00149	0	-0.00141	0	-0.00016	0	6.07E-05	0	0.000132	0.13163
-0.00148	0	-0.00142	0	-0.00018	0	4.53E-05	0	0.000149	0.149206
-0.00148	0	-0.00144	0	-0.00019	0	3.09E-05	0	0.000167	0.167389
-0.00147	0	-0.00145	0	-0.00021	0	1.77E-05	0	0.000186	0.186006
-0.00147	0	-0.00146	0	-0.00023	0	5.8E-06	0	0.000205	0.204878
-0.00147	0	-0.00147	0	-0.00025	0	-4.8E-06	0	0.000224	0.223819
-0.00147	0	-0.00148	0	-0.00027	0	-1.4E-05	0	0.000243	0.242643
-0.00147	0	-0.0015	0	-0.00029	0	-2.2E-05	0	0.000261	0.261164
-0.00148	0	-0.00151	0	-0.00031	0	-2.9E-05	0	0.000279	0.279203
-0.00148	0	-0.00152	0	-0.00032	0	-3.4E-05	0	0.000297	0.296591
-0.00149	0	-0.00153	0	-0.00034	0	-3.8E-05	0	0.000313	0.313171
-0.00149	0	-0.00154	0	-0.00036	0	-4.2E-05	0	0.000329	0.328801
-0.0015	0	-0.00155	0	-0.00037	0	-4.4E-05	0	0.000343	0.343358
-0.00151	0	-0.00156	0	-0.00039	0	-4.5E-05	0	0.000357	0.356739

E.9 Possible resonance speed summary

	Frequency	10	Hz												
Repititive Spacing	Posible Critical Speeds[m/s]	Multple of possible critical speed [km/h]													
		1		1		2		3		4		5		6	
			km/h		km/h		km/h		km/h		km/h		km/h		km/h
2.13	20	10	37	20	74	41	147	61	221	82	294	102	368	221	795
11.43	109	55	197	109	394	219	788	328	1183	438	1577	547	1971	1183	4257
3.73	36	18	64	36	129	71	257	107	386	143	514	179	643	386	1389
19.49	187	93	336	187	672	373	1344	560	2016	747	2689	934	3361	2016	7259

Key	
	Continously increasing acceleration
	Unrealistic speed for selected bridge which is ignored but critical
	Possible resonance spped: Critical in causing maximum amplitude above 4m/s2
	Cancellation effect observed

APPENDIX F

FINITE ELEMENT MODELLING OUTPUTS

APPENDIX F FINITE ELEMENT MODELLING OUTPUT

F.1 Natural frequency of the first vertical bending mode from FEM using beam elements observed at mode 4 (all pin supports)

Job No.	Sheet No.	Rev.
MSc		
Drg. Ref.		
Made by: RD	Date: 24-Feb-2015	Checked

Dynamic Analysis
Steel railway bridge
Beam model..Truss bridge at irene

ANALYSIS LAYER
Scale: 1:176.8
Highlighted:
Coincident Nodes
Coincident Elements
Deformation magnification: 2.500
Case: A237 : Modal50 : Mode 4
Mode 4
Frequency: 10.06 Hz
Period: 0.09944 s

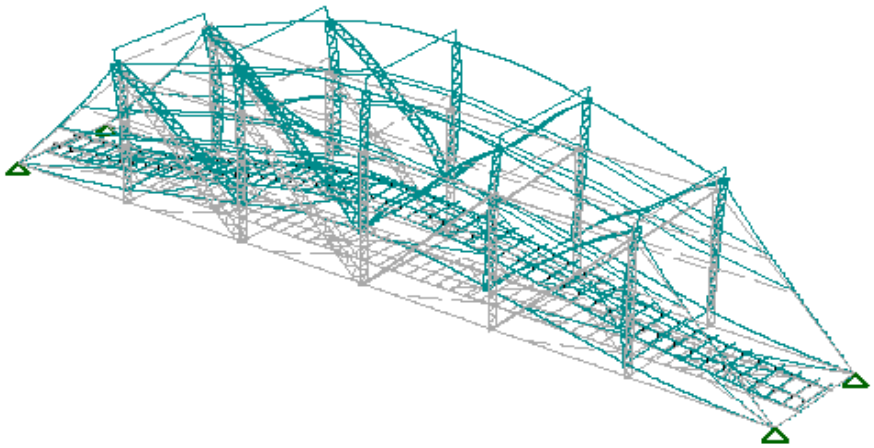

Program GSA Version 8.6.1.23 Copyright © Oasys 1985-2012 Page 1
C:\RAHEL D. SHIBESHI\M.SC FINITE ELEMENT MODEL\FEM rishi\T...\Beam model with pin.gwb Printed 26-Feb-2015 Time 23:43

F.2 Natural frequency of the second vertical bending mode from FEM using beam elements observed at mode 12 (all pin supports)

Job No.	Sheet No.	Rev.
MSc		
Drg. Ref.		
Made by RD	Date 24-Feb-2016	Checked

Dynamic Analysis
Steel railway bridge
Beam model..Truss bridge at irene

ANALYSIS LAYER
Scale: 1:206.2
Highlighted:
Coincident Nodes
Coincident Elements
Deformation magnification: 2.500
Case: A245 : Modal50 : Mode 12
Mode 12
Frequency: 16.96 Hz
Period: 0.05895 s

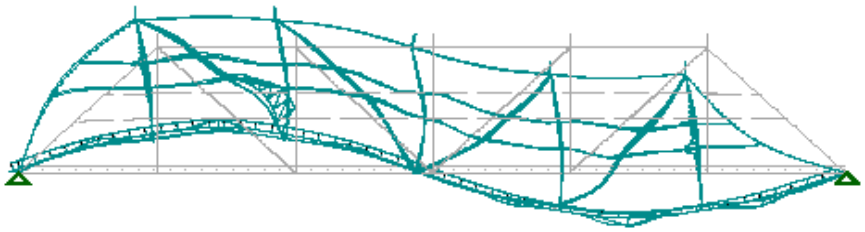

Program GSA Version 8.6.1.23 Copyright © Oasys 1986-2012 Page 1
C:\RAHEL D. SHIBESHI\M.SC FINITE ELEMENT MODEL\FEM rioh\T...\Beam model with pin.gwb Printed 26-Feb-2016 Time 23:50

F.3 Natural frequency of the first vertical bending mode from FEM using beam elements observed at mode 4 (two roller and two pin supports)

Job No.	Sheet No.	Rev.
MSc		
Drg. Ref.		
Made by: RD	Date: 27-Feb-2016	Checked

Dynamic Analysis
Steel railway bridge
Beam model..Truss bridge at irene

ANALYSIS LAYER
Scale: 1:199.9
Highlighted:
Coincident Nodes
Coincident Elements
Deformation magnification: 2.500
Case: A237 : Modal50 : Mode 4
Mode 4
Frequency: 8.659 Hz
Period: 0.1155 s

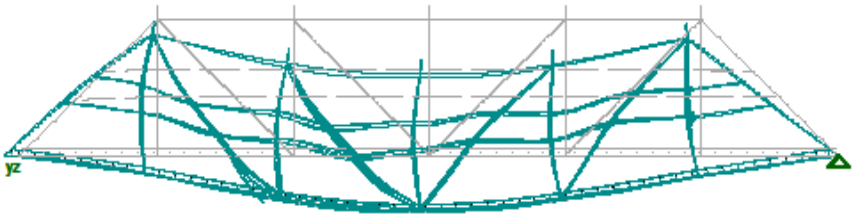

Program GSA Version 8.6.1.23 Copyright © Oasys 1985-2012 Page 1
Beam model with rollers one two support movement in the longitudinal direction.gwb Printed 27-Feb-2016 Time 03:39

F.4 Axial force in members from FEM using beam elements (all pin supports)

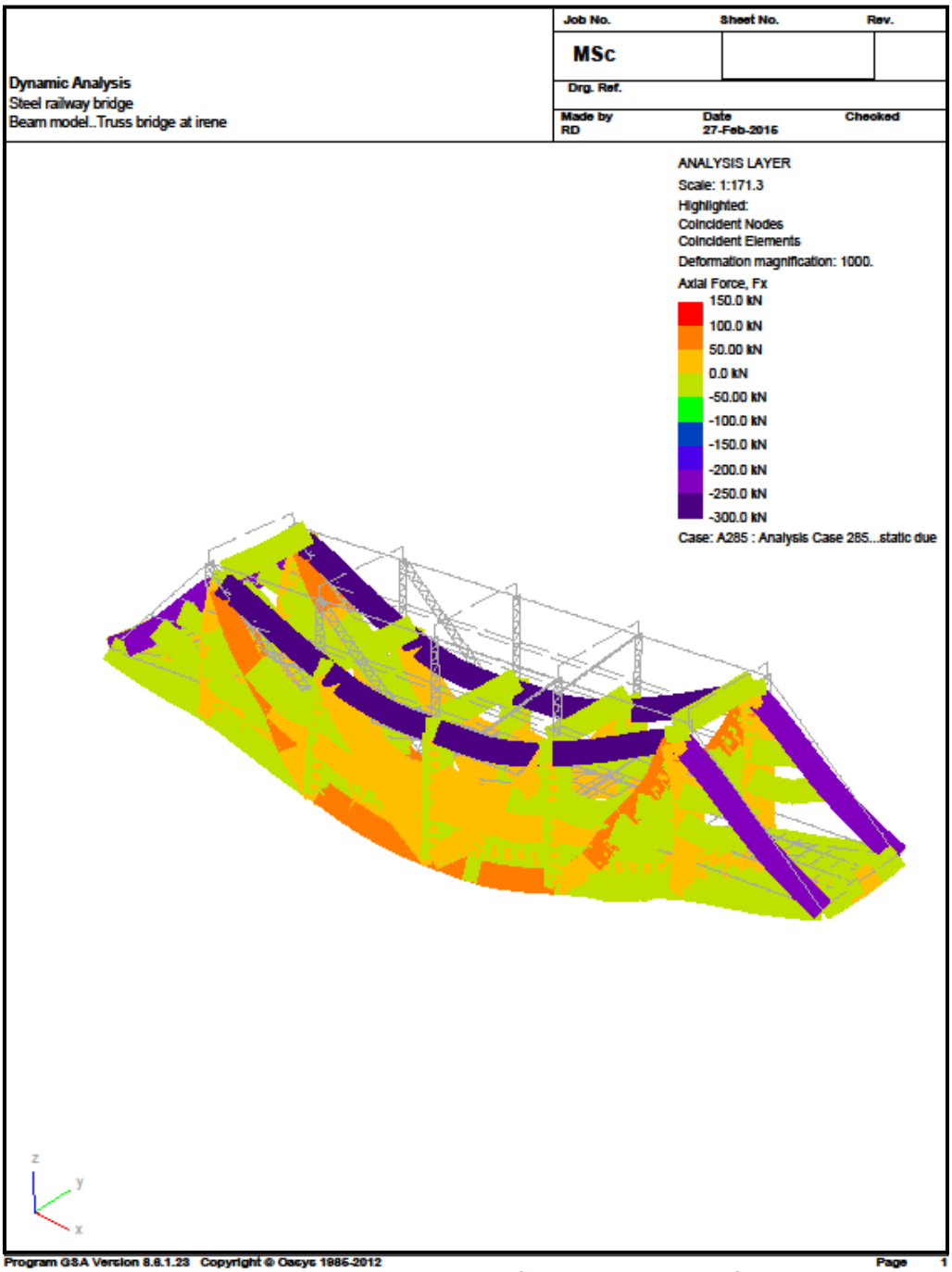

F.5 Reaction force in members from FEM using beam elements (all pin supports)

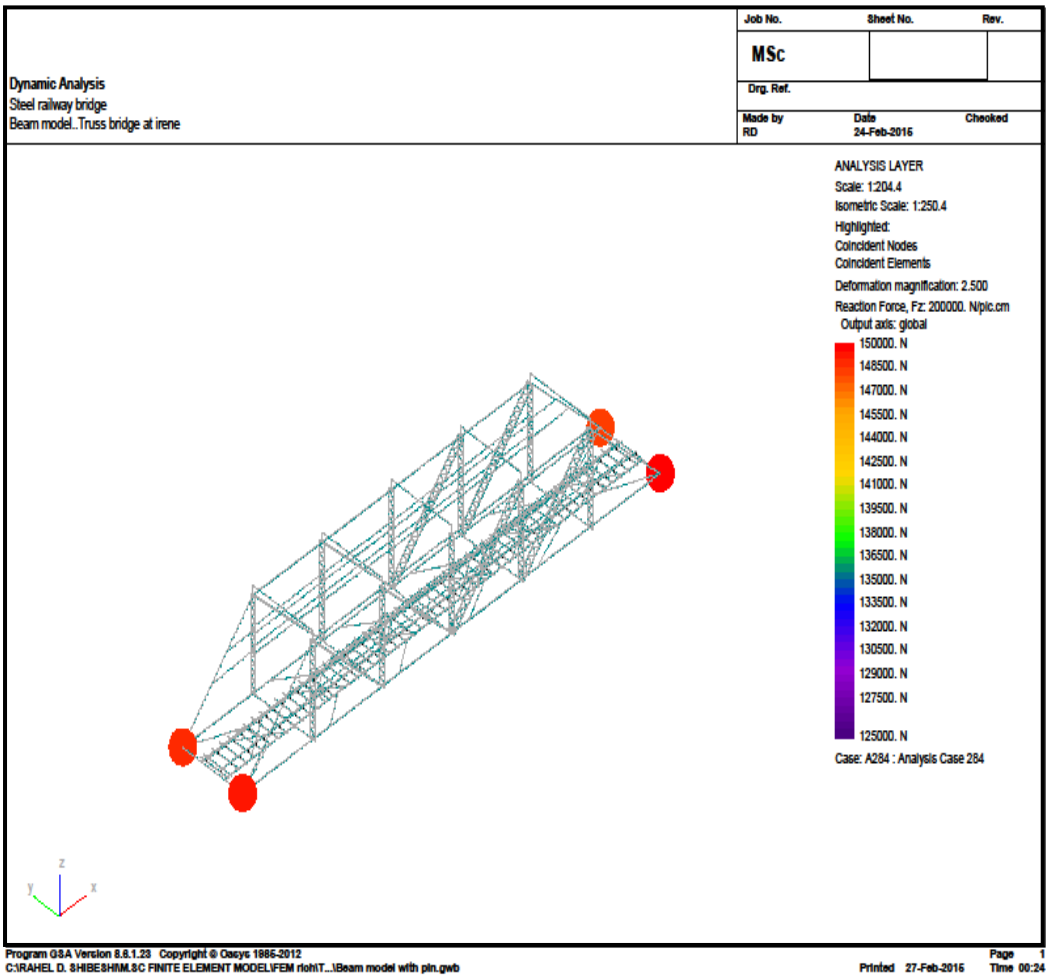

F.6 Reaction force in members from FEM using beam elements with the selfweight displayed (all pin supports)

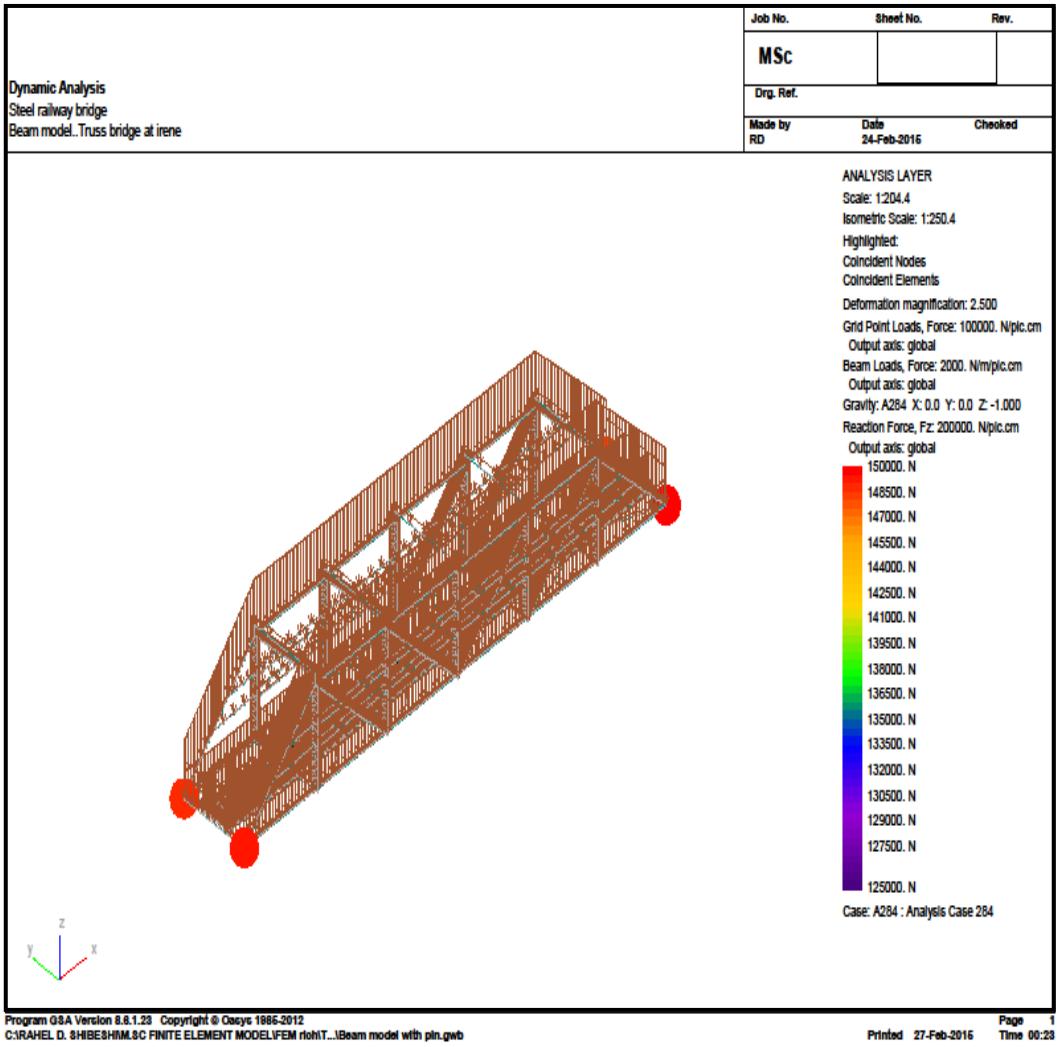

F.7 Maximum bending stresses in members from FEM using shell elements (all pin supports)

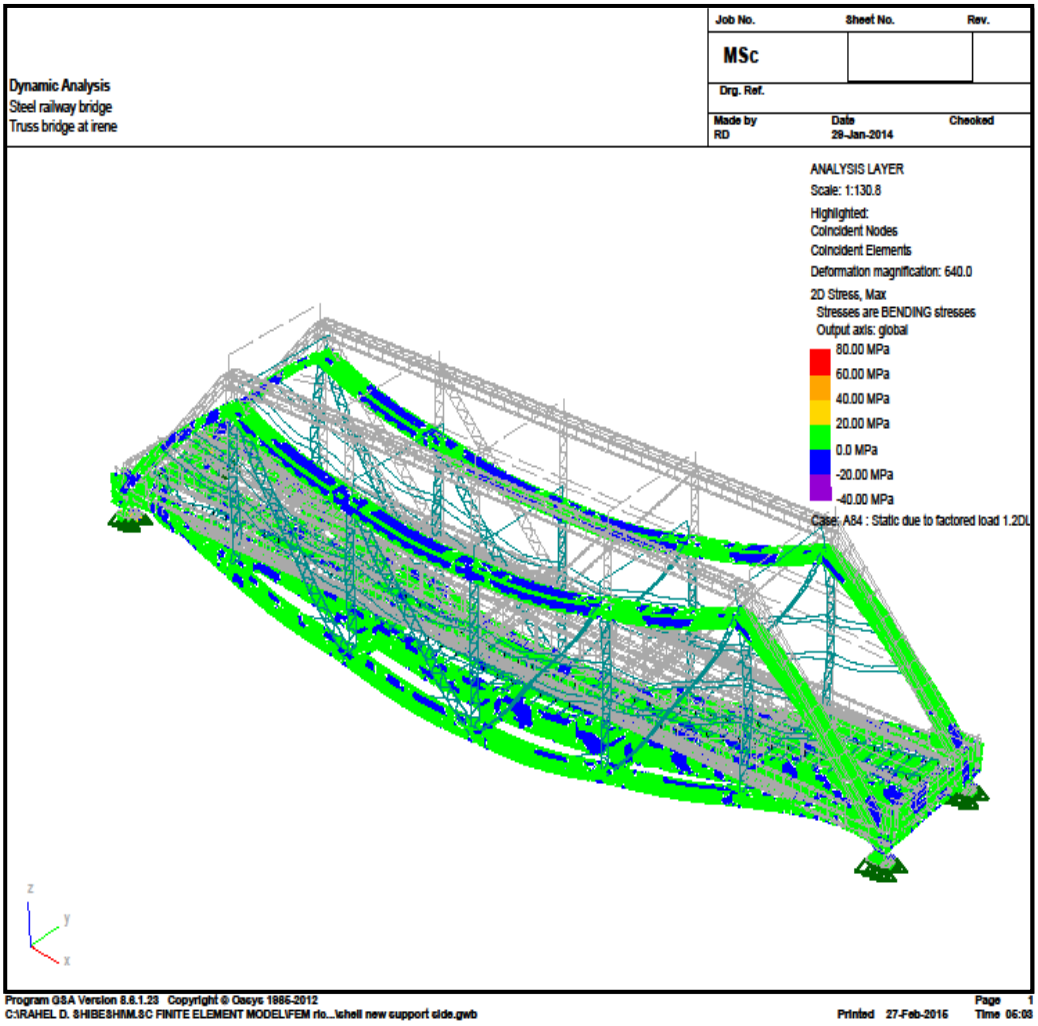

F.8 Von mises bending stresses in members from FEM using shell elements (all pin supports)

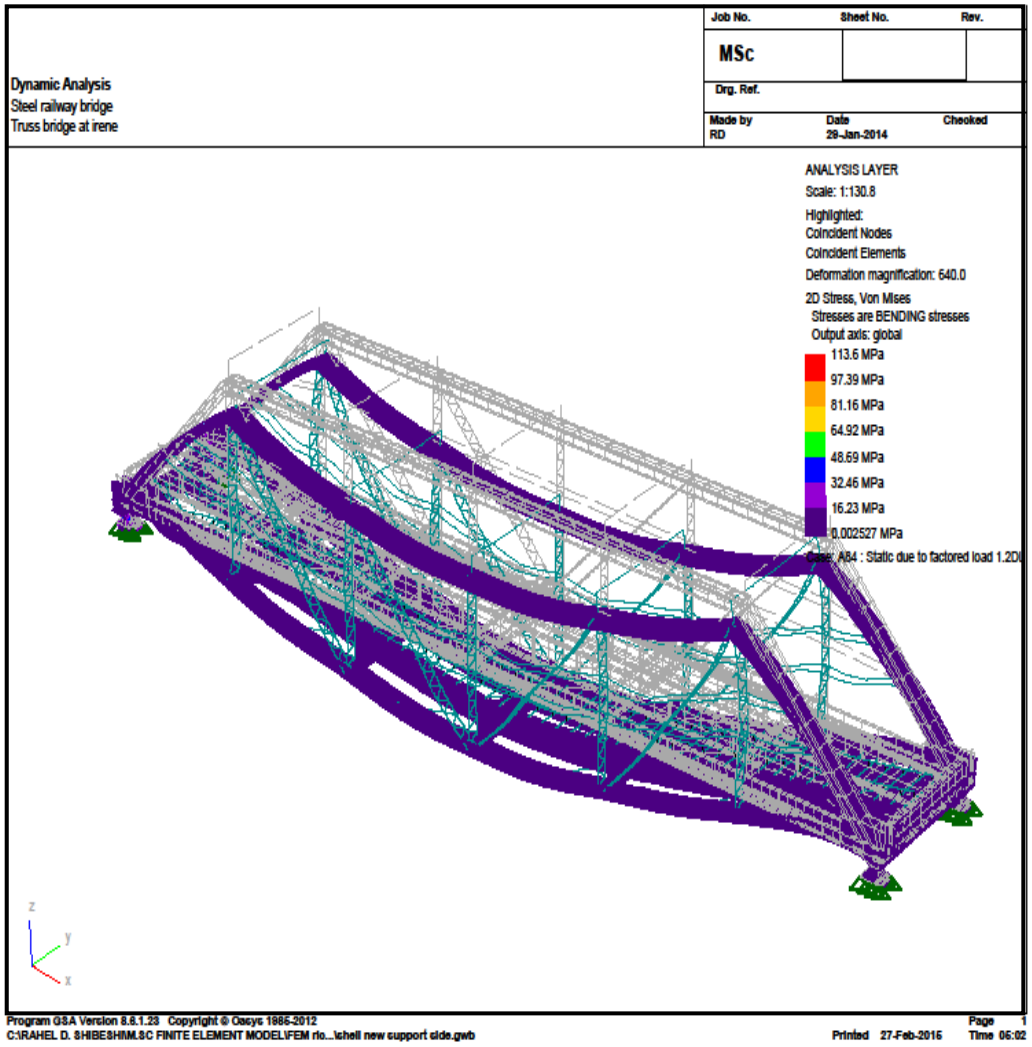

F.9 Natural frequency of the first vertical bending mode from FEM using shell elements observed at mode 5 (all pin supports)

Job No.	Sheet No.	Rev.
MSc		
Drg. Ref.		
Made by: RD	Date: 29-Jan-2014	Checked

Dynamic Analysis
Steel railway bridge
Truss bridge at irene

ANALYSIS LAYER
Scale: 1:200.3
Highlighted:
Coincident Nodes
Coincident Elements
Deformation magnification: 2.500
Case: A78 : Task 6 : Mode 5
Mode 5
Frequency: 10.03 Hz
Period: 0.09965 s

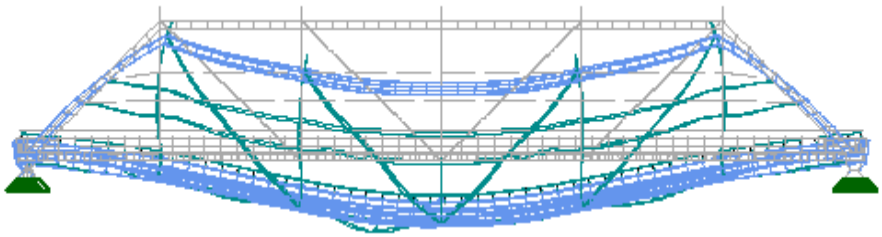

Program GSA Version 8.6.1.23 Copyright © Oasys 1985-2012 Page 1
C:\RAHEL D. SHIBESHI\M.SC FINITE ELEMENT MODEL\FEM rio...\shell new support side.gwb Printed 27-Feb-2015 Time 04:36

F.10 Natural frequency of the first vertical bending mode from FEM using shell elements observed at mode 5 (two roller and two pin supports)

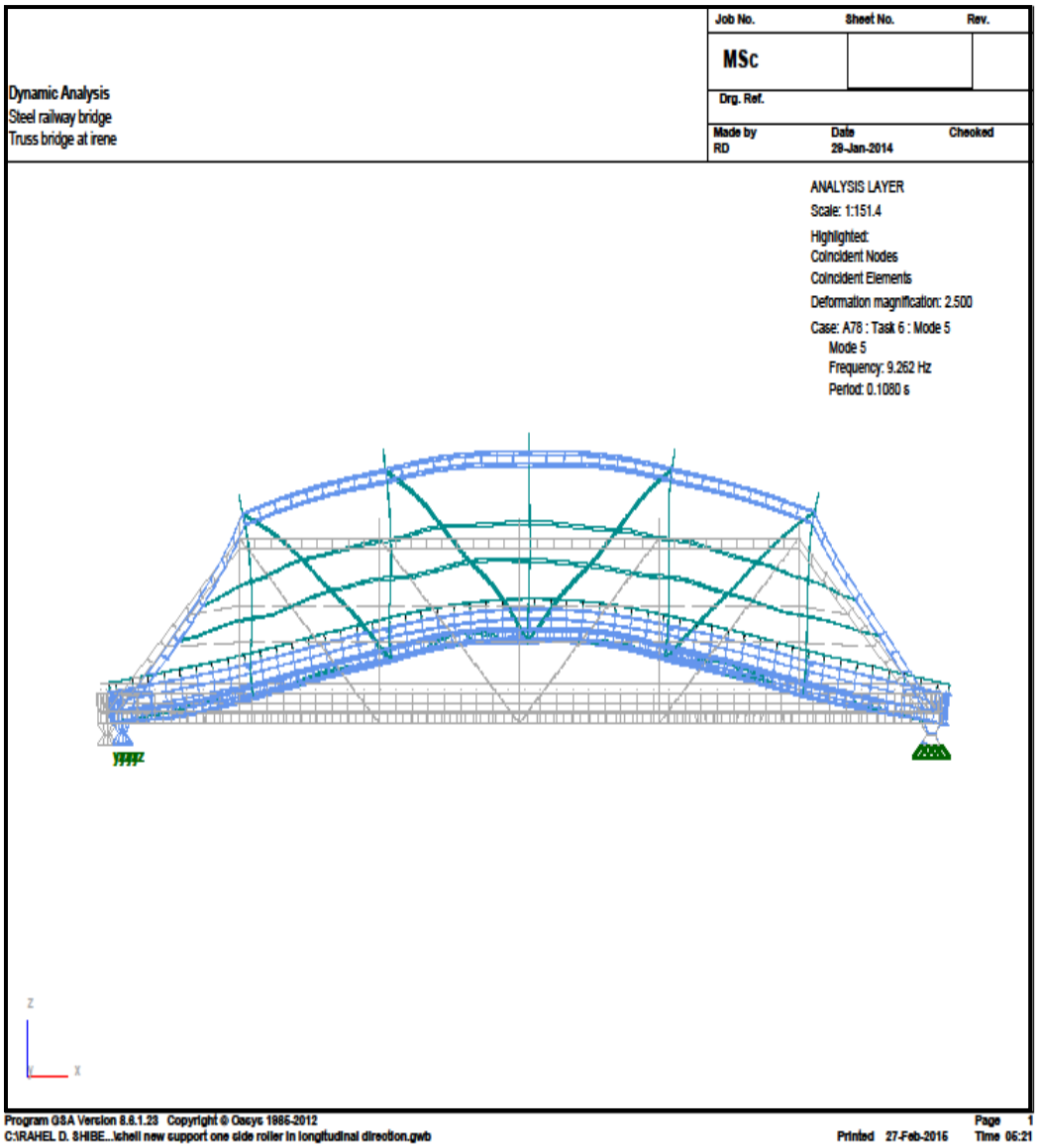

F.11 Displacement out put summary using shell elements due to selfweight only (all pin supports)

Job No.	Sheet No.	Rev.
MSc		
Drg. Ref.		
Made by: RD	Date: 28-Jan-2014	Checked

Dynamic Analysis
Steel railway bridge
Truss bridge at irene

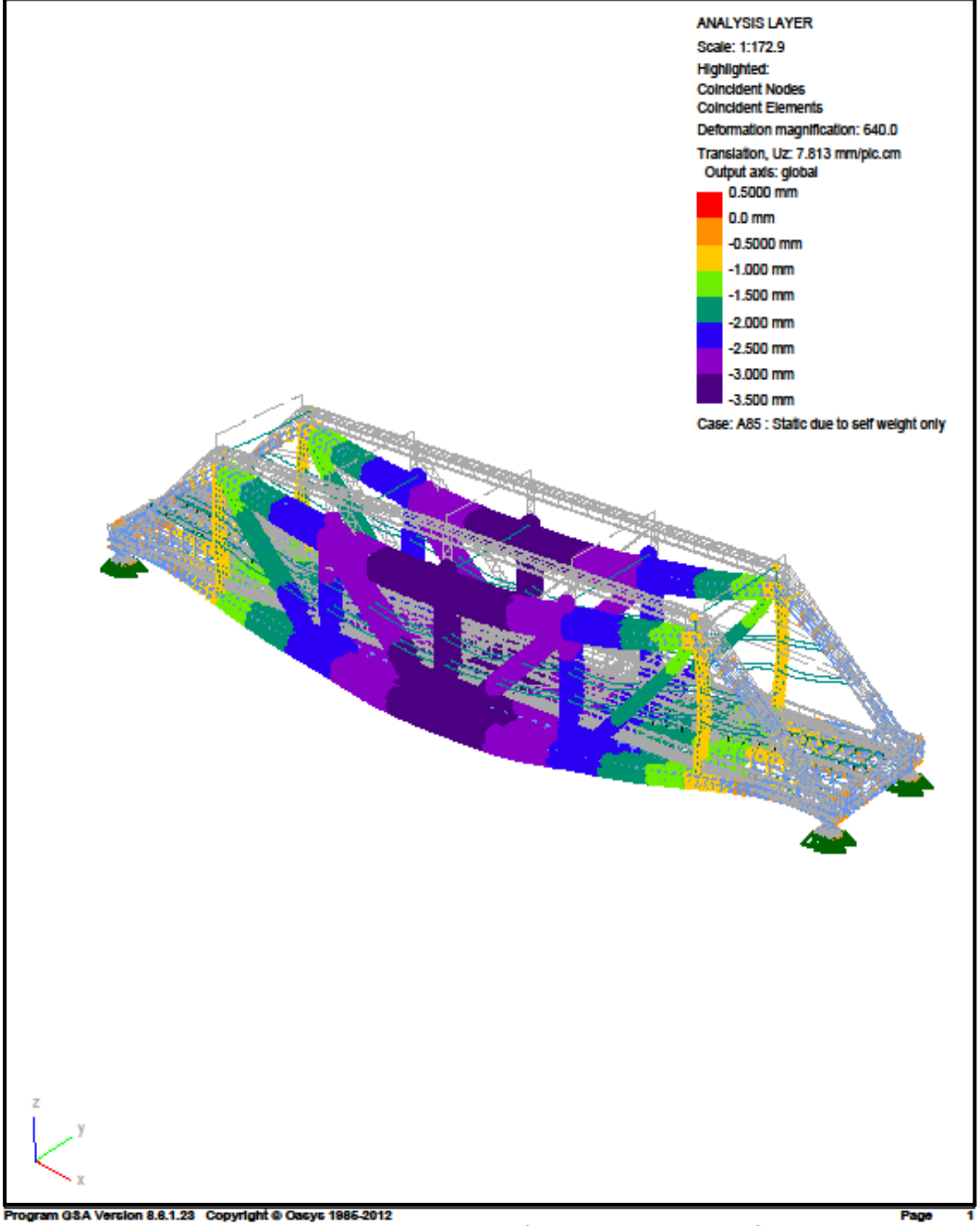

Program GSA Version 8.6.1.23 Copyright © Oasys 1985-2012 Page 1
C:\RAHEL D. SHIBESHI\M.SC FINITE ELEMENT MODEL\FEM rio...\shell new support side.gwb Printed 27-Feb-2015 Time 04:40

F.12 Displacement out put summary using shell elements due to selfweight only (two roller and two pin supports)

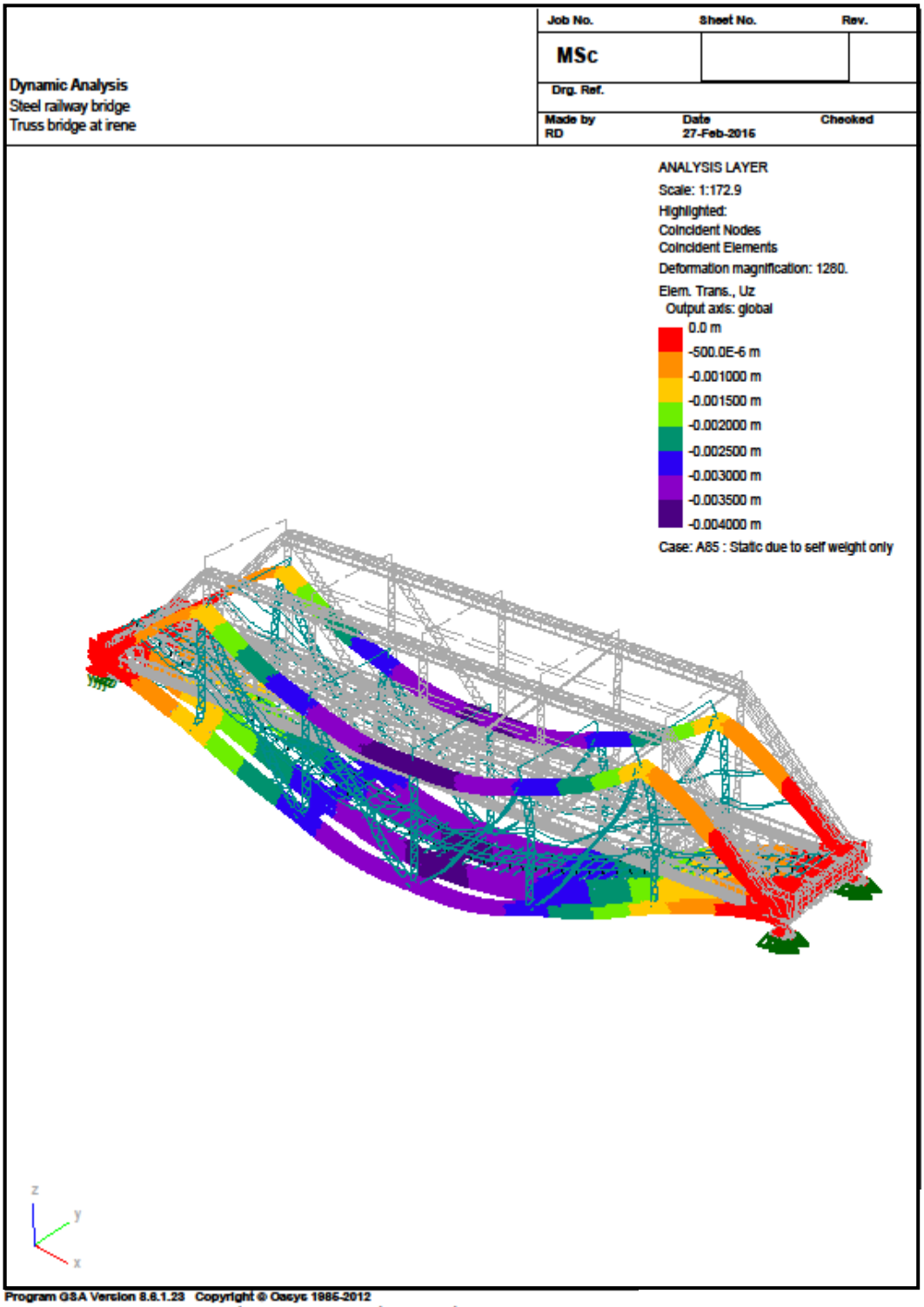

F.13 Displacement out put summary using beam elements due to selfweight only (all pin supports)

Job No.	Sheet No.	Rev.
MSc		
Drg. Ref.		
Made by RD	Date 27-Feb-2015	Checked

Dynamic Analysis
Steel railway bridge
Beam model..Truss bridge at irene

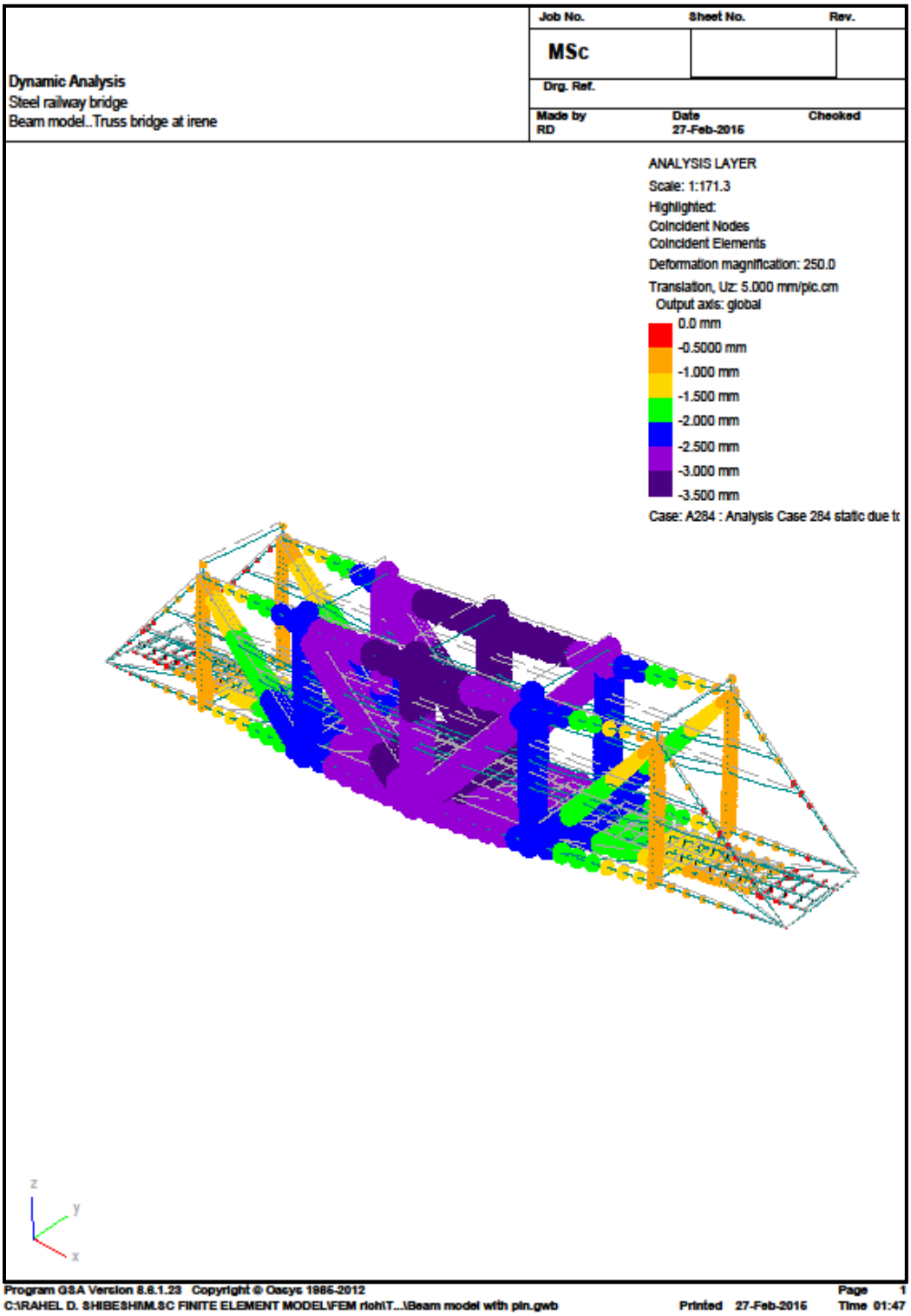

Program GSA Version 8.6.1.23 Copyright © Oasys 1985-2012 Page 1
C:\RAHEL D. SHIBESHI\M.SC FINITE ELEMENT MODEL\FEM rioh\T...\Beam model with pin.gwb Printed 27-Feb-2015 Time 01:47

F.14 A typical displacement and stress out put summary

Dynamic Analysis Steel railway bridge Beam model..Truss bridge at irene	Job No. **MSc**	Sheet No.	Rev.
	Drg. Ref.		
	Made by RD	Date 27-Feb-2015	Checked

Displacements

Displacements reported at nodes, fully restrained nodes are excluded
Output axes: global
Node list: 4
Case list: A2E5 : Analysis Case 2E5...static due to factored load(1.2DL+1.6LL)

Node	Case	Ux [m]	Uy [m]	Uz [m]	|U| [m]	Rxx [rad]	Ryy [rad]	Rzz [rad]	|R| [rad]	Uxy [m]
Maxima										
4	A2E5	***1.233E-6***	-26.62E-6	-0.003508	0.003508	-124.1E-6	-14.24E-6	-3.512E-6	125.0E-6	26.65E-6
4	A2E5	1.233E-6	***-26.62E-6***	-0.003508	0.003508	-124.1E-6	-14.24E-6	-3.512E-6	125.0E-6	26.65E-6
4	A2E5	1.233E-6	-26.62E-6	***-0.003508***	0.003508	-124.1E-6	-14.24E-6	-3.512E-6	125.0E-6	26.65E-6
4	A2E5	1.233E-6	-26.62E-6	-0.003508	***0.003508***	-124.1E-6	-14.24E-6	-3.512E-6	125.0E-6	26.65E-6
4	A2E5	1.233E-6	-26.62E-6	-0.003508	0.003508	***-124.1E-6***	-14.24E-6	-3.512E-6	125.0E-6	26.65E-6
4	A2E5	1.233E-6	-26.62E-6	-0.003508	0.003508	-124.1E-6	***-14.24E-6***	-3.512E-6	125.0E-6	26.65E-6
4	A2E5	1.233E-6	-26.62E-6	-0.003508	0.003508	-124.1E-6	-14.24E-6	***-3.512E-6***	125.0E-6	26.65E-6
4	A2E5	1.233E-6	-26.62E-6	-0.003508	0.003508	-124.1E-6	-14.24E-6	-3.512E-6	***125.0E-6***	26.65E-6
4	A2E5	1.233E-6	-26.62E-6	-0.003508	0.003508	-124.1E-6	-14.24E-6	-3.512E-6	125.0E-6	***26.65E-6***
Minima										
4	A2E5	***1.233E-6***	-26.62E-6	-0.003508	0.003508	-124.1E-6	-14.24E-6	-3.512E-6	125.0E-6	26.65E-6
4	A2E5	1.233E-6	***-26.62E-6***	-0.003508	0.003508	-124.1E-6	-14.24E-6	-3.512E-6	125.0E-6	26.65E-6
4	A2E5	1.233E-6	-26.62E-6	***-0.003508***	0.003508	-124.1E-6	-14.24E-6	-3.512E-6	125.0E-6	26.65E-6
4	A2E5	1.233E-6	-26.62E-6	-0.003508	***0.003508***	-124.1E-6	-14.24E-6	-3.512E-6	125.0E-6	26.65E-6
4	A2E5	1.233E-6	-26.62E-6	-0.003508	0.003508	***-124.1E-6***	-14.24E-6	-3.512E-6	125.0E-6	26.65E-6
4	A2E5	1.233E-6	-26.62E-6	-0.003508	0.003508	-124.1E-6	***-14.24E-6***	-3.512E-6	125.0E-6	26.65E-6
4	A2E5	1.233E-6	-26.62E-6	-0.003508	0.003508	-124.1E-6	-14.24E-6	***-3.512E-6***	125.0E-6	26.65E-6
4	A2E5	1.233E-6	-26.62E-6	-0.003508	0.003508	-124.1E-6	-14.24E-6	-3.512E-6	***125.0E-6***	26.65E-6
4	A2E5	1.233E-6	-26.62E-6	-0.003508	0.003508	-124.1E-6	-14.24E-6	-3.512E-6	125.0E-6	***26.65E-6***

Accelerations

This table is empty.

Beam Derived Stresses

Stresses are calculated only for elements that have unmodified Area, Iyy and Izz or for which the 'Stress Calc. Basis' is specified as 'Section'.
The 'Stress Calc. Basis' is reported only for sections that have modified Area, Iyy or Izz.

+ve stresses: tensile

SSy and SSz are the maximum elastic shear stresses. (Refer to the GSA manual for details.)

Torsional stress: St = Mxx/Ct
(where Ct is the 'torsion modulus'. (Refer to the GSA manual for details.)

Von Mises stress: This is calculated assuming the maximum through thickness stress and torsional stress coexist.
In most cases this is an over-estimate of the von Mises stress.

Case list: A2E5 : Analysis Case 2E5...static due to factored load(1.2DL+1.6LL)

Elem	Case	Stress Calc. Basis	Pos	SSy [Pa]	SSz [Pa]	St [Pa]	Von Mises [Pa]
Maxima							
14547	A2E5		310	***33.73E+6***	-25.80E+6	-1.201E+6	133.8E+6
1943	A2E5		1140	20.29E+6	***31.0E+6***	-474100.	114.1E+6
13434	A2E5		24519	356300.	-503500.	***2.364E+6***	19.63E+6
14547	A2E5		10497	55.73E+6	-25.72E+6	-1.201E+6	***141.0E+6***
Minima							
14562	A2E5		10200	***-33.73E+6***	2.068E+6	1.164E+6	105.2E+6
1944	A2E5		1145	20.11E+6	***-30.33E+6***	-528200.	115.1E+6
13542	A2E5		23909	8.577E+6	834300.	***-4.384E+6***	111.0E+6

Program GSA Version 8.6.1.23 Copyright © Oasys 1985-2012 Page 1
C:\RAHEL D. SHIBESHI\MSC FINITE ELEMENT MODEL\FEM right\T...\Beam model with pin.gwb Printed 27-Feb-2015 Time 03:19